University of Szeged
Albert Szent-Györgyi Medical School
Doctoral School of Interdisciplinary Medicine

INVESTIGATING CIRCULATING EXTRACELLULAR VESICLES FOR ENHANCED BRAIN TUMOR DIAGNOSIS AND PROGNOSIS

PhD Thesis

Gabriella Dobra

Supervisor:
Krisztina Buzás, PhD

Szeged,
2024

The dissertation is based on the following publications:

I. **Dobra, G.**; Bukva, M.; Szabo, Z.; Bruszel, B.; Harmati, M.; Gyukity-Sebestyen, E.; Jenei, A.; Szucs, M.; Horvath, P.; Biro, T.; et al. Small Extracellular Vesicles Isolated from Serum May Serve as Signal-Enhancers for the Monitoring of CNS Tumors. *Int. J. Mol. Sci.* **2020**, 21, 5359, doi:10.3390/ijms21155359. IF=5.924; Q1

II. **Dobra, G.**; Gyukity-Sebestyén, E.; Bukva, M.; Harmati, M.; Nagy, V.; Szabó, Z.; Pankotai, T.; Klekner, Á.; Buzás, K. MMP-9 as Prognostic Marker for Brain Tumors: A Comparative Study on Serum-Derived Small Extracellular Vesicles. *Cancers* **2023**, 15, 712, doi:10.3390/cancers15030712. IF: 5.064; Q1

Other publications related to the subject of the dissertation:

III. Bukva, M.; **Dobra, G.**; Gomez-Perez, J.; Koos, K.; Harmati, M.; Gyukity-Sebestyen, E.; Biro, T.; Jenei, A.; Kormondi, S.; Horvath, P.; et al. Raman Spectral Signatures of Serum-Derived Extracellular Vesicle-Enriched Isolates May Support the Diagnosis of CNS Tumors. *Cancers* **2021**, 13, 1407, doi:10.3390/cancers13061407. IF: 6.575; Q1

Other papers published during the PhD fellowship:

IV. Bukva, M.; **Dobra, G.**; Gyukity-Sebestyen, E.; Boroczky, T.; Korsos, MM.; Meckes, DG Jr.; Horvath, P.; Buzas, K.; Harmati, M. Machine learning-based analysis of cancer cell-derived vesicular proteins revealed significant tumor-specificity and predictive potential of extracellular vesicles for cell invasion and proliferation - A meta-analysis. *Cell Commun Signal*. **2023**, 21(1):333. doi: 10.1186/s12964-023-01344-5. IF: 8.228; Q1

V. Böröczky, T.; **Dobra, G.**; Bukva, M.; Gyukity-Sebestyén, E.; Hunyadi-Gulyás, É.; Darula, Z.; Horváth, P.; Buzás, K.; Harmati, M. Impact of Experimental Conditions on Extracellular Vesicles' Proteome: A Comparative Study. *Life* **2023**, 13, 206, doi:10.3390/life13010206. IF: 3.253; Q2

VI. Decsi, G.; Soki, J.; Pap, B.; **Dobra, G.**; Harmati, M.; Kormondi, S.; Pankotai, T.; Braunitzer, G.; Minarovits, J.; Sonkodi, I.; et al. Chicken or the Egg: Microbial Alterations in Biopsy Samples of Patients with Oral Potentially Malignant Disorders. *Pathol. Oncol. Res*. **2019**, 25, 1023–1033, doi:10.1007/s12253-018-0457-x. IF: 2.826; Q2

VII. Gyukity-Sebestyén, E.; Harmati, M.; **Dobra, G**.; Németh, I.B.; Mihály, J.; Zvara, Á.; Hunyadi-Gulyás, É.; Katona, R.; Nagy, I.; Horváth, P.; et al. Melanoma-Derived Exosomes Induce PD-1 Overexpression and Tumor Progression via Mesenchymal Stem Cell Oncogenic Reprogramming. *Front. Immunol.* **2019**, 10, 2459, doi:10.3389/fimmu.2019.02459. IF: 5.085; Q1

VIII. Harmati, M.; Gyukity-Sebestyen, E.; **Dobra, G**.; Janovak, L.; Dekany, I.; Saydam, O.; Hunyadi-Gulyas, E.; Nagy, I.; Farkas, A.; Pankotai, T.; et al. Small Extracellular Vesicles Convey the Stress-Induced Adaptive Responses of Melanoma Cells. *Sci. Rep*. **2019**, 9, 15329, doi:10.1038/s41598-019-51778-6. IF: 3.998; D1

IX. Harmati, M.; Tarnai, Z.; Decsi, G.; Kormondi, S.; Szegletes, Z.; Janovak, L.; Dekany, I.; Saydam, O.; Gyukity-Sebestyen, E.; **Dobra, G**.; et al. Stressors Alter Intercellular Communication and Exosome Profile of Nasopharyngeal Carcinoma Cells. *J. Oral Pathol. Med.* **2017**, 46, 259–266, doi:10.1111/jop.12486. IF: 2.237; Q2

X. Harmati, M.; Gyukity-Sebestyen, E.; **Dobra, G**.; Terhes, G.; Urban, E.; Decsi, G.; Mimica-Dukić, N.; Lesjak, M.; Simin, N.; Pap, B.; et al. Binary Mixture of Satureja Hortensis and Origanum Vulgare Subsp. Hirtum Essential Oils: In Vivo Therapeutic Efficiency against Helicobacter Pylori Infection. *Helicobacter* **2017,** 22, e12350, doi:10.1111/hel.12350. IF: 4.123; Q1

XI. Zsedenyi, A.; Farkas, B.; Abdelrasoul, G.N.; Romano, I.; Gyukity-Sebestyen, E.; Nagy, K.; Harmati, M.; **Dobra, G**.; Kormondi, S.; Decsi, G.; et al. Gold Nanoparticle-Filled Biodegradable Photopolymer Scaffolds Induced Muscle Remodeling: In Vitro and in Vivo Findings. *Mater. Sci. Eng. C* **2017**, 72, 625–630, doi:10.1016/j.msec.2016.11.124. IF: 5.080; Q1

Cumulative IF: 52.393

Participation in a position paper as a member of the MISEV Consortium:

I. Welsh, J.A.; Goberdhan, D.C.I.; O'Driscoll, L.; Buzas, E.I.; Blenkiron, C.; Bussolati, B.; Cai, H.; Di Vizio, D.; Driedonks, T.A.P.; Erdbrügger, U.; et al. Minimal Information for Studies of Extracellular Vesicles (MISEV2023): From Basic to Advanced Approaches. *J. Extracell. Vesicles* **2024**, *13*, e12404, doi:10.1002/jev2.12404.

IF: 15.485; Q1

Table of contents

Abbreviations

AFM	Atomic force microscopy
AFP	Alpha-fetoprotein
AUC	Area under the curve
BBB	Blood-brain barrier
BM	Brain metastasis originating from non-small-cell lung cancer
CA125	Cancer antigen 125
CNS	Central nervous system
CT	Computed tomography
CTC	Circulating tumor cells
ctDNA	Circulating tumor DNA
CTRL	Controls – lumbar disc hernia patients
DIA	Data independent acquisition
ECM	Extracellular matrix
EGFR	Epidermal growth factor receptor
ELISA	Enzyme-Linked Immunosorbent Assay
EPI test	ExoDx Prostate IntelliScore test
EVs	Extracellular Vesicles
FDA	U.S. Food and Drug Administration
GBM	Glioblastoma multiforme
GPC1	Glypican-1
IPA	Ingenuity Pathway Analysis
ISEV	International Society for Extracellular Vesicles
LC-MS	Liquid chromatography-mass spectrometry
M	Meningioma
MMPs	Matrix metalloproteinases
MRI	Magnetic resonance imaging
NGS	Next generation sequencing
NTA	Nanoparticle tracking analysis
PBS	Phosphate Buffered Saline
PCA	Principal component analysis
PSA	Prostate-specific antigen
ROC	Receiver operating characteristic
sEVs	Small extracellular vesicles
TEM	Transmission electron microscopy
WB	Western blot analysis
WHO	World Health Organization

1. Introduction

1.1. The prevalence and diagnosis of cancer diseases

According to the World Health Organization (WHO), cancer is one of the leading causes of death worldwide[1,2]. Between 1990 and 2019, the registered incidence of early-onset cancer increased by 79.1% globally, while the number of early-onset cancer fatalities rose by 27.7%[3]. In 2020, there were an estimated 19.3 million new cases, and cancer was accounting for almost 10 million deaths[2]. The prevalence of cancer continues to grow, exerting tremendous physical, emotional, and financial strain on individuals, families, communities, and health systems.

The dreaded cancer is a generic term for a large group of diseases that can affect any part of the body. Other terms used are malignant tumors and neoplasms. During tumorigenesis, normal cells acquire a set of functional capabilities, so-called cancer hallmarks, making their way from normalcy to neoplastic growth states[4,5,6]. One defining feature of cancer is the rapid creation of abnormal cells that grow beyond their usual boundaries, which can then invade adjoining parts of the body and spread to other organs; the latter process is called metastasis. Widespread metastases are the primary cause of death from cancer[7], however, the likelihood of metastasis can be diminished with early detection of the initial tumor[8].

In tumor diagnostics, computed tomography (CT) and magnetic resonance imaging (MRI) scans are used to determine disease status and evaluate the response to treatments[9]; however, these techniques have well-known limitations[10]. CT scans, for instance, cannot be repeated frequently due to overexposure to radiation, and radiocontrast agents can also cause serious side effects. MRI can only detect tumor masses of sufficient size, and the treatment-related changes may overlap with residual or recurrent tumors[11], and it has limited applicability to identify long-term recurrence[12].

Further common methods for tumor profiling require invasive surgical procedures to collect tumor samples. In addition to the high risk of complications, the disadvantages of such invasive procedures include the difficulty of obtaining tumor samples from highly heterogeneous or inaccessible locations, the need for multiple biopsies in the event of metastasis, and the inability to monitor tumor response or relapse. These challenges are exacerbated if the tumor is located within the skull. Thus, a crucial goal of neuro-oncological research is to develop novel methods for monitoring brain tumors in clinical practice[13].

1.2. Classification of brain and spinal cord tumors

The central nervous system (CNS) is a complex network of tissues and organs that play a crucial role in coordinating bodily functions. Within the CNS, tumors can arise, posing significant challenges to human health. These tumors originate from abnormal cell growth within the brain or spinal cord, disrupting normal function. There are over 130 different types of CNS tumors, they are usually named after the type of cell they develop from.

The two most common types of primary brain tumors in adults are the malignant glioblastoma multiforme (GBM), and the mainly benign meningioma. GBM - also referred to as a grade IV astrocytoma - can arise in the brain *de novo* or evolve from lower-grade astrocytoma. There is a general concept that GBM can originate from three distinct cell types: neural stem cells, astrocytes generated from neural stem cells, and oligodendrocyte precursor cells[14]. Meningioma is a tumor of the meninges, the tissue layers covering the brain and spinal cord. Meningiomas originate predominantly from meningothelial arachnoid cells, however, they can also occur as a primary tumor in other locations, such as the ventricles of the CNS[15].

Besides the primary ones, secondary brain cancer, so-called brain metastasis, is the most frequent type of brain tumor[16]. In general, the sources of brain metastases (in descending order) are cancers of the lung, breast, skin, kidney, and gastrointestinal tract[17,18,19]. Thus, lung cancer is the leading primary tumor that develops metastasis, and approximately 85% of patients have a group of histological subtypes collectively known as non-small cell lung cancer (NSCLC)[20].

The current international classification standard for CNS malignancies was established by the WHO in 2021. The WHO CNS5 classification standard (the abbreviation refers to the fifth edition) includes taxonomy, nomenclature, key diagnostic genes, molecules, and pathways in primary CNS tumors, as well as the grading criteria[21].

Accurate classification of CNS tumors requires tumor tissue obtained by biopsy or resection[21]. This is basically a morphological approach, but in an increasing number of instances, samples are also subjected to molecular profiling to decide between therapies. However, the tissue sample is not always available, and due to its heterogeneity and the dynamic changes as a result of the treatments, it is insufficient for therapeutic decision-making[22]. In addition, these procedures are extremely invasive, have a considerable risk of complications, and provide limited information about the tumor status. Due to these shortcomings and the spread of molecular profiling, attention has shifted towards the molecular investigation of biofluids, also known as liquid biopsy[23,24].

1.3. Liquid biopsy in tumor diagnosis

Every single cell, including neoplastic cells, releases molecular information into the circulation, which accumulates in urine, cerebrospinal fluid, saliva, and blood[24,25], thus, these body fluids can serve as a rich source of tumor-associated molecules. Liquid biopsy comprises the process of detecting and measuring distinct tumor-associated materials, such as circulating tumor DNAs (ctDNA)[26], circulating tumor cells (CTCs)[27], circulating tumor proteins[28], and tumor-derived or other extracellular vesicles (EVs)[29]. Identifying these materials can be of great importance in patient care (**Figure 1**).

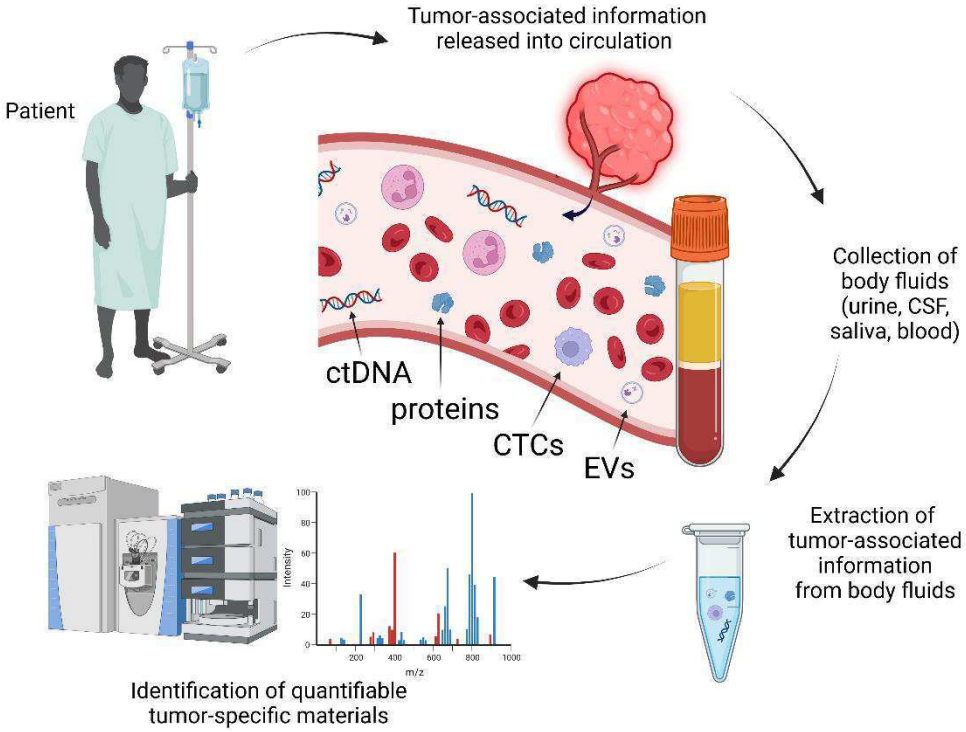

Figure 1. Schematic representation of liquid biopsy.
Abbreviations: ctDNA: circulating tumor DNA, CTCs: circulating tumor cells, proteins: tumor proteins, EVs: extracellular vesicles, CSF: cerebrospinal fluid

1.4. Potential targets of liquid biopsy

The first cancer liquid biopsy test, a ctDNA-based mutation assay called the cobas® EGFR Mutation Test v2, was approved by the U.S. Food and Drug Administration (FDA) in 2016[30]. This single-gene assay is based on the fact that epidermal growth factor receptor (EGFR) mutations are present in 10-30% of NSCLC patients. Today, not only assays examining single mutations but also strategies enabling extensive molecular profiling have been accepted. The first profiling test, a next-generation sequencing (NGS) ctDNA test, was adopted in 2020, to support osimertinib treatment decisions in NSCLC patients with EGFR

mutations. Despite the success of ctDNA-derived mutation tests, using them in early-stage cancers faces serious limitations, because for a successful analysis, the mutation should be present in sufficient quantity[31]. Furthermore, it has been reported that normal (non-cancerous) cells can also carry tumor-associated mutations[32] which significantly increases the false positive rate of ctDNA-derived liquid biopsy analysis[26].

Other possible targets are the CTCs generated when tumor cells detach from the tumor tissue and enter circulation. Once in circulation, tumor cells can serve as a minimally invasive source of tumor-associated material and have long been the focus of liquid biopsy[33,34,35]. Because CTCs are cellular analytes (as opposed to ctDNA, which is a nucleic acid), they carry a wide variety of molecular types that may be suitable as targets for clinical testing. Since 2004, the first and since then the only FDA-approved CTC analysis device has been able to quantify circulating tumor cells in the blood. Molecular characterization of CTCs could also be useful for the choice of therapy, however, most tumors release only limited amounts of CTCs into the circulation [36,37] and are mostly only suitable for evaluation in late-stage, metastatic diseases[38]. In addition to their rarity and unsuitability for early diagnostic use, the heterogeneity of CTCs also sets a serious limit to the use of this approach[39].

Liquid biopsy could also be based on the detection of proteins and have great potential for the diagnosis and monitoring of a disease[40]. For example, the disease status of the prostate, liver, and ovarian cancer can be assessed by using the serum concentration of the FDA-approved prostate-specific antigen (PSA), alpha-fetoprotein (AFP), and cancer antigen 125 (CA125) proteins, respectively[41,42,43]. Nevertheless, due to the lack of specificity of raised protein levels about a particular disease, and the possibility of normal serum concentrations even in advanced tumor cases, presently available protein tests do not meet the required diagnostic accuracy[28].

Last, but certainly not least, EVs are also potential liquid biopsy targets, since they possess various advantages in addition to the aforementioned benefits, such as access to the circulatory system[44,45], and a diverse range of diagnostically significant content[29]. Furthermore, EVs have a nanometer-scale dimension, and cells actively release substantial amounts of them; they are stable in all body fluids[46], and they can cross the blood-brain barrier (BBB)[47]. These valuable additional features make them ideal for liquid biopsy of brain tumors.

1.5. Extracellular vesicles

The term extracellular vesicles (EVs) endorsed by the International Society for Extracellular Vesicles (ISEV) as a "generic term for particles released from the cell that are delimited by a lipid bilayer and cannot replicate, i.e., do not contain a functional nucleus"[48,49]. EVs contain a sample of the cytosolic milieu of the donor cells, including abundant DNA, RNA, proteins, and other analytes, while outwardly resembling the donor cells[50,51,52].

Regarding biogenesis, EVs originate either from the endosomal system (used to be known as exosomes) or from the plasma membrane (e.g. other small extracellular vesicles, microvesicles, ectosomes); they comprise diverse subpopulations that can also differ in morphology, composition, or biological activity[53]. EVs are released of various sizes (small, medium, large) into the extracellular space[48,49]. The small EVs (shown in **Figure 2**) play the most significant part in tumor progression and have the greatest potential for utilization in the development of cancer diagnostics and therapeutics[54,55].

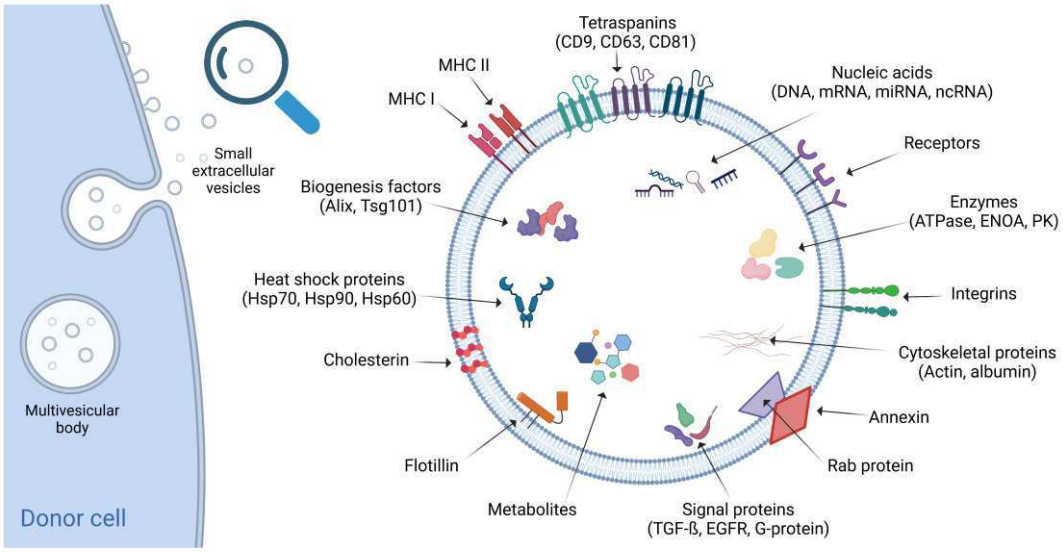

Figure 2. Biogenesis and structure of small extracellular vesicles

In the last few decades, EVs have become the target of intensive research, including their biological characteristics and physiological functions[56]; and their role was also described in cellular senescence[57], immunity[58], and communication between cells[53,59]. In the field of tumor biology, EVs have been extensively investigated and found to play a role in various aspects of the disease. These include tumor growth, development, invasion[60], inflammatory responses, immune suppression[61], epithelial-to-mesenchymal transition[62], angiogenesis, pre-metastatic niche formation[63,64], immunomodulation, tumor progression[65], and therapy resistance[66].

1.6. The role of small extracellular vesicles (sEVs) in tumor diagnosis

There is increasing evidence that sEVs contain a wealth of information that can be used for cancer diagnosis and prognostic evaluation[67,68]. Many studies focus primarily on nucleic acid content[69], but the EV proteome is also gaining increasing attention in cancer diagnostics[70]. Considering the number of proteins that can be produced by cells (which varies by time and stress), it seems that studying the proteome provides a greater understanding of the complexity of the tumor tissue and the evolution of tumors than studying the genetic material alone[71].

The first blood-based cancer diagnostic using extracellular vesicles, namely ExoDx Lung(ALK), was commercialized in the United States in 2016. The launch of this EV RNA-based liquid biopsy was a huge step in the development of extracellular vesicle science[72]. In another key event in EV diagnostics, Kalluri *et al.* found that glypican-1 (GPC1), a cell surface proteoglycan, is specifically enriched in circulating exosomes from pancreatic cancer patients. GPC1 can differentiate between early and late-stage pancreatic cancer and benign pancreatic diseases with 100% accuracy[73]. The development of such and similar diagnostic tools has been ongoing ever since. For instance, the ExoDx Prostate IntelliScore (EPI) test, which utilizes urine EVs to evaluate the risk of high-grade prostate cancer, has undergone three clinical trials[74,75] and has been granted FDA recognition. This achievement establishes the EPI test as the pioneering exosome-based LB test to receive a Breakthrough Device Designation[76]. Intensive research and product development is currently undergoing to bring EV-based diagnostics into routine clinical diagnostic practice, however, to date, there are no FDA-approved EV-based so-called biomarker tests for cancer diagnosis.

1.7. Biomarkers in clinical practice

According to the FDA/NIH Biomarker Working Group, the basic definition of a biomarker is deceptively simple: "A defined characteristic that is objectively measured and evaluated as an indicator of normal biological processes, pathogenic processes or responses to an exposure or intervention"[77]. Biomarkers can refer to characteristics that can be measured anywhere along the clinical continuum. In most cases, they are categorized based on the purpose of use, so we can talk about risk, diagnostic, monitoring, prognostic, predictive, response, and safety biomarkers (**Figure 3**).

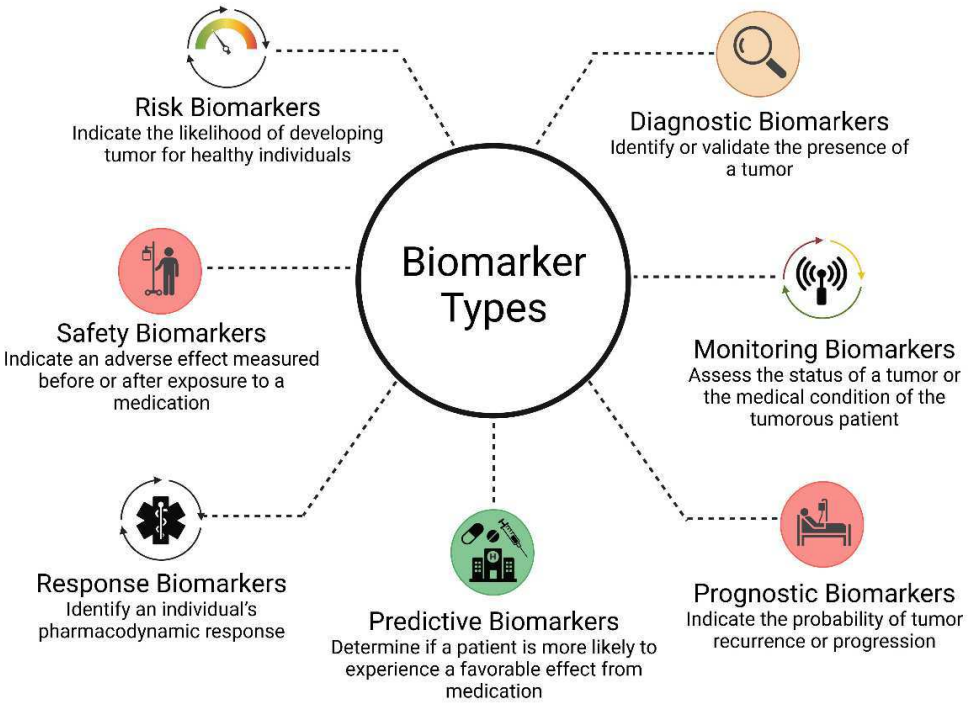

Figure 3. Types of tumor biomarkers

An ideal biomarker suitable for clinical application (1) is non-invasive, (2) comes from an easily accessible source, (3) is measured quickly and reliably using a standardized testing platform, (4) has high sensitivity, and (5) has high specificity. An ideal biomarker (6) also helps the risk assessment, (7) its level changes rapidly as a result of treatments, (8) it has a prognostic value, and, last but not least, (9) it is biologically acceptable[78,79].

To ensure most of the features above, biomarker tests undergo rigorous evaluation before being introduced into the clinic. Biomarkers must be validated, that is, the accuracy and reliability of the proposed test must be evaluated. Accuracy is a measure of how often a test is correct in a given population—in other words, its ability to differentiate the patient and healthy cases correctly. Accuracy is related to the sensitivity and specificity of the test and the prevalence of the target marker in the population being tested. A test's sensitivity is the distribution of true positives and false negatives—in other words, the test's intrinsic ability to identify a true positive when it exists. In contrast, specificity is the distribution of true negatives and false positives, or the intrinsic ability of a test to distinguish a true negative[80].

The rigorously evaluated and validated biomarker tests can therefore help, among other things, to accurately determine the type of tumors and the degree of malignancy, the latter being significantly related to the invasiveness of the tumor.

1.8. Extracellular matrix and MMPs in tumor invasion

The lack of effectiveness in treating certain aggressive brain tumors, such as GBM, can be attributed to the challenging task of completely removing the tumor due to the presence of peritumoral infiltration. This refers to the invasion of malignant cells into the surrounding healthy brain tissue. At the same time, brain metastases of similarly anaplastic carcinomas appear in the form of well-circumscribed intracerebral tumors, the complete resection of which is mostly considered a routine operation[81].

Peritumoral infiltration of aggressive cancers is caused by the increased invasion capacity of tumor cells. Tumor invasion is predominantly facilitated by extracellular matrix (ECM) molecules; consequently, the ECM is significantly involved in the tumor progression. Several ECM molecules, such as brevican, cadherin, fibronectin, neurocan, versican, tenascin-C, and matrix metalloproteinases (MMPs) are also associated with tumor invasion[81], of which MMPs are the main enzymes in collagen degradation[82].

MMPs compose a large family of secreted and membrane-associated proteinases essential for ECM remodeling. MMPs are zinc-dependent endopeptidases and are synthetized as inactive zymogens (pro-MMPs) and their activation requires a proteolytic cleavage that removes the pro-peptide. This pro-domain contains a cysteine that interacts with the Zn^{2+} ion present in the catalytic domain, preventing enzymatic proteolytic activity[83]. MMPs play an essential role in cell physiology by degrading the ECM components such as collagens, which are pivotal for normal physiological processes like wound healing, embryonic development, and tissue remodeling. Their ability to cleave proteins in the ECM and cell surface molecules also makes them critical in modulating cell behavior, influencing both cell-cell and cell-ECM interactions. This modulation can lead to alterations in cellular signaling pathways, impacting processes such as inflammation and cell proliferation[84].

In the context of pathology, MMPs are implicated in numerous processes. They enable cancer cells to breach the basal membrane barriers, facilitating metastasis and promoting cancer cell migration and invasion. Additionally, MMPs are involved in angiogenesis, which is essential for tumor growth as it provides the necessary blood supply for expanding tumors[85,86].

This intricate balance positions MMPs as double-edged swords; while they are essential for normal bodily functions, their dysregulation is linked to the progression of cancer. **Figure 4** indicates the importance of MMPs in biological processes and their potential as targets for therapeutic intervention in cancer treatment[87], aiming to suppress their cancer-facilitating roles while preserving their normal physiological functions.

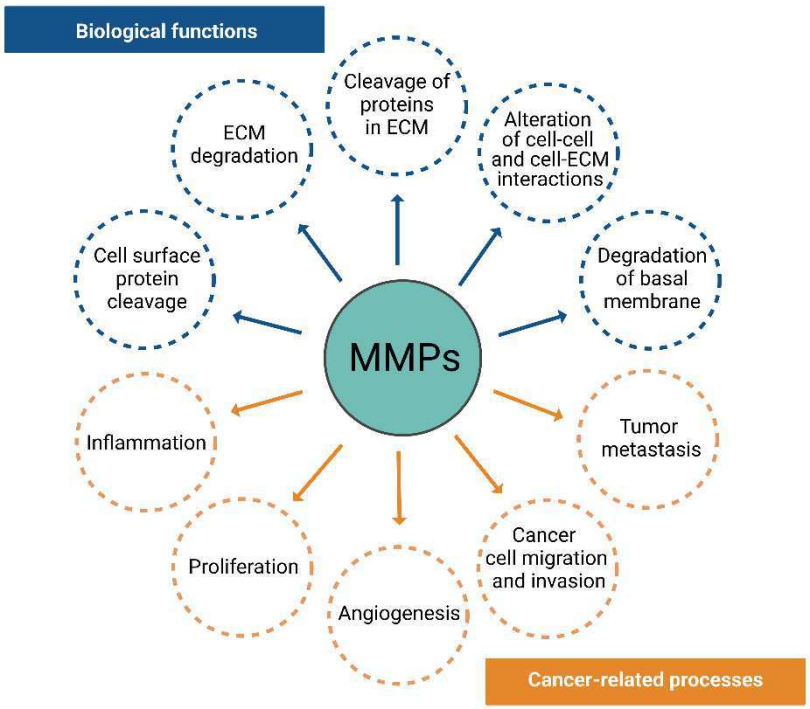

Figure 4. Roles of MMPs in the physiological and cancer-related processes
Abbreviations: ECM: extracellular matrix

Although they are associated with cancer cell survival and tumor spread, MMPs are synthesized in very small amounts by cancer cells. By secreting interleukin, interferon, growth factors, and extracellular MMP inducers, cancer cells stimulate the surrounding host cells to produce MMPs in a paracrine manner[82,88]. MMPs secreted by normal cells, key players of the tumor microenvironment, can bind to the cancer cell surface and be utilized by tumor cells[89].

Matrix metalloproteinase-9 (MMP-9, also known as 92 kDa type IV collagenase or gelatinase B) is one of the most complex forms of MMPs[84]. The role of MMP-9 in tumor tissue invasion and metastasis formation was already described in 1990[90], and the elevated levels of MMP-9 in human brain tumors were also reported in the 1990s[91]. Rao *et al*. also showed that the expression of MMP-9 is significantly upregulated in highly malignant gliomas and correlates with the progression, suggesting a role for MMP-9 in promoting the observed invasiveness[92].

1.9. Extracellular vesicle-associated MMPs

MMPs are crucial for ECM remodeling in both physiological and pathological conditions, including cancer, as was previously mentioned. MMPs are exposed to the microenvironment at two main locations: (1) the cell surface, at specialized plasma

membrane domains, such as invadopodia of cancer cells, and (2) associated with EVs. As a consequence, the activities of MMPs associated with the cell surface and EVs are unique. MMPs associated with cell surfaces may have a significant autocrine function via pericellular ECM remodeling, whereas EV-associated MMPs may primarily influence the activities of tumor microenvironment cells rather than influencing the producing cell activities[93].

MMPs have been identified as EV cargoes by multiple research groups[94,95,96]. In general, the topology of EVs is similar to that of cells, with extracellular ligands and receptors on the outside and cytoplasmic proteins and RNAs on the inside[97]. The proteolytic activity of EVs under non-permeabilized conditions suggests that membrane-anchored and secreted MMPs are present on the external surface of EVs[96].

Initial investigations have established that mouse melanoma cells and human colorectal carcinoma cells secrete EVs that exhibit gelatinolytic or collagenolytic properties[98,99] indicating the presence of MMPs. EVs derived from HT-1080 fibrosarcoma cells and 8701-BC breast cancer cells reportedly contain MMP-9 with degrading activity, according to the research of Ginestra *et al.*[100]. Subsequently, they discovered a positive correlation between the quantity of proteolytic enzymes carried by shed EVs and the invasive capability of various cell lines *in vitro*[101]. This finding emphasizes the clinical importance of proteolytic activities in EVs during the progression of tumors.

Kassassir *et al*. demonstrated that platelet-derived microparticles stimulate the invasiveness of colorectal cancer cells via the p38MAPK-MMP-2/MMP-9 axis[102]. A significant correlation has been observed between the quantity of EVs and MMPs associated with EVs and the invasive capability of cancer cells[103]. Wenzel *et al*. demonstrated that endosome-mediated protease shedding may transform non-invasive recipient cells to an invasive phenotype, thereby transferring the invasiveness of cancer cells intracellularly[104].

Shimoda and Khokha provided a comprehensive overview of the key discoveries and understandings related to MMPs in the field of EV biology. (1) EVs have been found to contain MMPs, (2) vesicular MMPs have been detected in various body fluids, (3) several MMPs in EVs hold proteolytic activities and alter EV contents, (4) vesicular MMPs might affect target cells and contribute to ECM degradation, thus (5) they actively participate in tumor progression[94]. These observations indicate that extracellular-associated MMPs might be used as biomarkers of disease progression.

1.10. Significance and rationale of the research

Non-invasive diagnostic tests are of great importance, especially in CNS tumors, because of their minimal burden and risk to the patient, their repeatability, low cost, high information content, and easy accessibility. Various papers report gene or protein expression analysis of CNS tumor tissue (mainly gliomas) allowing the identification of biomarkers secreted into the blood. Recent studies aimed to identify one or two specific biomarkers for blood-based assessment of actual tumor status[105,106,107]. However, studies on CNS tumors have halted at the initial phase, presumably explained by several reasons, including (1) the regulator function of BBB[108], (2) the presence of molecules released into the blood from other sources[109], and (3) possibly because of the intratumoral heterogeneity of tumor tissues[110]. These issues hamper attempts to use a single or only a few biomarkers to diagnose and monitor CNS tumors.

Since previous attempts to find surrogate serum markers for brain tumors failed when they were based on a single or only a few candidate factors, the solution may lie in identifying 10-20 candidate markers associated with brain tumors and creating a protein panel as a characteristic fingerprint of CNS diseases.

Another issue is that the potential biomarker candidates are difficult to detect because of their low concentrations in the blood, and the high levels of abundant serum proteins which may confound the analytical measurements. Hence, it is necessary to refine the sample to increase the concentration of potential biomarker candidates beyond the detection limit. This biomarker enrichment may be achieved by sEV isolation, but it is necessary to compare the two sample types (whole serum and serum-derived sEV) to determine which is more suitable to distinguish between patient groups.

As the content of EVs varies based on the patient's condition[111], the feasibility of utilizing sEVs for prognostic purposes was also an important issue. Hence, it is important to examine whether any of the proteins exhibiting the most significant differences among patient groups are appropriate for prognostic markers.

2. Aims

We aimed to identify circulating protein markers for liquid biopsy-based diagnosis, prognosis, and monitoring of central nervous system tumors utilizing patient-derived sera (later referred to as whole serum) and serum-derived extracellular vesicles (later referred to as serum sEV).

Four groups of patients with a disease affecting the central nervous system were included in the tests (glioblastoma, brain metastasis of non-small cell lung cancer, meningioma, and lumbar disc herniation as controls), a total of 222 patients were examined during this proteomic study.

Our specific aims were:

1. To compare the protein content of the whole serum and the serum sEV of four patient groups and identify non-invasive protein biomarkers by establishing characteristic protein panels that are suitable for classifying CNS tumors;
2. To compare the potential of the two proteome and the established protein panels in tumor classification and biological characterization of the disease;
3. To explore the factors underlying the differences in classification efficiency between the two sample types;
4. To select the most sufficient sEV protein for distinguishing the patient groups;
5. To examine the factors (gender, age, and clinical history of the patient) influencing the concentration of the protein biomarker candidates;
6. To determine the clinical potential of the most appropriate protein as a biomarker.

.

3. Materials and Methods

3.1. Patients

Blood samples of 222 patients treated in the Department of Neurosurgery, University of Debrecen were analyzed. Samples were obtained from patients with primary glioblastoma multiforme (GBM), meningioma (M), and single brain metastasis originating from non-small-cell lung cancer (BM). Control samples (CTRL) were collected from patients with spinal disc herniation without evidence of cancer. This non-tumor patient group served as the control group in comparison to the patients having different intracranial tumors to distinguish the effects of tumorous processes from the CNS involvement.

Blood samples were stored by the Neurosurgical Brain Tumor and Tissue Bank of Debrecen according to the criteria of the National Research Ethics Committee. An informed consent form was signed by each patient; the study was conducted in accordance with the Declaration of Helsinki. This study was carried out according to two ethical approvals, namely 51450-2/2015/EKU (0411/15), Medical Research Council, Scientific, and Research Ethics Committee, Budapest, October 30, 2015, and 121/2019-SZTE, University of Szeged, Human Investigation Review Board, Albert Szent-Györgyi Clinical Centre, Szeged, July 19, 2019.

The protein content of 96 whole sera and serum sEV samples originating from the four patient groups was analyzed by liquid chromatography-mass spectrometry (LC-MS). Each group contained 24 individuals with mixed ages and genders. As shown in **Table 1**, six-sample-pools were created from the individuals, allowing four parallel samples to be tested per group. Blood samples were collected one day prior to the neurosurgical procedure in each tumor case. None of the patients received radio- or chemotherapy before tumor resection.

Additional serum samples were involved in the vesicular MMP-9 analyses. Using ELISA, 222 serum sEV samples were investigated for MMP-9. In addition to collecting blood samples prior to surgery, samples were also taken after surgery. Some patients were undergoing treatment at the time of sampling, whereas others had tumor relapse and were tested following recurrence. Along with the four main groups, subgroups were defined based on histopathology, sampling time (before or after surgery), grading, recurrence, and treatment (**Table 2**).

Table 1. The patient cohort for the protein panel investigations and the comparison of the two sample types[1].

Characteristics	**Average**	**Pool1**	**Pool2**	**Pool3**	**Pool4**
♦ Glioblastoma multiforme	**GBM**	**GBM1**	**GBM2**	**GBM3**	**GBM4**
Total No. of patients	***n* = 24**	*n* = 6	*n* = 6	*n* = 6	*n* = 6
Age, Median (range)	**67 (33–82)**	64.5 (38–82)	69.5 (33–76)	67.5 (49–74)	66.5 (63–77)
Mean	**64.9**	62.7	63.8	64.7	68.5
Sex (%), Male	**13 (54.2)**	3 (50)	3 (50)	5 (83.3)	2 (33.3)
Female	**11 (45.8)**	3 (50)	3 (50)	1 (16.7)	4 (66.7)
■ Brain metastasis	**BM**	**BM1**	**BM2**	**BM3**	**BM4**
Total No. of patients	***n* = 24**	*n* = 6	*n* = 6	*n* = 6	*n* = 6
Age, Median (range)	**64 (42–82)**	66.5 (51–82)	68 (62–71)	63.5 (42–81)	59.5 (53–64)
Mean	**64**	67.7	67.5	59.7	59.5
Sex (%), Male	**13 (54.2)**	2 (33.3)	3 (50)	4 (66.7)	4 (66.7)
Female	**11 (45.8)**	4 (66.7)	3 (50)	2 (33.3)	2 (33.3)
▲ Meningioma	**M**	**M1**	**M2**	**M3**	**M4**
Total No. of patients	***n* = 24**	*n* = 6	*n* = 6	*n* = 6	*n* = 6
Age, Median (range)	**60 (30–79)**	54,5 (39–69)	62 (30–66)	61,5 (44–75)	66,5 (52–79)
Mean	**58.0**	53.5	53	59.3	66
Sex (%), Male	**4 (16.7)**	0 (0)	0 (0)	1 (16.7)	3 (50)
Female	**20 (83.3)**	6 (100)	6 (100)	5 (83.3)	3 (50)
● Control	**CTRL**	**CTRL1**	**CTRL2**	**CTRL3**	**CTRL4**
Total No. of patients	***n* = 24**	*n* = 6	*n* = 6	*n* = 6	*n* = 6
Age, Median (range)	**50.5 (20–81)**	46.5 (26–71)	47 (20–62)	70.5 (49–81)	52.5 (41–69)
Mean	**52,9**	46,5	45	67,2	53
Sex (%), Male	**9 (37.5)**	2 (33.3)	4 (66.7)	4 (66.7)	4 (66.7)
Female	**15 (62.5)**	4 (66.7)	2 (33.3)	2 (33.3)	2 (33.3)

[1] The table summarizes the main characteristics of the patient groups examined. Each group (average values highlighted in bald) included 24 individuals, converted into six-sample-pools to yield four samples per group for further analysis.

Table 2. The patient cohort for vesicular MMP-9 analyses

Characteristics	***n* = 222**	**%**
Glioblastoma multiforme (GBM)	**121**	**54%**
secondary glioblastoma (GBMsec)	*18*	*15%*
preoperative samples (GBMsec preop)	9	50%
postoperative samples (GBMsec postop)	9	50%
primary glioblastoma (GBMprim)	*103*	*85%*
preoperative samples (GBMprim preop)	69 (10) [1]	67%
recurrence-related analysis	69	67%
original tumor	54	78%
recurrence	15	22%
therapy involvement analysis	69	67%
patients before therapy	54	78%
patients with therapy	15	22%
survival analysis	27	39%
>65 Years	11	41%
≤65 Years	16	59%
high MMP-9 level (≥28 ppm)	17	63%
low MMP-9 level (<28 ppm)	10	37%
postoperative samples (GBMprim postop)	14 (10)[1]	33%
Brain Metastasis (BM)	**37**	**17%**
carcinoma planocellulare (BMplano)	*13*	*35%*
adenocarcinoma (BMadeno)	*24*	*65%*
preoperative samples (BMpreop)	27 (6)[2]	73%
postoperative samples (BMpostop)	10 (6)[2]	27%
Meningioma (M)	**28**	**13%**
meningioma Grade I (M_I)	*20*	*71%*
meningioma Grade II (M_II)	*8*	*29%*
Control (CTRL)	**36**	**16%**
lumbar disc herniation	*36*	*16%*
male	16	44%
female	20	56%

Percentages indicate the participation rates within each statistical analysis; [1] Number of GBM patients involved in paired t-test; [2] Number of BM patients involved in paired t-test

3.2. Preparation of serum samples

Blood samples were collected into BD Vacutainer SST II Advance Tubes (Becton, Dickinson and Company, Franklin Lakes, NJ, USA), allowed to clot for at least 1 h at room temperature, and centrifuged for 20 min at 3000 × *g*, 10 °C to remove cells; the supernatant serum was transferred to new Eppendorf tubes and stored on -80 °C until further usage.

3.3. sEV isolation

Following thawing on ice, the serum samples were centrifuged for 30 min at 10,000 × *g*, 4 °C to remove debris and large vesicles. One milliliter serum aliquot was diluted with DPBS (Ca^{2+}-free, Mg^{2+}-free, Lonza Group Ltd., Basel, Switzerland) to 8 mL and ultracentrifuged for 70 min, at 100,000 × *g*, 4 °C (polycarbonate tubes, fixed angle T-1270 rotor, Thermo Fisher Scientific, Waltham, MA, USA). The pellet was resuspended in 100 uL DPBS and stored at −80 °C until further processing. This sEV isolation protocol served to reach intermediate recovery and intermediate specificity according to MISEV2018 [48] [49].

3.4. sEV characterization

sEVs were characterized by atomic force microscopy (AFM), transmission electron microscopy (TEM), Western blot analysis (WB), and nanoparticle tracking analysis (NTA). The TEM and WB measurements were performed on a representative sample of every main group.

To examine sEV morphology, AFM measurements were carried out with an Asylum MFP-3D head and controller (Asylum Research, Santa Barbara, CA, USA). The driver program MFP-3D Xop was written in IGOR Pro Software (Wavemetrics, Lake Oswego, OR, USA). For imaging, gold-coated silicon nitride rectangular cantilevers were used with a typical spring constant of 0.03 N/m in the air (BL-RC150 VB, Olympus Optical Co. Ltd., Tokyo, Japan). The spring constant for each cantilever was determined by thermal calibration followed by Sader's method[112]. For the measurements, freshly cleaved, negatively charged 1 × 1 cm mica (SPI-Chem Mica Sheets) surfaces were incubated in 2% APTES ((3-aminopropyl)triethoxysilan, Sigma, St. Louis, MO, USA) dissolved in isopropanol for 90 min in shaking condition at RT to create free amine groups on their surface[113]. EVs were attached to the modified surface with glutaraldehyde. The measurements presented here are 1.5 × 1.5 μm^2 flattened heights. Experiments were repeated three to five times.

Regarding the sEV morphology, TEM analysis was also performed using a Tecnai G2 20 X-Twin type instrument (FEI, Hillsboro, OR, USA), operating at an acceleration voltage of 200 kV. The samples were dropped on a carbon film with 200 mesh copper grids (CF200-Cu, Electron Microscopy Sciences, Hatfield, PA, USA) and dried without staining or other fixation procedures.

For measuring the particle distribution, sEVs were diluted in particle-free DPBS and analyzed using a NanoSight NS300 instrument with a 532 nm laser (Malvern Panalytical

Ltd., Malvern, UK). The measurements were performed on the 16 sEV sample pools (described in 4.1). Six videos of 60 s were recorded for each sample under constant settings (Camera level: 15; Threshold: 4, 25 °C; 60–80 particles/frame) and analyzed to obtain data on the size distribution and particle concentration.

Confirming the presence of sEVs, Alix, CD81, CD5L, and calnexin markers were presented by Western blot analyses using NuPAGE reagents and an XCell SureLock Mini-Cell System (Thermo Fisher Scientific, Waltham, MA, USA) according to the manufacturer's protocols. The protein content of sEV samples was determined using a Pierce BCA Protein assay kit (Thermo Fisher Scientific, Waltham, MA, USA) and a benchtop microplate reader (Multiskan RC, Thermo Labsystems, Waltham, MA, USA) according to the manufacturer's instructions. For detection of the sEV markers in the four main groups, rabbit anti-human Alix (1:1000), rabbit anti-human CD81 (1:1000), rabbit anti-human CD5L (1:2000), and rabbit anti-human Calnexin (1:10,000) primary antibodies (all from Sigma-Aldrich, St. Louis, MO, USA), and HRP-conjugated anti-rabbit IgG (1:1000, R&D Systems, Minneapolis, MN, USA) secondary antibody were used. THP-1 cell line (ATCC, Manassas, VA, USA) lysate was used for the positive control for Calnexin. Bound antibodies were visualized by chemiluminescence using an ECL Plus Western Blotting detection system (Advansta, Menlo Park, CA). Immunoreactive signals were detected by using LI-COR ODYSSEY Fc (Dual-mode imaging system) imager followed by analysis with Odyssey v1.2, Image Studio Lite v5.2.

Characterizing proteins expressed on the surface of the serum-derived sEV, we used bead-based multiplex EV analysis by flow cytometry (MACSPlex Exosome Kit, human, Miltenyi Biotec, Germany). The kit consists of a set of 39 hard-dyed capture bead populations, each coated with different monoclonal antibodies specific for one of 37 proteins reported to be expressed on the sEV surface, together with antibodies of two control proteins. The antibody-coated beads capture sEV expressing the relevant molecule, which can then be quantified by flow cytometry after tagging with labeled antibodies to CD9, CD63, or CD81. Sample pools of sEV from ten donors in each group were analyzed by Cytoflex S fluorescent flow cytometer (Beckman Coulter, IN, USA). The markers were regarded as present when their median APC fluorescence intensities were based on more than 10 events. GraphPad Prism 8 (San Diego, CA, USA) was used for creating the heatmaps.

3.5. Proteomic Analysis by liquid chromatography-mass spectrometry (LC-MS)

3.5.1. 'In Solution' Digestion

Individual samples containing 20 µg protein were diluted to 10 µL with 0.1 M NH_4HCO_3 (pH = 8.0) buffer; 12 µL 0.1% RapiGest SF (Waters, Milford, MA, USA) and 2 µL 55 mM dithioeritritol solution was added and kept at 60 °C for 30 min to unfold and reduce proteins. A volume of 2 µL 200 mM iodo acetamide solution was added to alkylate the proteins which were kept for an additional 30 min in the dark at room temperature. The samples were digested overnight at 37 °C with trypsin (Thermo Scientific, Waltham, MA, USA, enzyme/protein ratio: 0.4 to 1). The digestion was stopped by the addition of 1 µl of concentrated formic acid.

3.5.2. LC-MS

The separation of the digested samples was carried out on a nanoAcquity UPLC, (Waters, Milford, MA, USA) using Waters ACQUITY UPLC M-Class Peptide C18 (130 Å, 1.78 µm, 75 µm × 250 mm) column with a nonlinear 90 min gradient. Eluents were water (A) and acetonitrile (B) containing 0.1 *V/V*% formic acid and the separation of the peptide mixture was performed at 45 °C with 0.35 µl/min flow rate using an optimized nonlinear LC gradient (3–40% B). The LC was coupled to a high-resolution Q Exactive Plus quadrupole-orbitrap hybrid mass spectrometer (Thermo Scientific, Waltham, MA, USA). The quantitative measurements of digested individual samples were performed in DIA mode. The survey scan for the DIA method operated with 35,000 resolution. The full scan was performed between 380 to 1020 *m/z*. The AGC target was set to 5 × 106 or 120 ms maximum injection time. In the 400–1000 *m/z* region, 22 *m/z* wide overlapping windows were acquired at 17,500 resolution (AGC target: 3 × 106 or 100 ms injection time, normalized collision energy: 27 for charge 2). The quantitative analysis was performed in Encyclopedia 0.81 [114] using default settings after deconvolution, peak picking, and conversion of raw MS files to mzML format in Proteowizard[115]. A comprehensive spectral library[116] of 10,000 human proteins was used for peptide identification. Protein quantities calculated by the Encyclopedia software based on summed intensities of the automatically filtered peptides were used in further statistical evaluations.

3.6. MMP-9 Analysis by Enzyme-Linked Immunosorbent Assay (ELISA)

To accurately measure the MMP-9 content of serum sEV, LEGEND MAX Human MMP-9 ELISA Kit (Biolegend, San Diego, CA, USA) was used according to the manufacturer's protocol. sEV isolates of 222 serum samples were measured individually, and the vesicles were disrupted in a detergent-free manner by five repeated freeze–thaw cycles to expose the entire protein content. As we examined sEV isolates, potential interferences—observed in clinical immunoassays of sera[117]—are avoided. The assay procedures are briefly summarized below.

A standard curve was applied for each assay, and all samples were run in duplicate on separate plates. In the first step, 50 µL assay buffer and 50 uL standard dilutions or 12× diluted samples were added to the appropriate wells, and the plates were sealed and incubated at room temperature for 2 h while shaking at 200 rpm. After the incubation, plates were washed four times with a 1× wash buffer. The first step was followed by three more incubation steps, namely 100 µL of human MMP-9 detection antibody solution, 100 µL of Avidin-HRP solution, and 100 µL of substrate solution D were added to each well and incubated at room temperature for 1 h, 30 min, and 15 min, respectively. The plates were washed four times with a 1× wash buffer between each incubation procedure. The last step was performed in the dark, and then the reaction was stopped by adding 100 µL of stop solution; the absorbance was immediately read at 450 nm and 570 nm on a benchtop microplate reader (Multiskan RC, Thermo Labsystems, Waltham, MA, USA).

3.7. Statistical Analysis

3.7.1. Statistical analysis of LC-MS data

The collected data about the whole serum and extracellular vesicles were reduced and analyzed using statistical methods. Pearson's correlation analysis was used to investigate the outlier samples[118], contaminating proteins (cytokeratins), and proteins with missing values were excluded from the proteomic data[119]. Data were log-transformed to reduce skewness and increase linearity[120]. Cohen's d effect size was calculated to measure the difference between the protein intensity means, and outcomes in two different groups. The formula of Cohen's d effect size

$$d = \frac{|\bar{X}_1 - \bar{X}_2|}{\sqrt{\frac{(n_1 - 1)SD_1^2 + (n_2 - 1)SD_2^2}{n_1 + n_2 - 2}}}$$

where X is the mean protein intensity in a given group, SD is the standard deviation and n is the sample size[121,122]. In this study, we say that the effect size should be at least 2. It indicates that the mean of group 1 is at the 97.7 percentile of group 2, and the nonoverlapping area of the two distributions at least is 81.1%[122].

Pairwise ROC analysis allowed us to find those proteins that can separate at least one group from the others[123]. The ROC analysis uses the true positive rate (sensitivity) and the true negative rate (specificity) at various threshold settings. The calculated ROC AUC (area under the ROC curve) values are accepted if it equals 1.

To transform several (potentially) correlated proteins into a (smaller) number of uncorrelated variables, and visualize the dataset, principal component analysis (PCA) with k-means clustering was performed. The goal of PCA is to reduce a large number of correlated variables with a set of uncorrelated principal components. These components can be thought of as linear combinations of the original variables that are optimally weighted and derived from the correlation matrix of the data[124–127]. Homogeneity and completeness scores of the clusters were calculated to measure the performance of k-means clustering[128].

Two-tailed Welch's *t*-test was performed to identify the significantly enriched or depleted proteins in sEV samples. The statistical analyses were performed using the R statistical program (version 3.6.3 with pROC, FactoMineR, factoextra, and ggplot2 packages; Vienna, Austria), Python programming language (version 3.8, Scotts Valley, CA, USA) and Perseus (MaxQuant, Munich, Germany). Values of $p < 0.05$ were considered significant (see Appendix A for more details). GraphPad Prism 8 (San Diego, CA, USA) was used for further data visualization.

3.7.2. Statistical analysis of ELISA data

Before conducting any statistical tests, the MMP-9 level was normalized to the protein content of serum sEV, meaning that the MMP-9 concentration (ng/mL) was divided by the protein concentration of the sEV-enriched isolates (ng/mL) for every sample. The results of all the analyses are notated in parts-per-million (ppm), describing the individual values of MMP-9 in patients.

Outliers from the analyzed groups were always excluded using the ROUT (robust regression followed by outlier identification) method with the Q parameter set to 1%. Then we examined the assumptions of normal distribution utilizing the Shapiro–Wilk test and the homogeneity of variances by using the F test (comparing two groups) and the Brown–Forsythe test (comparing more than two groups).

The MMP-9 ppm concentrations of independent groups and matched samples were compared with Welch's test and the paired t-test, respectively. One-way ANOVA was used to examine differences between more than two groups.

To determine the relationship between continuous variables, linear regression analyses were conducted. To improve linearity in regression, skewed data were logarithmized.

The diagnostic potential of the MMP-9 ppm was evaluated using receiver operating characteristic (ROC) analyses. Kaplan–Meier analyses with log-rank tests were used to compare the overall survival rates of different groups.

The collected data about the MMP-9 content of serum sEV were analyzed statistically using GraphPad Prism 8.3.4 (San Diego, CA, USA).

3.8. In Silico Analysis of LC-MS Data

Protein data derived from the LC-MS were analyzed by the Ingenuity Pathway Analysis (IPA, Qiagen Bioinformatics, Hilden, Germany). Using fold change values, 'Core Analysis' was performed for whole serum and sEV data separately to identify 'Diseases and Functions,' which can be significantly influenced by the described proteomes ($p < 0.05$). After 'Comparison Analysis,' we created heatmaps of the relevant 'Diseases and Functions,' that is, tumor-related and immunological functions showing regulatory differences between the three CNS tumor groups. Activation z-score calculated by IPA indicates the extent and direction of the effect that given proteins have on function/disease.

The selected 10 whole serum proteins and 17 sEV proteins were introduced to custom pathways as well. Then, the 'Connect tool' of IPA was used to reveal the relationships between these molecules, and the 'Grow tool' was applied to search the top ten 'Diseases and Functions' assigned to the 10 whole serum proteins or 17 sEV proteins. Results are displayed in two networks created by the IPA Path Designer.

The confidence level was set to 'Experimentally observed' for all IPA procedures, which enables literature data-based analysis but excludes unproven predictions.

3.9. Data Availability

We have submitted all relevant data of our experiments to the EV-TRACK knowledgebase[129]. EV-TRACK ID: EV200080 and EV230005.

4. Results

4.1. Workflow of the research

Figure 5 illustrates the schematic workflow that covered the entire experimental design employed in our study on whole serum and serum sEV to identify biomarkers in tumors of the CNS. The workflow describes the key steps of the study, starting from the selection of patient cohorts to the complex analysis of proteomic data and MMP-9 levels. Each step includes several additional analyses not shown in this figure. Detailed results are presented in the Results section with tables and figures indicated in the workflow.

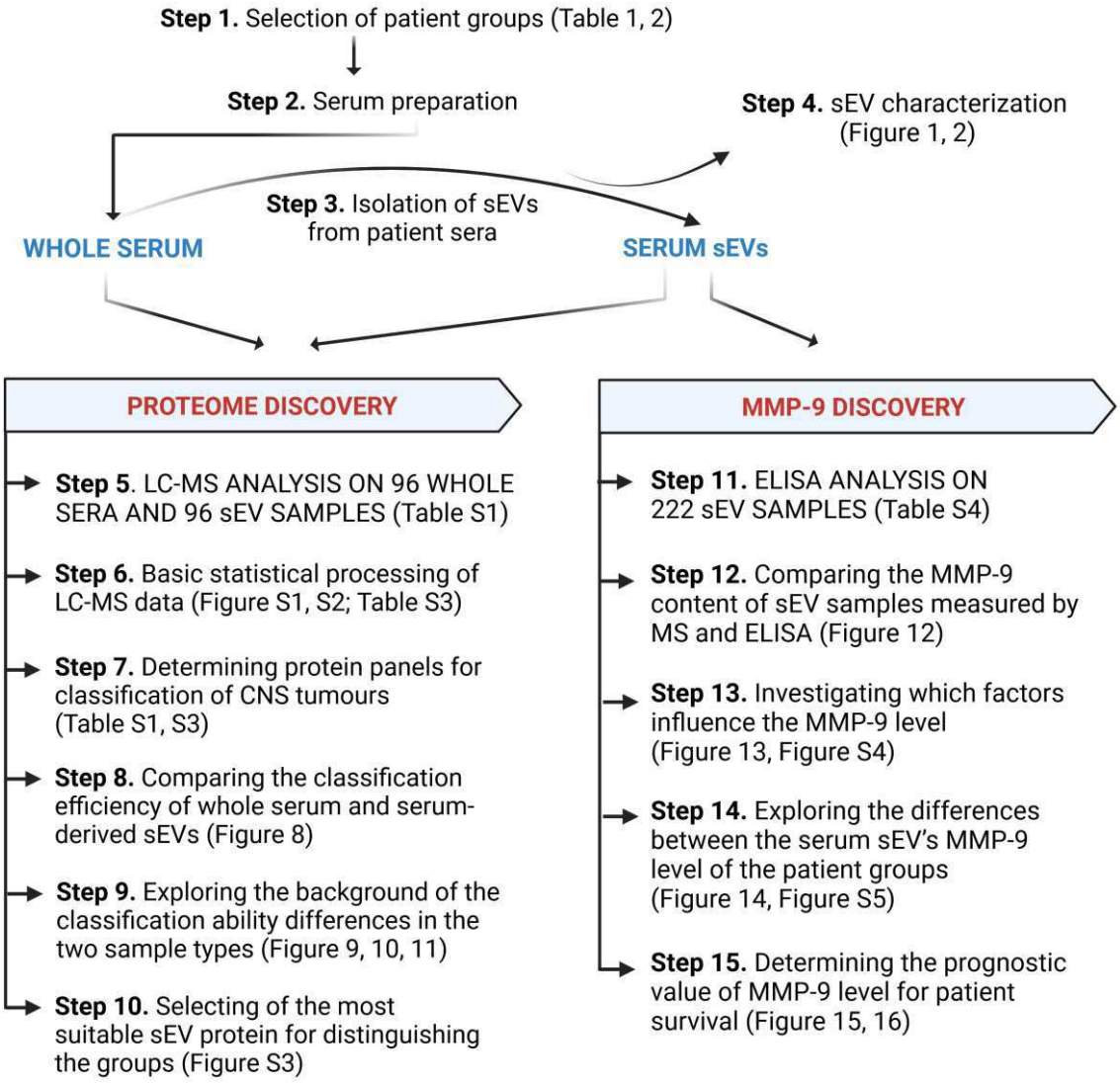

Figure 5. Experimental workflow of the research.
Summarizing the steps, tables, and figures.

The initial objective of these investigations was to identify biomarkers for CNS tumors that were non-invasive, reliable, and easily implementable in clinical practice. For this purpose, four patient groups were established (Step 1) and **blood samples** were collected by the Department of Neurosurgery at the University of Debrecen and provided to our group for processing, vesicle isolation, and subsequent analyses.

Following the serum preparation (Step 2)**, sEV isolation** (Step 3), and detailed **characterization** (Step 4), 96 whole sera and 96 serum sEV samples were introduced to the **proteomic analyses by LC-MS** (Step 5) to address the aforementioned issue. For the LC-MS measurements, individual samples in each group (n = 24) were arranged into 4 pools to eliminate individual variances, reduce sample number, shorten the time, and reduce the need for materials.

After constructing the spectral library, Pearson's correlation analyses were performed to investigate the outlier samples, contaminating proteins (e.g. cytokeratins), and proteins with missing values to be excluded from the proteomic data. This **data cleaning** is necessary to ensure that irrelevant data do not interfere with the results (Step 6).

Following this basic statistical processing, the up- and down-regulated proteins were discovered using Cohen's d effect size as an indicator of clinically relevant incidence. After that, ROC analysis was used to identify **protein panels**, that can be used for classification (Step 7).

After the protein selection, PCA was performed to visualize the dataset, and K-means clustering was applied to evaluate the **classification efficacy** of the two sample types (Step 8). These analyses led to one of the most important findings of the dissertation.

To investigate the **background of the differences** in the classification efficacy, quantitative and qualitative analyses were carried out, including a two-tailed Welch's t-test on the proteome, and Ingenuity Pathway Analysis on the proteome and the protein panels (Step 9).

We wanted to identify the **sEV protein** that is the **most effective** at distinguishing the groups. Therefore, we performed a multi-ROC analysis on the 17 panel members to determine the one with the highest AUC value (Step 10).

This protein was the MMP-9, therefore, we decided to measure the **MMP-9 content of each serum sEV sample**. Since mass spectrometry is not commonly used in clinical practice, and concentrations are more suitable for determining the selectivity/specificity of the assay, we performed ELISA.

To make sure that the ELISA interprets the same MMP-9 pattern as the LC-MS, we performed ANOVA and correlation analysis on the MMP-9 content measured by the two distinct methods. After confirming the suitability of the new method for group separation, we measured all the **222 sEV samples individually by ELISA** (Steps 11, 12) to investigate the correlation between the MMP-9 level and the clinical data of the patients.

First, we investigated which **factors** may **influence** MMP-9 levels of serum sEV. Hence, we conducted correlation analysis on age, paired t-tests on the time of sampling, and Welch tests on gender, and recurrence, and administered therapy to investigate the factors which might bias the differences between the groups of interest (Step 13).

Once the influencing factors have been identified, all analyses exploring **differences between patient groups** were conducted exclusively on samples obtained prior to surgical resection and therapy administration. Welch's test was used to distinguish between controls and tumorous patients, ANOVA was utilized to compare the different tumor types, and ROC and multiROC analyses were carried out to check the AUC values and the sensitivity/specificity of the tests (Step 14).

In the last step, we aimed to determine whether **MMP-9 levels of serum sEV** correlate with **patient survival.** ANOVA and ROC analyses were performed into the differences in survival time based on MMP-9 levels, correlation analyses were conducted on the connection between survival and MMP-9 level/age, and the possibility of survival was estimated by Kaplan-Meier charts (Step 15).

The comprehensive findings of the aforementioned analyses will be elaborated upon in the following eight subsections.

4.2. Particles isolated from serum show sEV properties

Particles were isolated by differential centrifugation from 222 serum samples of patients with GBM, BM, M, and CTRL. Isolated sEVs were characterized by AFM, TEM, and NTA, as well as by examining characteristic sEV markers (CD81, Alix, CD5L, and calnexin) by WB (**Figure 6**).

AFM and TEM images of sEV isolates display vesicles with diameters within the range of 50–140 nm. The average concentration, mean, and mode diameter of the particles were measured as 2.28×10^{12} particles/mL, 81.35 nm, and 59,82 nm, respectively. CD81, Alix, and CD5L positivity and calnexin negativity were determined.

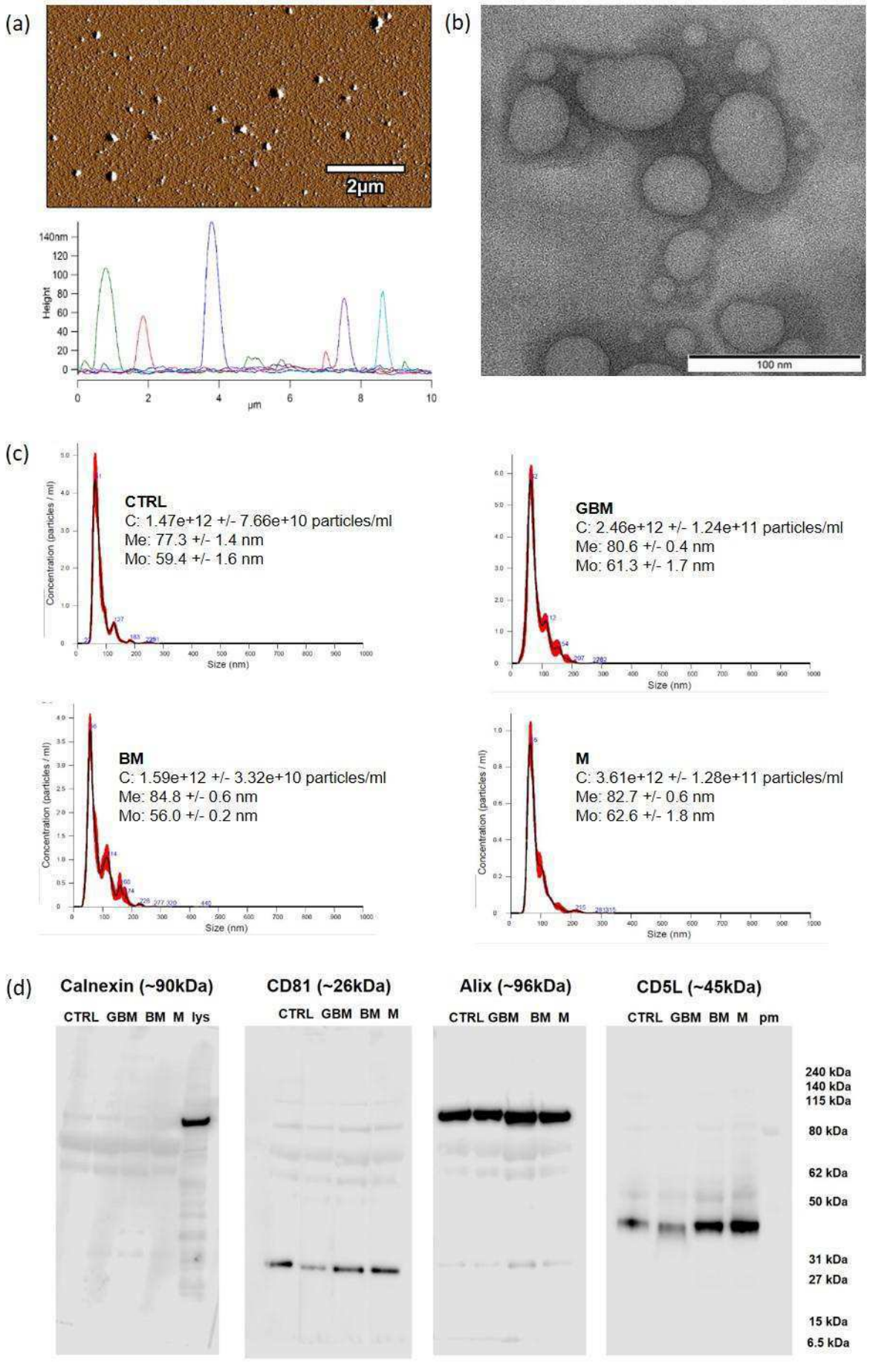
(a)
2µm
140nm
120
100
80
60
40
20
0
Height
0
2
4
6
8
10
µm
(b)
100 nm
(c)
CTRL
C: 1.47e+12 +/- 7.66e+10 particles/ml
Me: 77.3 +/- 1.4 nm
Mo: 59.4 +/- 1.6 nm
GBM
C: 2.46e+12 +/- 1.24e+11 particles/ml
Me: 80.6 +/- 0.4 nm
Mo: 61.3 +/- 1.7 nm
BM
C: 1.59e+12 +/- 3.32e+10 particles/ml
Me: 84.8 +/- 0.6 nm
Mo: 56.0 +/- 0.2 nm
M
C: 3.61e+12 +/- 1.28e+11 particles/ml
Me: 82.7 +/- 0.6 nm
Mo: 62.6 +/- 1.8 nm
Concentration (particles / ml)
Size (nm)
(d)
Calnexin (~90kDa)
CTRL GBM BM M lys
CD81 (~26kDa)
CTRL GBM BM M
Alix (~96kDa)
CTRL GBM BM M
CD5L (~45kDa)
CTRL GBM BM M pm
240 kDa
140 kDa
115 kDa
80 kDa
62 kDa
50 kDa
31 kDa
27 kDa
15 kDa
6.5 kDa

Figure 6. Characterization of serum-isolated particles.
(a) Representative AFM image of the tested samples with a 2 µm scale bar. (b) Representative TEM image of the tested samples with a 100 nm scale bar. (c) The diagrams display the concentration and size distributions of the serum-derived particles of the four main groups measured by NTA presenting the mean +/−95% CI values. (d) The figure shows CD81, Alix, CD5L markers, and Calnexin examined by WB analyses. *Abbreviations: CTRL, control; GBM, glioblastoma multiforme; BM, brain metastasis; M, meningioma; lys, cell lysate; pm, protein marker*; C, particle concentration; Me, mean diameter size; Mo, mode diameter size.)

No statistically significant differences were identified among the patient groups in any of the physical parameters of the isolated particles.

4.3. Serum samples obtained from the four patient groups comprise distinct populations of sEVs

The sEV diversity of the serum samples was also investigated. We used bead-based multiplex EV analysis by flow cytometry to characterize proteins expressed on the surface of the serum-derived sEVs. In the serum-derived sEV samples, we obtained APC fluorescence intensities above the limit of detection for 11 of the 37 sEV proteins. These summary data are mirrored by the mean APC fluorescence intensities of each specific exosome marker CD9, CD63, or CD81 (**Figure 7**).

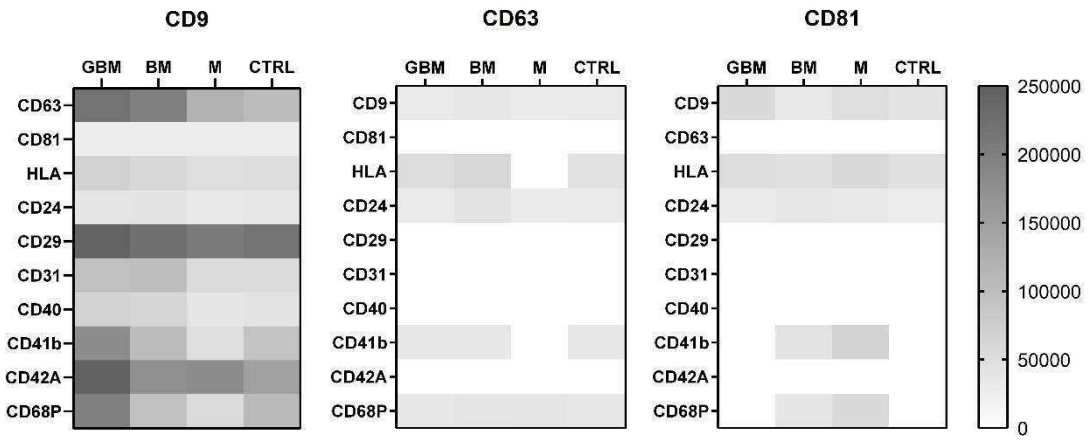

Figure 7. MACSPlex assay of small extracellular vesicle (sEV) samples.
Heat-map representation of the mean APC fluorescence values for the different bead populations detected with anti-CD9, anti-CD63, or anti-CD81 antibodies. Mean intensity values are based on the representative pool, i.e. samples of ten patients in each group. *Abbreviations: CTRL, control; GBM, glioblastoma multiforme; BM, brain metastasis; M, meningioma*

The MACSPlex assay also allowed us to characterize the populations of sEV in our samples by comparing the APC fluorescence intensities of the identified surface proteins. The previously described heat map (**Figure 7**) shows similarities and discrepancies between the patient groups. Beyond the exosomal markers (CD9, CD63, CD81), eight markers, namely HLA, CD24, CD29, CD31, CD40, CD41b, CD42a and CD68p were present in each patient group. The most abundant population was found to be the CD9+ vesicles, all 10 markers were present on their surface. The CD63+ and the CD81+ populations were less abundant and showed marked differences between the patient groups, as only 3-5 markers from the 10 were present on their surface.

Taken together, the MACSPlex data demonstrate that each group contains different populations of sEV. They also provide information about the source of the sEVs, since there were signals suggesting leukocytes (CD24, CD40), cell adhesion molecules (CD29, CD41b), platelet and endothelial cell-related molecules (CD42a, CD62P), and immunoglobulins (HLA, CD31).

The data also show that the co-purified proteins do not interfere with antibody-based strategies for characterizing proteins expressed on the sEV membrane.

4.4. Instead of individual biomarker proteins, a protein panel should be utilized to differentiate between patient groups

We aimed to identify the differences between the four patient groups to reveal the characteristic protein profiles associated with the CNS tumors in point. Using an intensity ratio of >2 or <0.5 with Cohen's d effect size of 2 as a cut-off, we investigated which proteins show reliable intensity difference and which proteins can separate at least one group from the others based on a receiver operating characteristic (ROC) analysis. Moreover, utilizing principal component analysis (PCA) with k-means clustering, we were able to compare the suitability of the two different sample types to distinguish between the CNS tumors in point.

Proteomics analyses by LC-MS were performed on whole serum and sEV samples obtained from patients with GBM, BM, M, and CTRL. Individual samples (n = 24) in each group were arranged into four pools (see **Table 1**) to eliminate individual variances, reduce sample number, shorten the time of LC-MS measurements, and reduce the need for materials. The Data Independent Acquisition (DIA) mode constructed spectral library revealed 311 proteins (see **Table S1**). Based on Pearson's correlation analyses, one of the sEV control samples had to be excluded from further statistical analyses (**Table S2**). After

excluding unreliable proteins, as well as proteins with missing values, a total of 262 proteins remained for the final analysis.

Following basic processing, up- and down-regulated protein discovery resulted in 41 whole serum proteins and 45 sEV proteins. In addition to comparing each CNS tumor group to CTRL, between group differences among the CNS tumor groups were also assessed in the protein selection process. As clinically relevant incidence is an important consideration for selecting the proteins identified, Cohen's d effect size was adopted as an indicator of between-group difference. Cohen's d effect size analysis with a threshold of d >2 yielded 10 and 21 proteins in the whole serum and sEV samples, respectively.

In the ROC analyses 10 whole serum proteins (MMP-9, HSPB1, CASP14, HBG1, IGHG4, DEFA1, VWF, HNRNPA1, S100A8, TLN1) and 17 sEV proteins (MMP-9, HSPB1, CASP14, HBG1, FGB, GGCT, PF4, S100A7, FN1, ANPEP, FLG2, HSPA8, IGLL1, MMRN1, S100A14, SBSN, SPRR2E) were found to meet the AUC = 1 selection criteria. **Table S3** includes the UniProt ID, Gene symbol, ratio of intensity means >2 or <0.5, and Cohen's d effect size >2 parameters for the selected proteins. The two sample groups shared four significantly altered proteins (highlighted in **Table S3**), namely MMP-9, CASP14, HBG1, and HSPB1.

4.5. Serum sEV is more suitable to distinguish CNS tumors than whole serum

Following protein selection, PCA was performed to visualize the dataset, where several potentially correlated proteins were projected into a smaller number of variables. K-means clustering on the whole serum PCA biplot resulted in three inhomogeneous or incomplete clusters. Calculated cluster homogeneity and completeness scores are 0.56 and 0.73, respectively. In contrast to whole serum samples, the clustering of sEV samples formed homogeneous and complete clusters, with homogeneity and completeness scores of 1. The results of the PCA analyses and k-means clustering indicate considerable differences between the whole serum and sEV samples (**Figure 8**). We found that the accuracy of distinguishing between various CNS tumors can be increased using a protein panel from serum sEV, compared to analyzing whole serum samples.

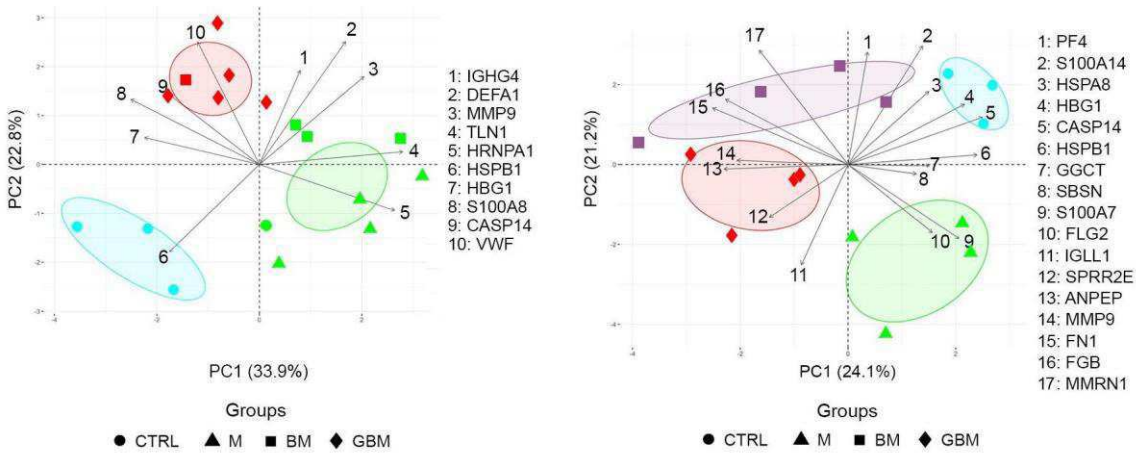

Figure 8. Principal component analysis (PCA) and k-means clustering on the protein panels*. The figure shows the PCA plots and protein panels of whole serum (left) and sEV (right). X and Y axes of PCA biplots show principal component 1 (PC1) and principal component 2 (PC2) with explained variances. Arrows represent the coefficients of each protein for PC1 versus the coefficients for PC2, showing the significance of each protein in influencing PCs. Different dots represent the 4 patient groups. Colors indicate the clusters formed by k-means clustering; ellipses indicating the 95% confidence interval were constructed around the barycenters of the clusters.*

4.6. Quantitative changes of the proteome may affect the suitability of sEV samples to provide biomarkers for CNS tumors

Statistical comparison of the proteome of sEV and whole serum samples was performed to reveal quantitative differences affecting the suitability of different sample types to provide biomarkers for CNS tumor status monitoring. Pairwise statistical comparison (Welch's test) was used to identify proteins significantly enriched or depleted in sEV samples compared to whole serum samples (**Figure 9**). Sixty-five proteins were found to be significantly enriched in sEV samples, while 129 proteins were significantly depleted ($p < 0.05$). Using our sEV purification protocol detailed in the Methods section, we obtained a uniform particle size range of sEVs but the magnitude of quantitative changes in the sEV versus whole serum proteome suggested the possible presence of lipoprotein and serum protein contaminations. The level of apolipoproteins was decreased in sEV-enriched samples (sEV/serum mean ratio is 0.66), however, this fraction could not be completely eliminated. Besides, well-known high-abundance serum proteins (e.g., ALB) dominated the protein content of sEV-enriched samples too. However, the enrichment of non-tissue specific (ITGA2B, ITGB3, LGALS3BP), epithelial cell (CD5L), and platelet related (STOM, TSPAN9) EV marker proteins[130] confirms sEV enrichment (sEV/serum mean ratio is 26.58), while it also demonstrates the presence of sEVs produced during clotting.

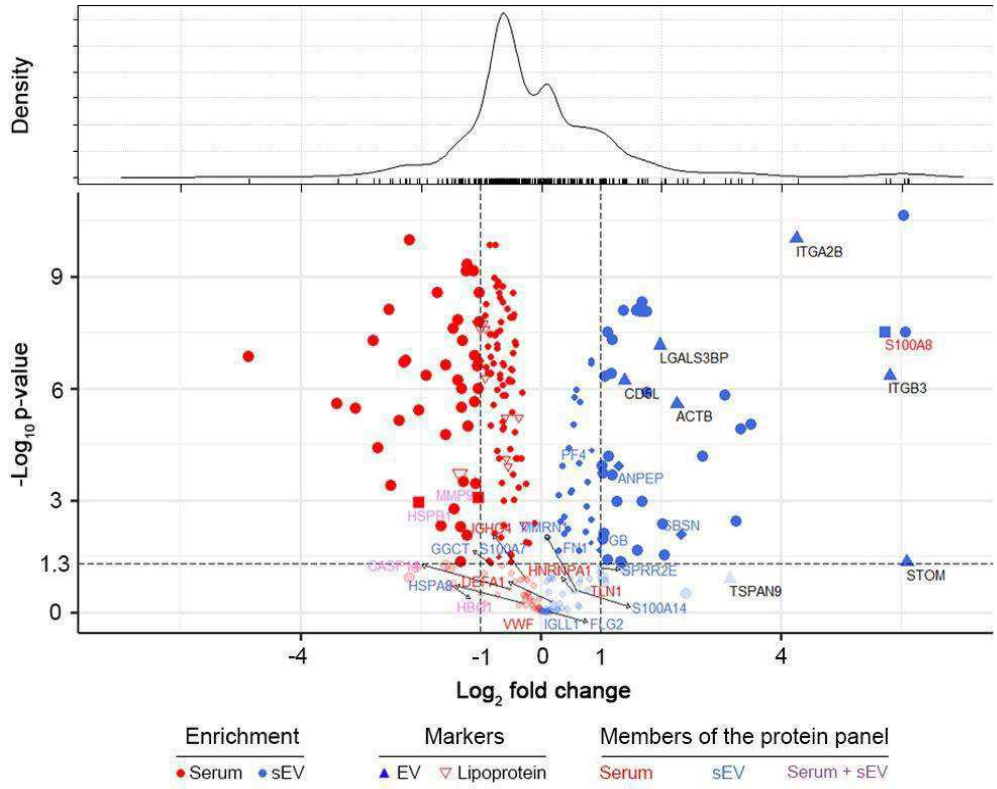

Figure 9. Quantitative comparison of the proteome of serum sEV and whole serum samples. *The volcano plot represents the observed changes in average MS intensities in paired sEV vs. serum comparisons. Protein enrichment is marked with red and blue colored symbols in whole serum and serum sEV, respectively. Lipoproteins (empty red upside-down triangles), elements of our whole serum protein panel (red letters, square symbols), sEV protein panel (blue letters, diamond symbols), and common members of the two protein panels (purple letters) are highlighted. Values of –log (p) were obtained from paired Welch's test in sEV/serum comparisons. Density estimation of log2 (fold change) values is shown on top.*

Among the 17 proteins of the sEV marker panel described in Section 2.2, only 6 were significantly enriched in the sEV samples and 5 of the 10 proteins comprising the specific serum panel had higher abundance in the whole serum (**Figure 9**). These findings suggest that the better suitability of sEV-enriched samples to serve as a biomarker source is not explained by a total increase in the abundance of specific proteins. (Detailed proteomics findings, protein annotation, and sEV enrichment data are available in **Table S1**).

Additional sample processing (sEV isolation) may introduce higher technical variance in the case of sEV samples, thus it may reduce the analytical suitability of this sample type. However, our analysis revealed a similar level of variance for proteins quantified in each sample type median coefficients of variation within each patient group were in the ranges of

20.78%–23.87% for sEV and 20.21%–24.45% for serum samples (see **Figure S1** for CV distributions).

4.7. Biological background might be responsible for the increased suitability of sEV samples in distinguishing CNS tumors

To gain insight into the biological background of the obtained proteomics data, IPA was applied.

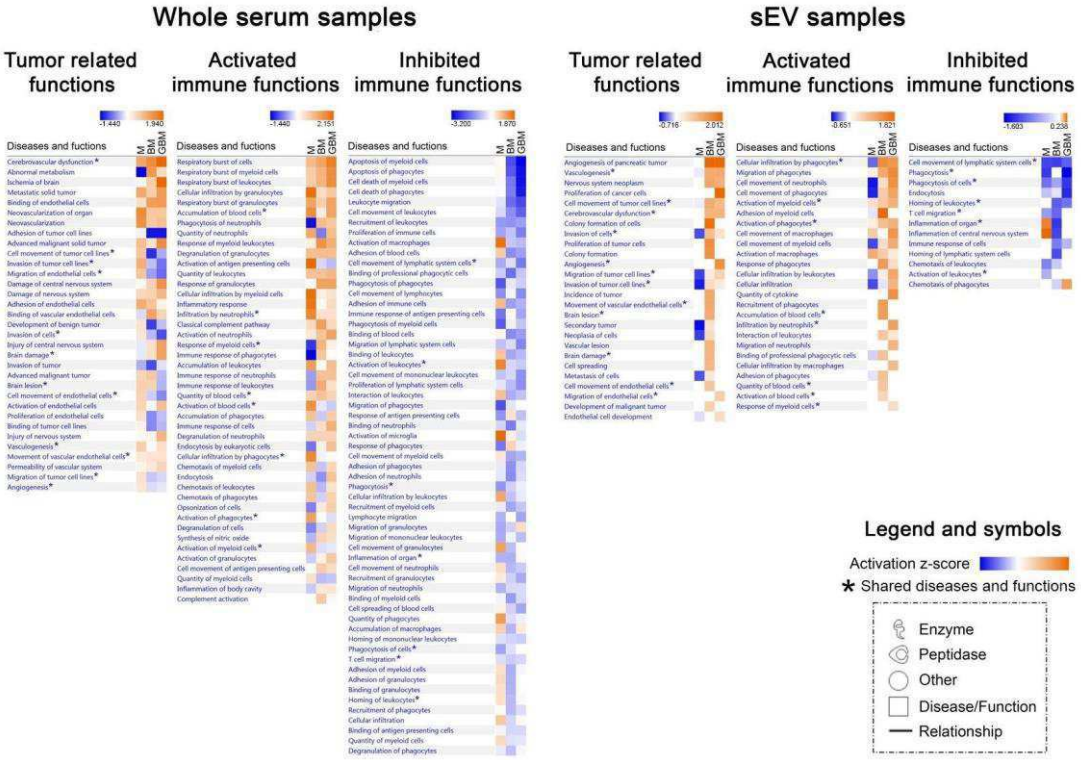

Figure 10. Relevant diseases and functions are based on the proteome of different patient groups. *Heatmaps of whole serum (left) and sEV (right) show relevant 'Diseases and Functions' in three separate panels related to systemic and tumor-related functions, as well as activated and inhibited immune functions. Z-score indicates activation or inhibition rates of the relevant 'Diseases and Functions' in the three tumorous patient groups compared to the control group. * symbol indicates the shared diseases and functions in whole serum and serum sEV.*

We performed 'Core Analyses' for whole serum and sEV data separately, yielding a list of significantly influenced 'Diseases and Functions' in each patient group ($p < 0.05$). Using 'Comparison Analysis,' we were able to develop heatmaps covering the relevant systemic and tumor-related functions, as well as the activated or inhibited immune functions (**Figure 10**). Regarding whole serum samples, many of the significantly influenced functions identified are related to CNS involvement and active immune regulatory processes but the

patient groups are not clearly distinguished on the heatmaps (**Figure 10**, left panels). In contrast, on two of the three sEV proteome-based heatmaps M was separated from the malignant tumor groups (**Figure 10**, right panels), where tumor progression-related functions (e.g., angiogenesis, proliferation, and migration of tumor cells) were detected to be highly activated and the activated immune functions (e.g., cell movement or activation of myeloid cells) predominate over inhibited immune functions (e.g., phagocytosis).

Next, we attempted to specify the common biological role of the characteristic protein profiles identified. Therefore, we elaborated two networks containing the selected 10 and 17 proteins identified based on whole serum and the sEV data, respectively (**Figure 11**). Using the 'Grow tool,' the top ten influenced 'Diseases and Functions' were integrated into the networks. In the case of the whole serum network (**Figure 11**, left panel), nine different related 'Diseases and Functions' were identified, including viral infection, apoptosis, necrosis, or cell movement of phagocytes and myeloid cells, and only one was cancer-related. In contrast, the top ten influenced diseases identified on the sEV network based on the sEV panel (**Figure 11**, right panel) were all tumor-associated, suggesting their potential involvement in the pathophysiology of cancers.

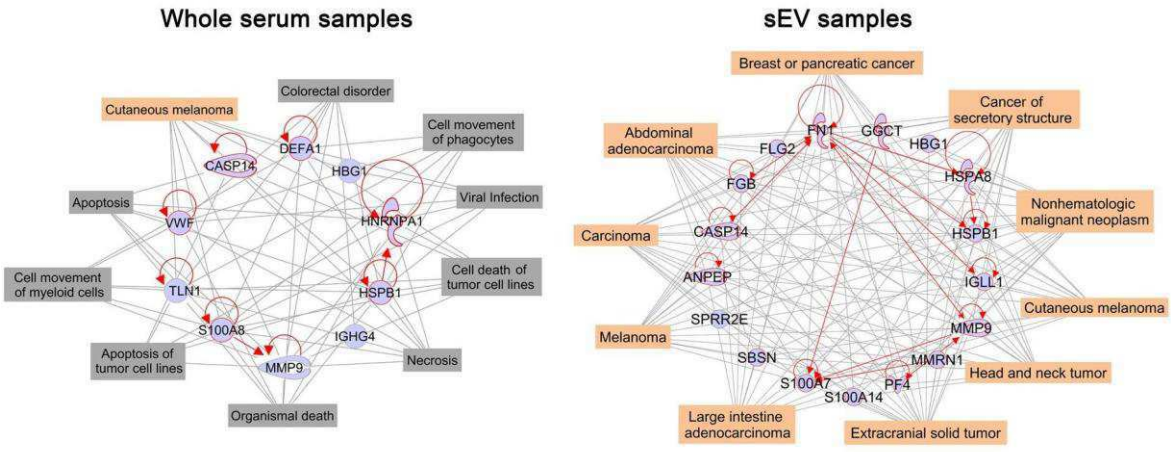

Figure 11. Related diseases and functions of the selected proteins.
Networks display the selected 10 whole serum or 17 sEV proteins (blue symbols) and their relationships (red lines). The top ten related 'Diseases (highlighted in orange symbols) and Functions (highlighted in gray)' are connected by gray lines.

4.8. Matrix metalloproteinase-9 is the most promising member of the sEV protein panel determined for separating the patient groups

Previously, LC-MS analysis was performed on 96 sEV samples. As a result of the statistical analyses (see 4.2.), a 17-membered protein panel was constructed from the

identified proteins which were able to separate the four groups with 100% efficacy. After that, we investigated which of the 17 sEV proteins was the most suitable for distinguishing patients, and found MMP-9 to be the most significant (*p = 0.0065*, multi ROC AUC = 0.86) (**Figure S3)**.

Following the candidate selection, the MMP-9 content of the 96 sEV samples was measured by ELISA, and the MMP-9 intensities (from LC-MS) were compared with the averaged MMP-9 concentrations (from ELISA) of the six-sample-pools to ascertain that ELISA is also capable of distinguishing the groups *(p = 0.0335*, multi ROC AUC = 0.83*).* The correlation analysis confirmed that the MMP-9 concentrations measured by ELISA were highly comparable to LC-MS measurements (r = 0.7264; p = 0.0022) (**Figure 12**), so it can be applied for further investigations.

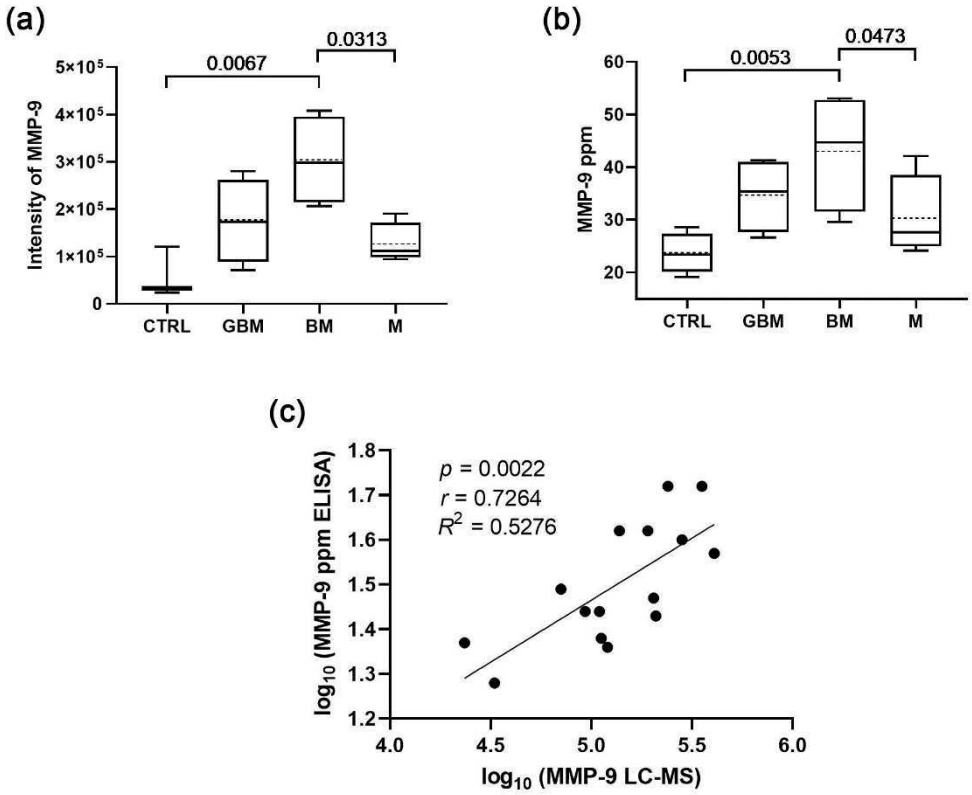

Figure 12. Comparison of the sEV MMP-9 content measured by ELISA with the LC-MS results. *(a) MMP-9 levels of serum sEV based on LC-MS data (boxplot shows median with interquartile range, mean with the dotted line, error bars range from the 5th–95th percentiles (nCTRL = 3, nGBM = 4, nBM = 4, nM = 4). (b) MMP-9 levels of serum sEV based on ELISA data (nCTRL = 4, nGBM = 4, nBM = 4, nM = 4). Dotted lines indicate mean values. (c) Correlation between the MMP-9 levels measured by LC-MS and ELISA.*

Therefore, we aimed to perform ELISA measurements on the larger cohort; the MMP-9 concentrations can be found in **Table S3**. The large sample size allowed us to investigate factors influencing the MMP-9 level and is suitable for examining whether there was a measurable, significant difference in the sEV MMP-9 level associated with different diseases and patient survival outcomes. Measuring the MMP-9 concentrations of serum EVs instead of MMP-9 intensities enabled the determination of the cut-off values required in the clinic, as well as the specificity and sensitivity of the test.

4.9. Several factors might influence the MMP-9 level of the serum sEV

Performing comparative studies between different tumors requires examining what factors (e.g. age, gender, surgical resection, recurrence, and therapy) may influence MMP-9 levels of serum sEV (**Figure 13**).

The MMP-9 level was normalized to the total protein content of serum sEV, meaning that the MMP-9 concentration (ng/mL) was divided by the protein concentration of the EV-enriched isolates (ng/mL) for every sample. The results of all analyses are notated in parts-per-million (ppm) describing the individual values of MMP-9 in patients (**Table S3**).

Age and gender analyses were carried out in the control group, eliminating the possible MMP-9-modifying effect of any tumor disease. Correlation analysis revealed that there is no distinct relationship between age and MMP-9 levels (**Figure 13a**). The MMP-9 level of sEVs shows no significant difference between male and female patients, as determined by Welch's test (**Figure 13b**). Based on these findings, further data analyses were conducted regardless of the age or gender of the patients.

Examining the effects of surgical resection on the MMP-9 level of serum sEV, paired t-tests were completed in the GBM and BM groups (**Figure 13c,d**, respectively). The MMP-9 levels were similar ($p = 0.1843$, fold change = 15%) before and after the surgical resection in the case of primary GBM patients, while BM samples showed a marked increase ($p = 0.0065$, fold change = 209%) after resection.

Further examination of preoperative GBM samples found a distinct difference between the original tumor and the recurrence based on MMP-9 levels of serum sEV (**Figure 13e**), and the recurrence showed a lower level of MMP-9 on average ($p < 0.0001$).

Determining the influence of the administered therapy, MMP-9 levels were also compared based on whether or not GBM patients had received treatment at the time of sampling. Our result ($p < 0.0001$) indicates that therapy might decrease the MMP-9 levels of the circulating sEVs (**Figure 13f**).

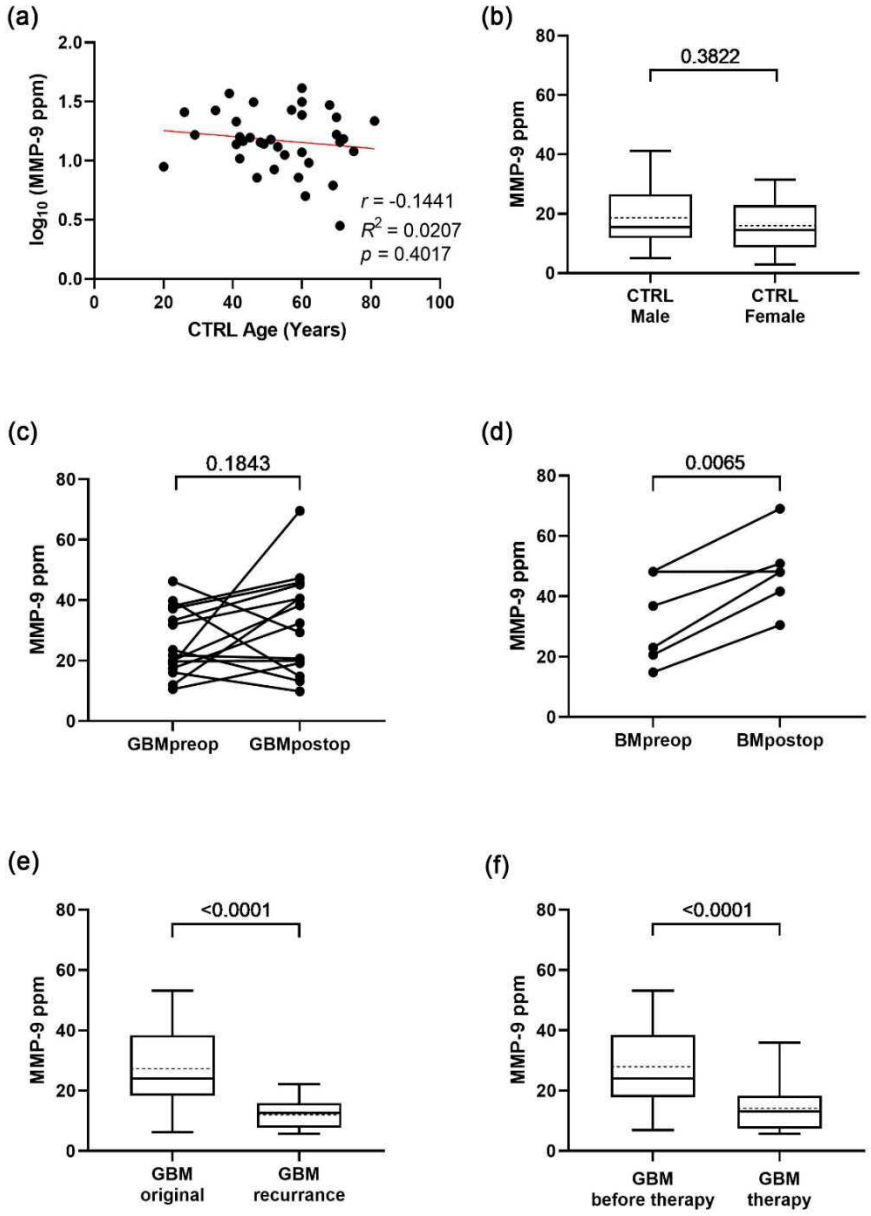

Figure 13. Factors influencing MMP-9 level of serum sEVs.

(a) Relationship between age and MMP-9 levels in the control group. (nCTRL = 36). (b) MMP-9 levels of the two genders in the control group (boxplots show the median with interquartile range, mean with dotted line, error bars range from the 5th–95th percentiles; nCTRL male = 16, nCTRL female = 20). (c,d) Changes in individual patient's MMP-9 levels before and after surgical resection for the GBM and BM groups, respectively (nGBM preop-postop = 14, nBM preop-postop = 6). (e) MMP-9 levels of serum sEV regarding the original tumor and the recurrence in the GBM group prior to surgical resection (nGBM original = 52, nGBM recurrence = 14). (f) MMP-9 levels in the GBM group according to treatment status (nGBM before therapy = 52, nGBM therapy = 15).

In addition to the paired t-test shown in **Figure 13c,d**, unpaired t-tests (Welch's tests) were performed on all primary and secondary GBM samples, as well as on all BM samples to determine the effect of surgical resection on a broader cohort (**Figure S4**). First, all the preoperative and postoperative samples were evaluated; then, subsequent exclusions were made for individuals who had relapsed or received therapy. The unpaired t-tests on primary GBM and BM samples (**Figure S4a,c**) yielded the same results as the paired t-tests (**Figure 4c,d**); however, for the secondary GBM samples, the significant differences were erased when the recurrent or treated samples were excluded from the analysis (**Figure S4b**).

Based on our findings, we can conclude that in addition to the disease types, surgical resection, recurrence, and therapy might influence the MMP-9 level of the serum sEV. Due to these findings, all subsequent analyses were conducted exclusively on samples obtained prior to surgical resection and therapy administration.

4.10. MMP-9 level of serum sEV differs in various CNS tumors showing a positive correlation with tumor aggressiveness

Further statistical analyses were performed to identify if there was a difference between the MMP-9 levels of the patient groups (**Figure 14**).

As a first step, Welch's test was used to compare the control group with all the tumor patients (**Figure 14a**). Based on ROC analysis, the two groups were significantly distinguishable ($p = 0.0002$) using a cut-off point of 16 MMP-9 ppm with 74% sensitivity, 61% specificity, and an AUC of 0.70 (**Figure 14b**).

The tumor patients then were divided into M, GBM, and BM, and we found that the differences remained significant between controls and malignant tumors, as well as between the benign and malignant tumors (**Figure 14c**). The separate comparison resulted in increased specificity, sensitivity values, and AUC scores in the case of control-malignant tumor comparisons at the expense of control-benign comparisons (**Figure 14d**).

In the last step, the patients were divided into further subgroups based on histopathology. In the subgroup analysis, primary and secondary GBM, patients with grade I and II meningiomas, and brain metastases from patients with adenocarcinoma and carcinoma planocellulare were distinguished. The detailed results are presented in **Figure S5**. The comparisons of the patient groups showing significant differences in MMP-9 levels resulted in AUC scores up to 0.77.

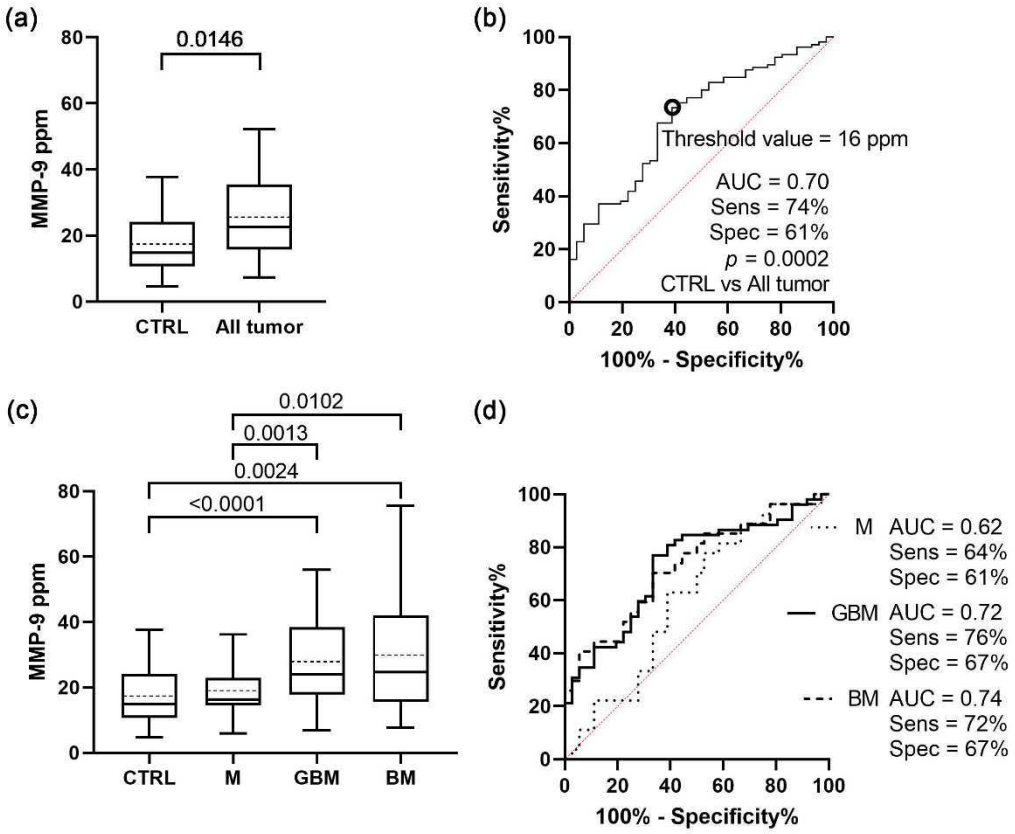

Figure 14. Comparative analyses of MMP-9 level of serum sEV on the four main groups. *(a) The graph shows the MMP-9 level of the control group comparing all the tumor patients (median with interquartile range, mean with the dotted line, error bars range from the 5th–95th percentiles; nCTRL = 36, nAll tumor = 105). (b) ROC curves for exploring the differences between the MMP-9 level of the control group and all the tumor patients (nCTRL = 36, nAll tumor = 109). (c) The diagram shows the MMP-9 level of serum sEV among the four patient groups (nCTRL = 36, nM = 27, nGBM = 52, nBM = 27). (d) ROC curves for comparing the three tumor groups to controls (nCTRL = 36, nM = 27, nGBM = 52, nBM = 27).*

Our data indicate that patients with malignant, but not benign brain tumors can be distinguished from CTRL patients based on the MMP-9 level of serum sEV, and that the MMP-9 level of serum sEV differs between CNS tumor types, showing a positive correlation with tumor aggressiveness.

4.11. The MMP-9 level of serum sEV might be a prognostic marker for overall survival in glioblastoma patients

After comparing the patient groups, we aimed to determine whether MMP-9 levels of sEV correlate with disease progression/patient survival. To assess the prognostic value of MMP-9 levels in serum sEV, we analyzed the preoperative serum samples from 27 GBM patients. Patients in this study were not administered any treatment at the time of sampling.

To reveal the prognostic value of serum sEVs' MMP-9 level on survival, subjects were divided into three groups based on their survival time (short-, medium- and long-term) using 0–2, 3–8, 10–23 months as the cut-offs (**Figure 15a**). Long-term survival was found to be associated with a significantly lower MMP-9 level compared to the MMP-9 levels of the other two groups (**Figure 15b–d**). These differences represent a high specificity and sensitivity of 80–89% at a threshold of 28 MMP-9 ppm, and AUC values of 0.83–0.87 in ROC analyses allow efficient distinction of these survival groups.

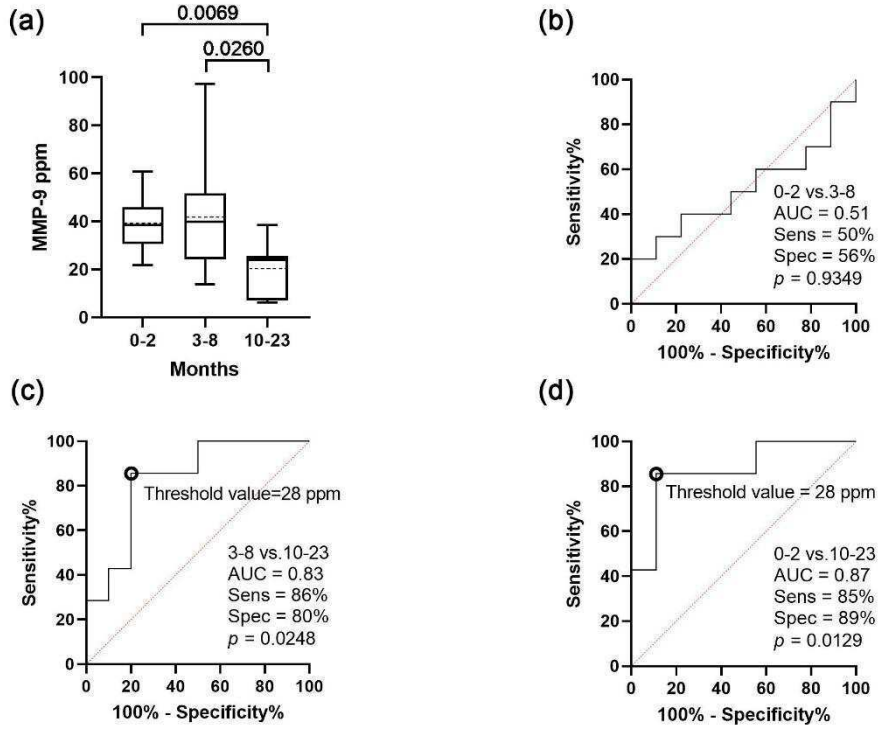

Figure 15. Establishing the critical MMP-9 level of serum sEV as a function of survival time. *(a) Differences among the short-, medium- and long-term survival based on MMP-9 level of serum sEV of GBM patients (median with interquartile range, mean with dotted line, error bars range from the 5th–95th percentiles, dotted lines indicate mean values). (b–d) Receiver operating characteristic (ROC) curves for comparing the short- (0–2 months), medium- (3–8 months), and long-term (10-23 months) survival groups (threshold values of the group-membership score are marked with black circles).*

These results suggest that there should be a correlation between the MMP-9 level of serum sEV and the probability of survival, so we performed an analysis where we observed that lower survival time was associated with higher MMP-9 levels (**Figure 16a**). To determine the extent of the influencing effect of MMP-9 levels on survival, patients were separated into two groups, with the previously established threshold of 28 ppm. Based on the Kaplan–Meier chart, patients with low MMP-9 level (<28 ppm) presented with a

significant survival benefit (HR 2.401, 95% CI 1.095 to 5.261, p = 0.0063), which represents an eight-month increase in the median survival (**Figure 16b**).

The probability of survival also decreased with age (**Figure 16c**); therefore, we repeated the examination with a cut-off of 65 years. According to the Kaplan–Meier chart, patients under the age of 65 had a five-month increase (HR 2.037, 95% CI 0.8524 to 4.869, p = 0.0340) in median survival (**Figure 16d**). It is crucial to note that age and MMP-9 level are independent (see **Figure 13a**); we can conclude that the MMP-9 level of serum sEV may influence survival regardless of age.

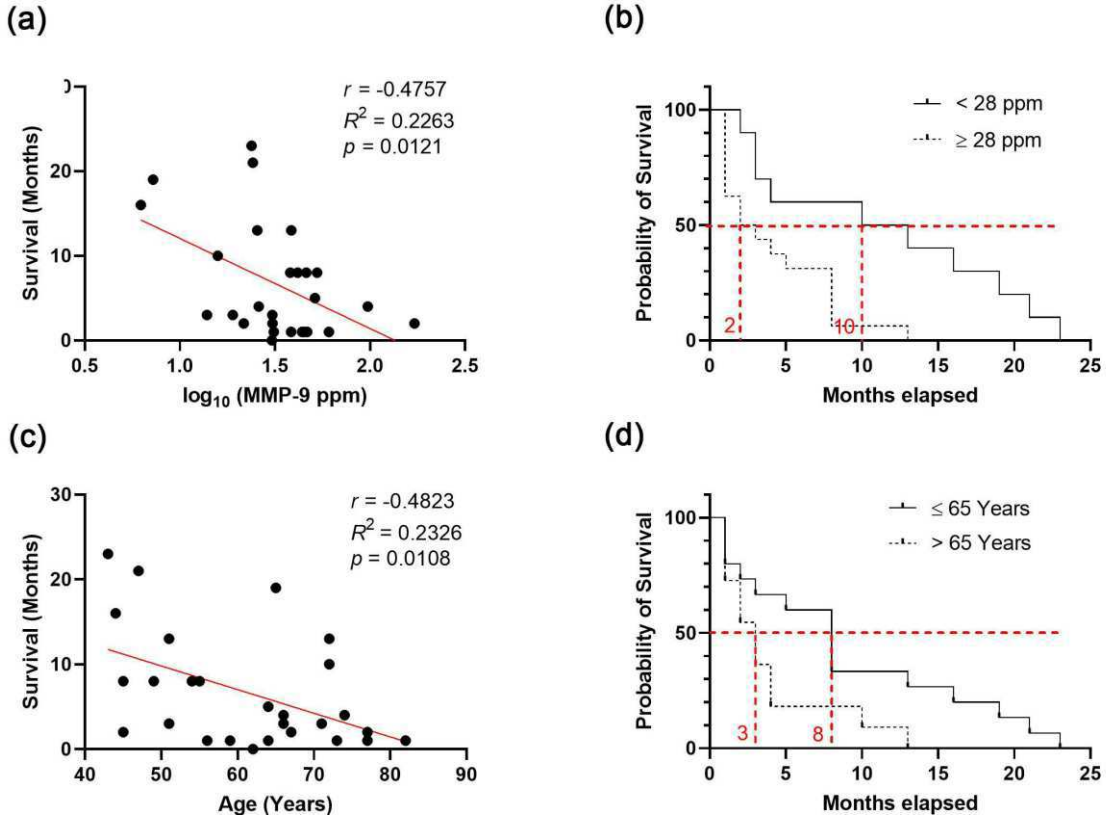

Figure 16. Investigation of vesicular MMP-9 concentration-dependent survival in GBM patients. *(a) Correlation between MMP-9 level and survival in the GBM group (nGBM = 27). (b) Overall survival according to low and high (n < 28 ppm = 10 and n ≥ 28 ppm = 17) MMP-9 levels. (c) Relationship between age and survival in the GBM group (nGBM = 27); (d) Overall survival according to the age (n ≤ 65 years = 16 and n > 65 years = 11).*

To summarize the main findings, analysis of samples taken prior to surgical resection and the administration of therapy revealed a negative correlation between higher vesicular MMP-9 levels and survival, and long-term (10–23 months) survival was found to be associated with low vesicular MMP-9 levels (<28 ppm). Our results support that the high level of MMP-9 in serum sEV might be a negative prognostic marker of the probability of survival in GBM patients.

5. Discussion

5.1. Small extracellular vesicles isolated from serum may serve as signal-enhancers for monitoring CNS tumors

Our investigations aimed to identify protein markers for liquid biopsy-based diagnosis, prognosis, and monitoring of CNS tumors utilizing patient-derived sera and serum-derived sEVs.

Covering the most common CNS tumors, we analyzed a total of 222 serum samples of patients with GBM, BM, M, and controls. Particles were isolated by differential centrifugation from serum samples, the isolated sEVs were characterized by AFM, TEM, and NTA, as well as by examining sEV markers (CD81, Alix, CD5L, and calnexin) by WB. As the quantitative description of the isolation efficiency is required for the proper interpretation of the analytical results[131], we provided a detailed description of the sEV/serum mean ratio of sEV-marker proteins, marked the remained contaminants (high-abundance serum proteins and lipoproteins), and also submitted all relevant data from our experiments to the EV-TRACK knowledgebase[129].

Blood is the most commonly used body fluid for the collection and study of EVs[132]. However, utilizing serum as a source of EVs introduces numerous challenges. For example, there is a lack of established serum preparation protocol tailored for EV research[133]. It should be taken into account, that a significant proportion of EVs may be eliminated during coagulation and that blood components such as platelets may also release vesicles during clotting[134]. Beyond previous ones, the co-purification of proteins[135] and lipoprotein particles[136] in EV isolation methods is also a common and well-known challenge[130,137]. Although we achieved only medium purity and recovery of serum sEVs with the differential centrifugation method, our findings support that even an sEV enrichment may be appropriate to enhance the analytical applicability of serum samples for cancer monitoring.

We demonstrated that serum samples obtained from the four patient groups comprise distinct populations of sEVs. We also provided some information about the source of the sEVs, since our results suggested the presence of leukocyte sEVs (CD24, CD40), cell adhesion molecules (CD29, CD41b), platelet and endothelial cell-related molecules (CD42a, CD62P), and immunoglobulins (HLA, CD31).

The cellular origin of serum EVs has been widely studied using detection methods, such as electron microscopy[138], and flow cytometry[139]. Blood EVs are mainly derived from blood cells and to a lesser extent from endothelial cells, and the cells that line the inside of the blood vessels. In addition, low levels of EVs from tissues and organs may be present[140,141], and EVs derived from cancer cells are indeed a rare population[142,143] in the blood. Therefore, it is difficult to find reliable information on the tissue source of blood EVs. Although the cell sources of non-blood cell-derived EVs are barely known, it is generally accepted that EVs vary depending on pathological states[133,111].

We aimed to identify the differences between the four patient groups to reveal the characteristic protein profiles associated with the CNS tumors in point. Using an intensity ratio of >2 or <0.5, Cohen's d effect size of 2 as a cut-off, and AUC = 1 from ROC analysis as selection criteria, we investigated which proteins can separate at least one group from the others. Our research revealed that in order to distinguish between patient groups, it is more effective to employ a protein panel as opposed to a single biomarker protein.

Numerous ongoing research aim to identify non-invasive biomarkers for various types of cancer to monitor a broad range of malignant diseases[144,145]. However, studies on CNS tumors have halted at the initial phase due to several reasons, including (1) the regulatory function of the BBB[108], (2) the presence of molecules released into the blood from other sources[109], and (3) possibly because of the intratumoral heterogeneity of tumor tissues[110,146]. These issues hinder attempts to use a single biomarker to diagnose and monitor CNS tumors. To improve efficiency, some research groups have decided to use serum biomarker panels instead of a single marker to distinguish between diseased and healthy groups. Usually, a panel consists of three or four proteins[147–153], although some may contain more than ten[154–157]. Our research supports the latter approach, as successful differentiation between patient groups was only achieved when using a protein panel consisting of 10-17 members. Using this sEV protein panel, we were able to discriminate not only between the tumorous and control patients but between four different patient groups, pointing the way toward the establishment of a general CNS biomarker panel.

Following protein selection, PCA and k-means clustering were used to compare the potential of the established protein panels in tumor classification. Our study revealed that the utilization of a serum sEV protein panel provides a more accurate way of differentiating among different types of CNS tumors than using the protein panel of whole serum samples.

sEVs offer several advantages over soluble proteins in serum for biomarker research. Every cell releases sEVs in relatively large amounts, including tumor cells and immune cells activated in the presence of disease[158,159]. The molecular cargo is selectively loaded into sEVs, thus it reflects the physiological and pathological state of the donor cells[111,160]. sEVs can cross the BBB[161], and the molecular content they carry is stable in biofluids due to the lipid membrane bilayer[162]. These properties make sEVs exceptionally suitable for liquid biopsy. There is increasing evidence, that serum sEV proteins can serve as reliable biomarkers for cancer detection and cancer type determinations[68,29]. However, the effectiveness of the blood-based and sEV-based biomarkers has not been compared. To the best of our knowledge, we are the first group to quantitatively compare the proteome of whole serum and serum-derived sEVs[163]. Our findings confirm the significance of sEVs in differentiating CNS tumors and underline their enhanced capability in categorizing CNS tumors compared to the whole serum.

We uncovered that quantitative changes and biological background might be responsible for the increased suitability of sEV samples in distinguishing CNS tumors.

On one hand, sEV enrichment increased the relative abundance of proteins present in higher concentrations within sEVs and decreased the suppressing effect of the uninformative protein fraction released from sources not specific to the target disease. The increased signal-to-noise ratio was beneficial for the quantitative LC-MS analysis of such proteins.

On the other hand, IPA analysis revealed that many functions related to tumor progression, such as angiogenesis, proliferation, and migration of tumor cells, were significantly activated on the sEV proteome-based heatmaps. The IPA heatmaps and networks showed that the proteome of sEV samples may offer more specific information on tumor-associated and immune reactions in patient groups compared to whole serum.

According to Anderson *et al.,* serum sEV is a dual source of biomolecular information on cancer, as it contains the molecules released by cancer cells as well as those released during tumor-specific immune responses[164]. It can therefore be concluded that the differences observed in the serum vesicles isolated from different patient groups may reflect not only tumor-specific processes[165] but also those related to the associated immune responses[166,167].

5.2. MMP-9 level of serum sEV can be used as a prognostic marker for brain tumors

From the determined sEV panel, MMP-9 was found to be the most successful protein in separating the patient groups. To the best of our knowledge, we were the first ones who performed comparative analyses on the MMP-9 content of serum sEVs[168]. We performed ELISA on 222 individual serum sEV samples and compared the results with the gender, age, and clinical history of the patients. Since there is no study on MMP-9 content of circulating vesicles in the literature, our findings can be compared only with blood-based ones.

Numerous studies discuss the clinical significance of serum MMP-9 in inflammation[169], and various cancers, such as breast cancer[170], ovarian cancer[171], colorectal cancer[172,173], lung cancer[174], bladder cancer[175], and melanoma[176]. In connection with CNS tumors, only a few serum MMP-9 investigations have been published with contradictory findings. Hormingo *et al*. found that YKL-40 and MMP-9 could be monitored in patients' serum and help confirm the absence of active disease in GBM[177]. However, after five years, the same group (Iwamoto *et al*.) conducted a longitudinal prospective study of MMP-9 as a serum marker in gliomas, and the larger cohort could not confirm the previous findings[178]. In contrast, Ricci *et al*. found that MMP-9 levels are significantly higher in high-grade glioma, in low- and high-grade meningioma samples, and in metastasis specimens compared to healthy individuals[179]. The latter study on serum MMP-9 levels aligns with our findings based on serum sEVs[179].

In addition to disease status, other characteristics of patients may influence MMP-9 levels in their sera. In our study on serum-derived sEVs, there was no distinct relationship between age and MMP-9 levels, and there was no significant difference between male and female patients in terms of the MMP-9 level. In contrast, Otero-Estévez *et al*. found that MMP-9 was significantly correlated with gender and age when examining the serum of colorectal cancer patients[180].

The surgical resection also can affect the extracellular vesicle concentration and the MMP-9 content of serum/plasma EVs. In our study, the MMP-9 level of serum sEVs were similar before and after the surgical resection in the case of primary GBM patients, while BM samples showed a marked increase after resection. Osti *et al*. measured a significant drop in plasma extracellular vesicle concentration after surgery of glioblastoma patients[181]. Hormigo *et al*. observed that levels of MMP-9 were higher in the sera samples of patients with high-grade glioma after surgery, suggesting that increases in the serum level of this

protein may be associated with brain inflammation and breakdown of the BBB, rather than be a true measure of tumor burden[177].

Determining the influence of the administered therapy, MMP-9 levels have to also be compared based on whether or not GBM patients had received treatment at the time of sampling. Our result indicated that therapy might decrease the MMP-9 level of circulating sEVs. Tabouret *et al*. also reported that urine protein levels of MMP-2 also decreased and were considered to be related to treatment response, although this was not confirmed in an additional patient cohort[182].

Our results support that the vesicular MMP-9 levels are partly influenced by some patient characteristics. Therefore, when conducting comparative analyses, it is crucial to consider factors such as the surgical resection and the administered therapy rather than gender and age.

We discovered that there are significant differences between the vesicular MMP-9 content of the malignant and the benign CNS tumors and the malignant tumor and the control groups. In other words, sEVs of more aggressive tumors had higher levels of MMP-9. Although our findings are indirect, we were the first to investigate this phenomenon at the serum vesicular level.

Numerous studies analyzing tumor tissue[183,184] have demonstrated the relationship between tumor aggressiveness and the MMP-9 levels. The higher level of MMP-9 in aggressive tumors compared to benign ones reflects its multifaceted role in promoting tumor progression. MMP-9 enhances invasion[185], metastasis[86], angiogenesis[186], and resistance to apoptosis[82], as well as modulating the immune response[186]. These activities contribute to the aggressive behavior and poor prognosis often associated with high MMP-9 expressing tumors. Our research on sEVs has led us to the same conclusion. However, a single blood test is sufficient to measure the MMP-9 content of serum vesicles eliminating the need for invasive tissue biopsies through the skull.

In our sEV-based study, a negative correlation was revealed between higher MMP-9 levels and survival, and the long-term (10–23-month) survival was found to be associated with a low MMP-9 level. We have been able to establish a threshold of 28 ppm to determine the patient's probability of survival. Our results support that the high level of MMP-9 in serum-derived sEVs might be a negative prognostic marker of the probability of survival in GBM patients.

Only a few studies have addressed the relationship between MMP-9 and survival in CNS tumors. According to Hormigo *et al*. MMP-9 can be monitored in patients' serum and help confirm the absence of active disease in glioblastoma, but serum MMP-9 cannot be used as a predictor of survival[177]. In Iwamoto's serum-based longitudinal prospective study, MMP-9 was not a clinically relevant prognostic marker for survival. Longitudinal increases in serum MMP-9 were weakly associated with shorter survival in patients with glioblastoma, but after adjusting for age, extent of resection, and performance status, they were not independently associated with survival[178]. In contrast, Jiguet-Jiglaire *et al*. tested patients with recurrent glioblastoma prior to treatment and found that decreased plasma levels of MMP-9 were associated with increased overall survival[88]. These serum-based studies have conflicting results, the latter being consistent with our findings based on serum sEVs.

5.3. Future perspectives

The clinical potential of a biomarker candidate can be determined by comparing its efficacy to that of existing clinical procedures. We were unable to correlate the sEVs' MMP-9 level of the patients with their MRI status; nevertheless, contradictory findings exist in the literature.

For example, in oral squamous cell carcinoma[187], and thyroid carcinoma[188], a strong correlation between MMP-9 level of serum and tumor size was identified. Hormigo *et al*. observed that the MMP-9 concentrations were significantly lower in glioblastoma patients with no radiographic evidence of disease in comparison to the subjects with active tumor[177].

In contrast, Iwamoto *et al*. found that there was no statistically significant correlation between serum MMP-9 levels and radiographic disease status[178]. Moreover, in a recent study by Jiguet-Jiglaire *et al*., MMP-9 did not correlate with glioblastoma tumor volume, invasion, or angiogenesis assessed by neuro-imaging[88].

This discrepancy may be explained by the fact that Macdonald's criteria are of limited value in certain clinical situations[10]. Macdonald's criteria use the enhancing tumor area as the primary measure while considering the use of steroids and changes in the neurologic status. Nevertheless, enhancement can also be induced by a variety of nontumoral processes, such as inflammation, seizure activity, postsurgical changes, and radiation necrosis[189–192]. As a result, changes in the enhancing area cannot be equated with changes in tumor size or tumor growth. Therefore, in addition to MRI status, another biomarker may be needed to predict tumor spread and prognosis.

EV-based products are still awaiting broad clinical approval from national regulatory agencies such as the FDA and the European Medicine Agency, although many are in late-stage clinical trials. Over 50 clinical trials have been registered on www.clinicaltrials.gov to assess the potential of EVs as biomarkers for disease diagnosis[193]. Thirteen studies have been completed, with seven of which have published results for pre-eclampsia (NCT03562715), non-small cell lung cancer (NCT03228277), high-grade prostate cancer (NCT02702856, NCT03031418, NCT04720599, and NCT03235687), and bladder cancer (NCT04155359). In addition to the completed trials, 40 clinical trials are currently ongoing in this field, nearly half of which are evaluating the potential of circulating cancer/tumor-derived EVs as liquid biopsies.

Although none of the EV-based trials address CNS tumors, it is expected that EV-based diagnostic of CNS tumors may be introduced into clinical practice in the future to transform patient care by allowing for non-invasive diagnosis of CNS tumors to avoid surgical risks and allow for early detection of tumor development and progression[194]. Our results support that the high level of MMP-9 in serum-derived sEVs might be a negative prognostic marker of the probability of survival in GBM patients.

Furthermore, our research findings may also have valuable therapeutic implications. The regulation and inhibition of MMP-9 is an important therapeutic approach for combating cancer. There are studies on targeting intracellular MMPs to inhibit tumor metastasis and angiogenesis[195], and there are attempts to develop selective inhibitors to increase effectiveness[196]. Inhibitors of MMP-9 can be used as anticancer agents, however, there are no selective MMP-9 inhibitors that passed the clinical trials[84].

The lack of success can be attributed to the Janus-faced nature of MMP-9[165]. This molecule plays an essential role in tumor pathogenesis and progression, however, MMP-9 also possesses antitumor activity and serves essential physiological functions[165]. Hence it is necessary to develop specific inhibitors of MMP-9. It may be advantageous to (1) investigate the invasion- and angiogenesis-related molecules co-expressed with MMP-9, or (2) develop strategies for inhibiting tumor-specific activators of MMP-9 instead of using direct inhibitors.

6. New Findings

From the comprehensive quantitative and qualitative analyses on four patient groups with a disease affecting the central nervous system (glioblastoma, brain metastasis of non-small cell lung cancer, meningioma, and lumbar disc herniation) by comparing the protein content of their whole serum and serum sEV, we can make the following conclusions:

1) Instead of one or two molecules, only a panel of 10-20 proteins can distinguish CNS tumors precisely.
2) The protein content of serum sEV is more suitable for the classification of CNS tumors than the protein content of whole serum.
3) The quantitative and qualitative differences between the protein content of whole serum and serum sEV may affect their suitability for providing biomarkers.
4) Among the proteome of serum sEV, the MMP-9 showed the greatest potential for distinguishing between patient groups.
5) The vesicular MMP-9 level is independent of gender and age, but there is a significant difference in the case of the original tumor and the recurrent tumor, and also in the case that the patient had already received therapy at the time of sampling.
6) There are significant differences between the vesicular MMP-9 content of the malignant and the benign CNS tumors and the malignant tumor and the control groups, and it has prognostic value regarding the probability of survival of glioblastoma patients.

7. Conclusions

We aimed to identify circulating protein biomarkers for prognosis, monitoring, and diagnosis of the most prevalent tumors of the central nervous system using liquid biopsy. To enhance the signal that brain tumors release into the bloodstream, sEVs were isolated from serum samples. In addition to that of the whole serum, the protein content of small extracellular vesicles isolated from the serum was also analyzed.

The comparative proteomic analysis showed that sEVs may be more suitable for investigating tumor-related molecular patterns because these molecules are present in higher concentrations in sEV samples than in whole serum samples and contain less "noise" that could introduce bias into the analytical results.

The research discovered that the number of proteins used for monitoring cannot be reduced to a few single molecules, instead, a specific protein panel is required for perfect differentiation.

The *in silico* analyses on the proteome of the two different samples (whole serum and serum sEV) revealed that the biological background of the sEV-based characteristic protein profile is more accurately associated with the tumor types than the whole serum-based protein profile. Samples enriched in sEVs may provide an enhanced source of relevant information, representing not only the specific tumor tissue but also the associated immune responses. This finding provides further evidence that sEVs may be more effective than whole serum samples for monitoring CNS tumors. It also highlights the advantages of introducing EV-based diagnostics into clinical practice.

Furthermore, the dissertation demonstrates the correlation between the survival of GBM patients and their MMP-9 levels of serum-derived sEVs. As MRI status has limited value in certain clinical situations for predicting tumor spread, and the average survival rate for glioblastoma patients is only 5.5% five years after diagnosis, the prognostic value of vesicular MMP-9 as a biomarker for glioblastoma is critical.

Therefore, given the above findings and the ease with which sEVs can be analyzed, incorporating sEV analysis into clinical practice could open new perspectives in the diagnosis and prognosis of CNS tumors.

8. Acknowledgments

I would like to start by expressing my gratitude to my supervisor, Krisztina Buzás, for inviting me to join her group and recognizing my potential and ability for scientific work. I am grateful to fate for bringing us together again on a playground ten years after our university days together. This allowed me to hear about the fascinating and significant work that Krisztina and her research group are engaged in. I am grateful to her for this exceptional opportunity, her guidance, and the excellent scientific milieu she has created in her research group.

My gratitude extends to my colleagues, Mária Harmati, Edina Gyukity-Sebestyén, Mátyás Bukva, Lilla Pintér, and Tímea Böröczky. I am thankful for their help and endless support, as well as the opportunity to learn from them. We are connected by countless collaborative research projects and experiences; without them, writing articles and dissertation would not have been feasible.

I would like to thank Professor Dr. Márta Széll, for my admission to the Microbiology, Antimicrobial Immunity Programme of the Doctoral School of Interdisciplinary Medicine.

I am grateful to Péter Horváth, head of the Institute of Biochemistry and the Laboratory of Image Analysis and Machine Learning in the Biological Research Centre, for the infrastructural support of my project.

Our cooperating partners, who are eminent representatives of their field of science, are to be thanked for their professional assistance. I am grateful to Álmos Klekner for having faith in our research group and providing valuable clinical samples and advice. I am grateful to Zoltán Szabó for taking on the challenge and showing enthusiasm for the examination of the previously unknown sample type, extracellular vesicles, as well as for performing the mass spectrometry measurements with great care and proficiency.

Furthermore, I appreciate the financial support, as my research was funded by the National Brain Research Program NAP 2.0; GINOP-2.3.2-15-2016-00015; GINOP-2.2.1-15-2017-00052; OTKA-K143255; and TKP-2021-EGA-09.

I am especially grateful to my parents for their love, and support. I always knew that you believed in me and wanted the best for me.

Last, but most certainly not least, my deepest gratitude is reserved for my husband and my three amazing children. I hope that my tenacity has been an inspiration to them as they have watched me patiently throughout this journey.

9. References

1. Mattiuzzi, C. & Lippi, G. Current Cancer Epidemiology: *J. Epidemiol. Glob. Health* **9**, 217 (2019).
2. Ferlay, J. *et al.* Cancer statistics for the year 2020: An overview. *Int. J. Cancer* **149**, 778–789 (2021).
3. Zhao, J. *et al.* Global trends in incidence, death, burden and risk factors of early-onset cancer from 1990 to 2019. *BMJ Oncol.* **2**, e000049 (2023).
4. Hanahan, D. & Weinberg, R. A. The Hallmarks of Cancer. *Cell* **100**, 57–70 (2000).
5. Hanahan, D. & Weinberg, R. A. Hallmarks of Cancer: The Next Generation. *Cell* **144**, 646–674 (2011).
6. Hanahan, D. Hallmarks of Cancer: New Dimensions. *Cancer Discov.* **12**, 31–46 (2022).
7. Chaffer, C. L. & Weinberg, R. A. A Perspective on Cancer Cell Metastasis. *Science* **331**, 1559–1564 (2011).
8. Hu, Z. & Curtis, C. Looking backward in time to define the chronology of metastasis. *Nat. Commun.* **11**, 3213 (2020).
9. Macdonald, D. R., Cascino, T. L., Schold, S. C. & Cairncross, J. G. Response criteria for phase II studies of supratentorial malignant glioma. *J. Clin. Oncol.* **8**, 1277–1280 (1990).
10. Van Den Bent, M. J., Vogelbaum, M. A., Wen, P. Y., Macdonald, D. R. & Chang, S. M. End Point Assessment in Gliomas: Novel Treatments Limit Usefulness of Classical Macdonald's Criteria. *J. Clin. Oncol.* **27**, 2905–2908 (2009).
11. Pope, W. B. & Brandal, G. Conventional and advanced magnetic resonance imaging in patients with high-grade glioma. *Q. J. Nucl. Med. Mol. Imaging* **62**, (2018).
12. Garden, G. A. & Campbell, B. M. Glial biomarkers in human central nervous system disease. *Glia* **64**, 1755–1771 (2016).
13. Staedtke, V., Dzaye, O. D. A. & Holdhoff, M. Actionable Molecular Biomarkers in Primary Brain Tumors. *Trends Cancer* **2**, 338–349 (2016).
14. Yao, M. *et al.* Cellular origin of glioblastoma and its implication in precision therapy. *Cell. Mol. Immunol.* **15**, 737–739 (2018).
15. Preusser, M., Brastianos, P. K. & Mawrin, C. Advances in meningioma genetics: novel therapeutic opportunities. *Nat. Rev. Neurol.* **14**, 106–115 (2018).
16. Fox, B. D., Cheung, V. J., Patel, A. J., Suki, D. & Rao, G. Epidemiology of Metastatic Brain Tumors. *Neurosurg. Clin. N. Am.* **22**, 1–6 (2011).
17. Posner, J. B. Brain metastases: 1995. A brief review. *J. Neurooncol.* **27**, 287–293 (1996).
18. Whittle, I. Brain tumors: an encyclopedic approach, 2nd edn: Edited by Andrew H Kaye and Edward Laws Jr (Pp 1052, pound175). Published by Harcourt Publishers Ltd, London, 2001. ISBN 0-4430-4261. *J. Neurol. Neurosurg. Psychiatry* **73**, 211–211 (2002).
19. Ene, C. I. & Ferguson, S. D. Surgical Management of Brain Metastasis: Challenges and Nuances. *Front. Oncol.* **12**, 847110 (2022).
20. Herbst, R. S., Morgensztern, D. & Boshoff, C. The biology and management of non-small cell lung cancer. *Nature* **553**, 446–454 (2018).
21. Louis, D. N. *et al.* The 2021 WHO Classification of Tumors of the Central Nervous System: a summary. *Neuro-Oncol.* **23**, 1231–1251 (2021).
22. Berzero, G., Pieri, V., Mortini, P., Filippi, M. & Finocchiaro, G. The coming of age of liquid biopsy in neuro-oncology. *Brain* awad195 (2023) doi:10.1093/brain/awad195.
23. Lone, S. N. *et al.* Liquid biopsy: a step closer to transform diagnosis, prognosis and future of cancer treatments. *Mol. Cancer* **21**, 79 (2022).
24. Connal, S. *et al.* Liquid biopsies: the future of cancer early detection. *J. Transl. Med.* **21**, 118 (2023).
25. Siravegna, G., Marsoni, S., Siena, S. & Bardelli, A. Integrating liquid biopsies into the management of cancer. *Nat. Rev. Clin. Oncol.* **14**, 531–548 (2017).

26. Cisneros-Villanueva, M. *et al.* Cell-free DNA analysis in current cancer clinical trials: a review. *Br. J. Cancer* **126**, 391–400 (2022).
27. Pantel, K. & Alix-Panabières, C. Circulating tumour cells in cancer patients: challenges and perspectives. *Trends Mol. Med.* **16**, 398–406 (2010).
28. Ding, Z., Wang, N., Ji, N. & Chen, Z.-S. Proteomics technologies for cancer liquid biopsies. *Mol. Cancer* **21**, 53 (2022).
29. Yu, W. *et al.* Exosome-based liquid biopsies in cancer: opportunities and challenges. *Ann. Oncol.* **32**, 466–477 (2021).
30. FDA. FDA. Summary of Safety and Effectiveness Data (SSED) P150047. cobas® EGFR Mutation Test v2. 2016. (2016).
31. Abbosh, C., Birkbak, N. J. & Swanton, C. Early stage NSCLC — challenges to implementing ctDNA-based screening and MRD detection. *Nat. Rev. Clin. Oncol.* **15**, 577–586 (2018).
32. Webster, P. A golden era of cancer clinical trials. *Nat. Med.* **28**, 602–605 (2022).
33. Cristofanilli, M. *et al.* Circulating tumor cells, disease progression, and survival in metastatic breast cancer. *N. Engl. J. Med.* **351**, 781–791 (2004).
34. Clifton, G. T. *et al.* Monitoring of circulating tumor cell trends in a prospective, randomized, placebo-controlled HER2 / neu peptide vaccine trial. *J. Clin. Oncol.* **29**, e11126–e11126 (2011).
35. Bidard, F.-C. *et al.* Clinical validity of circulating tumour cells in patients with metastatic breast cancer: a pooled analysis of individual patient data. *Lancet Oncol.* **15**, 406–414 (2014).
36. Dawson, S.-J. *et al.* Analysis of Circulating Tumor DNA to Monitor Metastatic Breast Cancer. *N. Engl. J. Med.* **368**, 1199–1209 (2013).
37. Bettegowda, C. *et al.* Detection of Circulating Tumor DNA in Early- and Late-Stage Human Malignancies. *Sci. Transl. Med.* **6**, (2014).
38. Castro-Giner, F. & Aceto, N. Tracking cancer progression: from circulating tumor cells to metastasis. *Genome Med.* **12**, 31 (2020).
39. Rossi, E. & Fabbri, F. CTCs 2020: Great Expectations or Unreasonable Dreams. *Cells* **8**, 989 (2019).
40. Landegren, U. & Hammond, M. Cancer diagnostics based on plasma protein biomarkers: hard times but great expectations. *Mol. Oncol.* **15**, 1715–1726 (2021).
41. Catalona, W. J. *et al.* Measurement of Prostate-Specific Antigen in Serum as a Screening Test for Prostate Cancer. *N. Engl. J. Med.* **324**, 1156–1161 (1991).
42. Colli, A. *et al.* Abdominal ultrasound and alpha-foetoprotein for the diagnosis of hepatocellular carcinoma in adults with chronic liver disease. *Cochrane Database Syst. Rev.* **2021**, (2021).
43. Herzog, T. J. *et al.* Correlation between CA-125 serum level and response by RECIST in a phase III recurrent ovarian cancer study. *Gynecol. Oncol.* **122**, 350–355 (2011).
44. Janowska-Wieczorek, A. *et al.* Microvesicles derived from activated platelets induce metastasis and angiogenesis in lung cancer. *Int. J. Cancer* **113**, 752–760 (2005).
45. Ostrowski, M. *et al.* Rab27a and Rab27b control different steps of the exosome secretion pathway. *Nat. Cell Biol.* **12**, 19–30 (2010).
46. Hu, T., Wolfram, J. & Srivastava, S. Extracellular Vesicles in Cancer Detection: Hopes and Hypes. *Trends Cancer* **7**, 122–133 (2021).
47. García-Romero, N. *et al.* DNA sequences within glioma-derived extracellular vesicles can cross the intact blood-brain barrier and be detected in peripheral blood of patients. *Oncotarget* **8**, 1416–1428 (2017).
48. Théry, C. *et al.* Minimal information for studies of extracellular vesicles 2018 (MISEV2018): a position statement of the International Society for Extracellular Vesicles and update of the MISEV2014 guidelines. *J. Extracell. Vesicles* **7**, 1535750 (2018).
49. Welsh, J. A. *et al.* Minimal information for studies of extracellular vesicles (MISEV2023): From basic to advanced approaches. *J. Extracell. Vesicles* **13**, e12404 (2024).

50. Skog, J. *et al.* Glioblastoma microvesicles transport RNA and proteins that promote tumour growth and provide diagnostic biomarkers. *Nat. Cell Biol.* **10**, 1470–1476 (2008).
51. Kahlert, C. *et al.* Identification of Double-stranded Genomic DNA Spanning All Chromosomes with Mutated KRAS and p53 DNA in the Serum Exosomes of Patients with Pancreatic Cancer. *J. Biol. Chem.* **289**, 3869–3875 (2014).
52. Al-Nedawi, K. *et al.* Intercellular transfer of the oncogenic receptor EGFRvIII by microvesicles derived from tumour cells. *Nat. Cell Biol.* **10**, 619–624 (2008).
53. Van Niel, G., D'Angelo, G. & Raposo, G. Shedding light on the cell biology of extracellular vesicles. *Nat. Rev. Mol. Cell Biol.* **19**, 213–228 (2018).
54. Willms, E., Cabañas, C., Mäger, I., Wood, M. J. A. & Vader, P. Extracellular Vesicle Heterogeneity: Subpopulations, Isolation Techniques, and Diverse Functions in Cancer Progression. *Front. Immunol.* **9**, 738 (2018).
55. Xu, R. *et al.* Extracellular vesicles in cancer - implications for future improvements in cancer care. *Nat. Rev. Clin. Oncol.* **15**, 617–638 (2018).
56. Yáñez-Mó, M. *et al.* Biological properties of extracellular vesicles and their physiological functions. *J. Extracell. Vesicles* **4**, 27066 (2015).
57. Estévez-Souto, V., Da Silva-Álvarez, S. & Collado, M. The role of extracellular vesicles in cellular senescence. *FEBS J.* **290**, 1203–1211 (2023).
58. Buzas, E. I. The roles of extracellular vesicles in the immune system. *Nat. Rev. Immunol.* **23**, 236–250 (2023).
59. Raposo, G. & Stahl, P. D. Extracellular vesicles: a new communication paradigm? *Nat. Rev. Mol. Cell Biol.* **20**, 509–510 (2019).
60. Clancy, J. W. & D'Souza-Schorey, C. Tumor-Derived Extracellular Vesicles: Multifunctional Entities in the Tumor Microenvironment. *Annu. Rev. Pathol. Mech. Dis.* **18**, 205–229 (2023).
61. Sheta, M., Taha, E. A., Lu, Y. & Eguchi, T. Extracellular Vesicles: New Classification and Tumor Immunosuppression. *Biology* **12**, 110 (2023).
62. Mastronikolis, N. S. *et al.* The Role of Exosomes in Epithelial–to-Mesenchymal Transition and Cell Functional Properties in Head and Neck Cancer. *Cancers* **15**, 2156 (2023).
63. Peinado, H. *et al.* Melanoma exosomes educate bone marrow progenitor cells toward a pro-metastatic phenotype through MET. *Nat. Med.* **18**, 883–891 (2012).
64. Costa-Silva, B. *et al.* Pancreatic cancer exosomes initiate pre-metastatic niche formation in the liver. *Nat. Cell Biol.* **17**, 816–826 (2015).
65. Marar, C., Starich, B. & Wirtz, D. Extracellular vesicles in immunomodulation and tumor progression. *Nat. Immunol.* **22**, 560–570 (2021).
66. Jahan, S. *et al.* Pioneer Role of Extracellular Vesicles as Modulators of Cancer Initiation in Progression, Drug Therapy, and Vaccine Prospects. *Cells* **11**, 490 (2022).
67. Kosaka, N. *et al.* Exploiting the message from cancer: the diagnostic value of extracellular vesicles for clinical applications. *Exp. Mol. Med.* **51**, 1–9 (2019).
68. Hoshino, A. *et al.* Extracellular Vesicle and Particle Biomarkers Define Multiple Human Cancers. *Cell* **182**, 1044-1061.e18 (2020).
69. Möhrmann, L. *et al.* Liquid Biopsies Using Plasma Exosomal Nucleic Acids and Plasma Cell-Free DNA Compared with Clinical Outcomes of Patients with Advanced Cancers. *Clin. Cancer Res.* **24**, 181–188 (2018).
70. Ruhen, O. & Meehan, K. Tumor-Derived Extracellular Vesicles as a Novel Source of Protein Biomarkers for Cancer Diagnosis and Monitoring. *PROTEOMICS* **19**, 1800155 (2019).
71. Mund, A., Brunner, A.-D. & Mann, M. Unbiased spatial proteomics with single-cell resolution in tissues. *Mol. Cell* **82**, 2335–2349 (2022).
72. Sheridan, C. Exosome cancer diagnostic reaches market. *Nat. Biotechnol.* **34**, 359–360 (2016).
73. Melo, S. A. *et al.* Glypican-1 identifies cancer exosomes and detects early pancreatic cancer. *Nature* **523**, 177–182 (2015).

74. Donovan, M. J. *et al.* A molecular signature of PCA3 and ERG exosomal RNA from non-DRE urine is predictive of initial prostate biopsy result. *Prostate Cancer Prostatic Dis.* **18**, 370–375 (2015).
75. McKiernan, J. *et al.* A Prospective Adaptive Utility Trial to Validate Performance of a Novel Urine Exosome Gene Expression Assay to Predict High-grade Prostate Cancer in Patients with Prostate-specific Antigen 2–10 ng/ml at Initial Biopsy. *Eur. Urol.* **74**, 731–738 (2018).
76. Bio-Techne Corporation, FDA Grants Breakthrough Device Designation to Bio- Techne's ExoDx™ Prostate intelliScore™ (EPI) Test. (2019).
77. FDA-NIH Biomarker Working Group. *BEST (Biomarkers, EndpointS, and Other Tools) Resource*. (Food and Drug Administration (US), Silver Spring (MD), 2016).
78. Bennett, M. R. & Devarajan, P. Characteristics of an Ideal Biomarker of Kidney Diseases. in *Biomarkers of Kidney Disease* 1–24 (Elsevier, 2011). doi:10.1016/B978-0-12-375672-5.10001-5.
79. Devarajan, P. Proteomics for Biomarker Discovery in Acute Kidney Injury. *Semin. Nephrol.* **27**, 637–651 (2007).
80. Cagney, D. N. *et al.* The FDA NIH Biomarkers, EndpointS, and other Tools (BEST) resource in neuro-oncology. *Neuro-Oncol.* **20**, 1162–1172 (2018).
81. Klekner, Á. *et al.* Expression pattern of invasion-related molecules in the peritumoral brain. *Clin. Neurol. Neurosurg.* **139**, 138–143 (2015).
82. Jabłońska-Trypuć, A., Matejczyk, M. & Rosochacki, S. Matrix metalloproteinases (MMPs), the main extracellular matrix (ECM) enzymes in collagen degradation, as a target for anticancer drugs. *J. Enzyme Inhib. Med. Chem.* **31**, 177–183 (2016).
83. Van Wart, H. E. & Birkedal-Hansen, H. The cysteine switch: a principle of regulation of metalloproteinase activity with potential applicability to the entire matrix metalloproteinase gene family. *Proc. Natl. Acad. Sci.* **87**, 5578–5582 (1990).
84. Mondal, S., Adhikari, N., Banerjee, S., Amin, S. A. & Jha, T. Matrix metalloproteinase-9 (MMP-9) and its inhibitors in cancer: A minireview. *Eur. J. Med. Chem.* **194**, 112260 (2020).
85. Chambers, A. F. & Matrisian, L. M. Changing views of the role of matrix metalloproteinases in metastasis. *JNCI J. Natl. Cancer Inst.* **89**, 1260–1270 (1997).
86. Barillari, G. The Impact of Matrix Metalloproteinase-9 on the Sequential Steps of the Metastatic Process. *Int. J. Mol. Sci.* **21**, 4526 (2020).
87. Mannello, F., Tonti, G. & Papa, S. Matrix Metalloproteinase Inhibitors as Anticancer Therapeutics. *Curr. Cancer Drug Targets* **5**, 285–298 (2005).
88. Jiguet-Jiglaire, C. *et al.* Plasmatic MMP9 released from tumor-infiltrating neutrophils is predictive for bevacizumab efficacy in glioblastoma patients: an AVAglio ancillary study. *Acta Neuropathol. Commun.* **10**, 1 (2022).
89. Noel, A., Jost, M. & Maquoi, E. Matrix metalloproteinases at cancer tumor–host interface. *Semin. Cell Dev. Biol.* **19**, 52–60 (2008).
90. Stetler-Stevenson, W. G. Type IV collagenases in tumor invasion and metastasis. *CANCER METASTASIS Rev.* **9**, 289–303 (1990).
91. Rao, J. S. *et al.* Elevated levels of M(r) 92,000 type IV collagenase in human brain tumors. *Cancer Res.* **53**, 2208–2211 (1993).
92. Rao, J. S. *et al.* Expression and localization of 92 kDa type IV collagenase/gelatinase B (MMP-9) in human gliomas. *Clin. Exp. Metastasis* **14**, 12–18 (1996).
93. Thuault, S., Ghossoub, R., David, G. & Zimmermann, P. A Journey on Extracellular Vesicles for Matrix Metalloproteinases: A Mechanistic Perspective. *Front. Cell Dev. Biol.* **10**, 886381 (2022).
94. Shimoda, M. & Khokha, R. Metalloproteinases in extracellular vesicles. *Biochim. Biophys. Acta BBA - Mol. Cell Res.* **1864**, 1989–2000 (2017).
95. Sanderson, R. D., Bandari, S. K. & Vlodavsky, I. Proteases and glycosidases on the surface of exosomes: Newly discovered mechanisms for extracellular remodeling. *Matrix Biol.* **75–76**, 160–169 (2019).

96. Shimoda, M. Extracellular vesicle-associated MMPs: A modulator of the tissue microenvironment. in *Advances in Clinical Chemistry* vol. 88 35–66 (Elsevier, 2019).
97. Maas, S. L. N., Breakefield, X. O. & Weaver, A. M. Extracellular Vesicles: Unique Intercellular Delivery Vehicles. *Trends Cell Biol.* **27**, 172–188 (2017).
98. Zucker, S. *et al.* Metastatic mouse melanoma cells release collagen-gelatin degrading metalloproteinases as components of shed membrane vesicles. *Biochim. Biophys. Acta BBA - Gen. Subj.* **924**, 225–237 (1987).
99. Murayama, T., Kataoka, H., Koita, H., Nabeshima, K. & Koono, M. Glycocalyceal bodies in a human rectal carcinoma cell line and their interstitial collagenolytic activities. *Virchows Arch. B Cell Pathol. Incl. Mol. Pathol.* **60**, 263–270 (1991).
100. Ginestra, A. *et al.* Urokinase Plasminogen Activator and Gelatinases Are Associated with Membrane Vesicles Shed by Human HT1080 Fibrosarcoma Cells. *J. Biol. Chem.* **272**, 17216–17222 (1997).
101. Ginestra, A. *et al.* The amount and proteolytic content of vesicles shed by human cancer cell lines correlates with their in vitro invasiveness. *Anticancer Res.* **18**, 3433–3437 (1998).
102. Kassassir, H., Papiewska-Pająk, I., Kryczka, J., Boncela, J. & Kowalska, M. A. Platelet-derived microparticles stimulate the invasiveness of colorectal cancer cells via the p38MAPK-MMP-2/MMP-9 axis. *Cell Commun. Signal.* **21**, 51 (2023).
103. Di Vizio, D. *et al.* Large Oncosomes in Human Prostate Cancer Tissues and in the Circulation of Mice with Metastatic Disease. *Am. J. Pathol.* **181**, 1573–1584 (2012).
104. Wenzel, E. M. *et al.* Intercellular transfer of cancer cell invasiveness via endosome-mediated protease shedding. *Nat. Commun.* **15**, 1277 (2024).
105. Gollapalli, K. *et al.* Investigation of serum proteome alterations in human glioblastoma multiforme. *PROTEOMICS* **12**, 2378–2390 (2012).
106. Gállego Pérez-Larraya, J. *et al.* Diagnostic and prognostic value of preoperative combined GFAP, IGFBP-2, and YKL-40 plasma levels in patients with glioblastoma: Plasma IGFBP-2, YKL-40, and GFAP in GBM. *Cancer* **120**, 3972–3980 (2014).
107. Figueroa, J. M. & Carter, B. S. Detection of glioblastoma in biofluids. *J. Neurosurg.* **129**, 334–340 (2018).
108. Badaut, J., Ghersi-Egea, J.-F., Thorne, R. G. & Konsman, J. P. Blood–brain borders: a proposal to address limitations of historical blood–brain barrier terminology. *Fluids Barriers CNS* **21**, 3 (2024).
109. Schaller, J., Gerber, S., Kämpfer, U., Lejon, S. & Trachsel, C. *Human Blood Plasma Proteins: Structure and Function*. (Wiley, 2008). doi:10.1002/9780470724378.
110. Patel, A. P. *et al.* Single-cell RNA-seq highlights intratumoral heterogeneity in primary glioblastoma. *Science* **344**, 1396–1401 (2014).
111. Harmati, M. *et al.* Small extracellular vesicles convey the stress-induced adaptive responses of melanoma cells. *Sci. Rep.* **9**, 15329 (2019).
112. Sader, J. E. *et al.* Spring constant calibration of atomic force microscope cantilevers of arbitrary shape. *Rev. Sci. Instrum.* **83**, 103705 (2012).
113. Ebner, A., Hinterdorfer, P. & Gruber, H. J. Comparison of different aminofunctionalization strategies for attachment of single antibodies to AFM cantilevers. *Ultramicroscopy* **107**, 922–927 (2007).
114. Searle, B. C. *et al.* Chromatogram libraries improve peptide detection and quantification by data independent acquisition mass spectrometry. *Nat. Commun.* **9**, 5128 (2018).
115. Chambers, M. C. *et al.* A cross-platform toolkit for mass spectrometry and proteomics. *Nat. Biotechnol.* **30**, 918–920 (2012).
116. Rosenberger, G. *et al.* A repository of assays to quantify 10,000 human proteins by SWATH-MS. *Sci. Data* **1**, 140031 (2014).
117. Luong, J. H. T. & Vashist, S. K. Chemistry of Biotin–Streptavidin and the Growing Concern of an Emerging Biotin Interference in Clinical Immunoassays. *ACS Omega* **5**, 10–18 (2020).

118. Metz, T. O. *et al.* Application of Proteomics in the Discovery of Candidate Protein Biomarkers in a Diabetes Autoantibody Standardization Program Sample Subset. *J. Proteome Res.* **7**, 698–707 (2008).
119. Hodge, K., Have, S. T., Hutton, L. & Lamond, A. I. Cleaning up the masses: Exclusion lists to reduce contamination with HPLC-MS/MS. *J. Proteomics* **88**, 92–103 (2013).
120. Curran-Everett, D. Explorations in statistics: the log transformation. *Adv. Physiol. Educ.* **42**, 343–347 (2018).
121. Lakens, D. Calculating and reporting effect sizes to facilitate cumulative science: a practical primer for t-tests and ANOVAs. *Front. Psychol.* **4**, (2013).
122. Cohen, J. *Statistical Power Analysis for the Behavioral Sciences*. (Routledge, 2013). doi:10.4324/9780203771587.
123. Fawcett, T. An introduction to ROC analysis. *Pattern Recognit. Lett.* **27**, 861–874 (2006).
124. Husson, F., Le, S. & Pagès, J. *Exploratory Multivariate Analysis by Example Using R*. (Chapman and Hall/CRC, 2017). doi:10.1201/b21874.
125. Hartigan, J. A. & Wong, M. A. Algorithm AS 136: A K-Means Clustering Algorithm. *Appl. Stat.* **28**, 100 (1979).
126. Ding, C. & He, X. *K* -means clustering via principal component analysis. in *Twenty-first international conference on Machine learning - ICML '04* 29 (ACM Press, Banff, Alberta, Canada, 2004). doi:10.1145/1015330.1015408.
127. Rousseeuw, P. J. Silhouettes: A graphical aid to the interpretation and validation of cluster analysis. *J. Comput. Appl. Math.* **20**, 53–65 (1987).
128. Pedregosa, F. *et al.* Scikit-learn: Machine Learning in Python. *J. Mach. Learn. Res.* **12**, 2825–2830 (2011).
129. EV-TRACK Consortium *et al.* EV-TRACK: transparent reporting and centralizing knowledge in extracellular vesicle research. *Nat. Methods* **14**, 228–232 (2017).
130. de Menezes-Neto, A. *et al.* Size-exclusion chromatography as a stand-alone methodology identifies novel markers in mass spectrometry analyses of plasma-derived vesicles from healthy individuals. *J. Extracell. Vesicles* **4**, 27378 (2015).
131. Xu, R., Greening, D. W., Zhu, H.-J., Takahashi, N. & Simpson, R. J. Extracellular vesicle isolation and characterization: toward clinical application. *J. Clin. Invest.* **126**, 1152–1162 (2016).
132. Royo, F., Théry, C., Falcón-Pérez, J. M., Nieuwland, R. & Witwer, K. W. Methods for Separation and Characterization of Extracellular Vesicles: Results of a Worldwide Survey Performed by the ISEV Rigor and Standardization Subcommittee. *Cells* **9**, 1955 (2020).
133. Nieuwland, R. & Siljander, P. R. A beginner's guide to study extracellular vesicles in human blood plasma and serum. *J. Extracell. Vesicles* **13**, e12400 (2024).
134. Liu, M.-L., Werth, V. P. & Williams, K. J. Blood plasma versus serum: which is right for sampling circulating membrane microvesicles in human subjects? *Ann. Rheum. Dis.* **79**, e73–e73 (2020).
135. Smolarz, M., Pietrowska, M., Matysiak, N., Mielańczyk, Ł. & Widłak, P. Proteome Profiling of Exosomes Purified from a Small Amount of Human Serum: The Problem of Co-Purified Serum Components. *Proteomes* **7**, 18 (2019).
136. Sódar, B. W. *et al.* Low-density lipoprotein mimics blood plasma-derived exosomes and microvesicles during isolation and detection. *Sci. Rep.* **6**, 24316 (2016).
137. Lucien, F. *et al.* MIBlood-EV: Minimal information to enhance the quality and reproducibility of blood extracellular vesicle research. *J. Extracell. Vesicles* **12**, 12385 (2023).
138. Arraud, N. *et al.* Extracellular vesicles from blood plasma: determination of their morphology, size, phenotype and concentration. *J. Thromb. Haemost.* **12**, 614–627 (2014).
139. Welsh, J. A. *et al.* A compendium of single extracellular vesicle flow cytometry. *J. Extracell. Vesicles* **12**, e12299 (2023).
140. Li, Y. *et al.* EV-origin: Enumerating the tissue-cellular origin of circulating extracellular vesicles using exLR profile. *Comput. Struct. Biotechnol. J.* **18**, 2851–2859 (2020).

141. Abdelmohsen, K. *et al.* Survey of organ-derived small extracellular vesicles and particles (sEVPs) to identify selective protein markers in mouse serum. *J. Extracell. Biol.* **2**, e106 (2023).
142. Nanou, A. *et al.* Tumor-Derived Extracellular Vesicles as Complementary Prognostic Factors to Circulating Tumor Cells in Metastatic Breast Cancer. *JCO Precis. Oncol.* e2200372 (2023) doi:10.1200/PO.22.00372.
143. Yang, Y. *et al.* Exosomal PD-L1 harbors active defense function to suppress T cell killing of breast cancer cells and promote tumor growth. *Cell Res.* **28**, 862–864 (2018).
144. Marrugo-Ramírez, J., Mir, M. & Samitier, J. Blood-Based Cancer Biomarkers in Liquid Biopsy: A Promising Non-Invasive Alternative to Tissue Biopsy. *Int. J. Mol. Sci.* **19**, 2877 (2018).
145. Batool, S. M. *et al.* The Liquid Biopsy Consortium: Challenges and opportunities for early cancer detection and monitoring. *Cell Rep. Med.* **4**, 101198 (2023).
146. Skaga, E. *et al.* Intertumoral heterogeneity in patient-specific drug sensitivities in treatment-naïve glioblastoma. *BMC Cancer* **19**, 628 (2019).
147. Song, J. *et al.* A panel of selected serum protein biomarkers for the detection of aggressive prostate cancer. *Theranostics* **11**, 6214–6224 (2021).
148. Jones, A. L. *et al.* Prostate Cancer Diagnosis in the Clinic Using an 8-Protein Biomarker Panel. *Anal. Chem.* **93**, 1059–1067 (2021).
149. Russell, M. R. *et al.* Diagnosis of epithelial ovarian cancer using a combined protein biomarker panel. *Br. J. Cancer* **121**, 483–489 (2019).
150. Wu, S. *et al.* Serum Biomarker Panel for Rapid Early Diagnosis of Lung Cancer. *Curr. Cancer Drug Targets* **23**, 534–546 (2023).
151. Fung, K. Y. C. *et al.* Blood-Based Protein Biomarker Panel for the Detection of Colorectal Cancer. *PLOS ONE* **10**, e0120425 (2015).
152. Nijaguna, M. B. *et al.* Definition of a serum marker panel for glioblastoma discrimination and identification of Interleukin 1β in the microglial secretome as a novel mediator of endothelial cell survival induced by C-reactive protein. *J. Proteomics* **128**, 251–261 (2015).
153. Popescu, I. D. *et al.* Potential serum biomarkers for glioblastoma diagnostic assessed by proteomic approaches. *Proteome Sci.* **12**, 47 (2014).
154. Erkan, E. P. *et al.* Circulating Tumor Biomarkers in Meningiomas Reveal a Signature of Equilibrium Between Tumor Growth and Immune Modulation. *Front. Oncol.* **9**, 1031 (2019).
155. Kim, J. Y. *et al.* Proteome Multimarker Panel for the Early Detection of Hepatocellular Carcinoma: Multicenter Derivation, Validation, and Comparison. *ACS Omega* **7**, 29934–29943 (2022).
156. Wu, D. *et al.* Serum biomarker panels for the diagnosis of gastric cancer. *Cancer Med.* **8**, 1576–1583 (2019).
157. Nijaguna, M. B. *et al.* An Eighteen Serum Cytokine Signature for Discriminating Glioma from Normal Healthy Individuals. *PLOS ONE* **10**, e0137524 (2015).
158. Qian, K. *et al.* The roles of small extracellular vesicles in cancer and immune regulation and translational potential in cancer therapy. *J. Exp. Clin. Cancer Res.* **41**, 286 (2022).
159. Li, C., Donninger, H., Eaton, J. & Yaddanapudi, K. Regulatory Role of Immune Cell-Derived Extracellular Vesicles in Cancer: The Message Is in the Envelope. *Front. Immunol.* **11**, 1525 (2020).
160. Luo, X., Jean-Toussaint, R., Sacan, A. & Ajit, S. K. Differential RNA packaging into small extracellular vesicles by neurons and astrocytes. *Cell Commun. Signal.* **19**, 75 (2021).
161. Shi, M., Sheng, L., Stewart, T., Zabetian, C. P. & Zhang, J. New windows into the brain: Central nervous system-derived extracellular vesicles in blood. *Prog. Neurobiol.* **175**, 96–106 (2019).
162. Asleh, K. *et al.* Extracellular vesicle-based liquid biopsy biomarkers and their application in precision immuno-oncology. *Biomark. Res.* **11**, 99 (2023).
163. Dobra, G. *et al.* Small Extracellular Vesicles Isolated from Serum May Serve as Signal-Enhancers for the Monitoring of CNS Tumors. *Int. J. Mol. Sci.* **21**, 5359 (2020).

164. Anderson, K. S. & LaBaer, J. The Sentinel Within: Exploiting the Immune System for Cancer Biomarkers. *J. Proteome Res.* **4**, 1123–1133 (2005).
165. Farina, A. & Mackay, A. Gelatinase B/MMP-9 in Tumour Pathogenesis and Progression. *Cancers* **6**, 240–296 (2014).
166. Wen, C. *et al.* Biological roles and potential applications of immune cell-derived extracellular vesicles. *J. Extracell. Vesicles* **6**, 1400370 (2017).
167. Veerman, R. E., Güçlüler Akpinar, G., Eldh, M. & Gabrielsson, S. Immune Cell-Derived Extracellular Vesicles – Functions and Therapeutic Applications. *Trends Mol. Med.* **25**, 382–394 (2019).
168. Dobra, G. *et al.* MMP-9 as Prognostic Marker for Brain Tumours: A Comparative Study on Serum-Derived Small Extracellular Vesicles. *Cancers* **15**, 712 (2023).
169. Halade, G. V., Jin, Y.-F. & Lindsey, M. L. Matrix metalloproteinase (MMP)-9: A proximal biomarker for cardiac remodeling and a distal biomarker for inflammation. *Pharmacol. Ther.* **139**, 32–40 (2013).
170. Wu, Z. *et al.* Prognostic significance of MMP-9 and TIMP-1 serum and tissue expression in breast cancer. *Int. J. Cancer* **122**, 2050–2056 (2008).
171. Li, W., Cui, Z., Kong, Y., Liu, X. & Wang, X. Serum Levels of S100A11 and MMP-9 in Patients with Epithelial Ovarian Cancer and Their Clinical Significance. *BioMed Res. Int.* **2021**, 7341247 (2021).
172. Liang, S. & Chang, L. Serum matrix metalloproteinase-9 level as a biomarker for colorectal cancer: a diagnostic meta-analysis. *Biomark. Med.* **12**, 393–402 (2018).
173. Huang, X. *et al.* Diagnostic values of MMP-7, MMP-9, MMP-11, TIMP-1, TIMP-2, CEA, and CA19-9 in patients with colorectal cancer. *J. Int. Med. Res.* **49**, 030006052110125 (2021).
174. Balla, M. M. S. *et al.* Differential diagnosis of lung cancer, its metastasis and chronic obstructive pulmonary disease based on serum Vegf, Il-8 and MMP-9. *Sci. Rep.* **6**, 36065 (2016).
175. Ramón de Fata, F. *et al.* The role of matrix metalloproteinase MMP-9 and TIMP-2 tissue inhibitor of metalloproteinases as serum markers of bladder cancer. *Actas Urol. Esp.* **37**, 480–488 (2013).
176. Redondo, P., Lloret, P., Idoate, M. & Inoges, S. Expression and serum levels of MMP-2 and MMP-9 during human melanoma progression. *Clin. Exp. Dermatol.* **30**, 541–545 (2005).
177. Hormigo, A. *et al.* YKL-40 and Matrix Metalloproteinase-9 as Potential Serum Biomarkers for Patients with High-Grade Gliomas. *Clin. Cancer Res.* **12**, 5698–5704 (2006).
178. Iwamoto, F. M. *et al.* Longitudinal prospective study of matrix metalloproteinase-9 as a serum marker in gliomas. *J. Neurooncol.* **105**, 607–612 (2011).
179. Ricci, S. *et al.* Evaluation of matrix metalloproteinase type IV-collagenases in serum of patients with tumors of the central nervous system. *J. Neurooncol.* **131**, 223–232 (2017).
180. Otero-Estévez, O. *et al.* Serum matrix metalloproteinase-9 in colorectal cancer family-risk population screening. *Sci. Rep.* **5**, 13030 (2015).
181. Osti, D. *et al.* Clinical Significance of Extracellular Vesicles in Plasma from Glioblastoma Patients. *Clin. Cancer Res.* **25**, 266–276 (2019).
182. Tabouret, E. *et al.* Association of matrix metalloproteinase 2 plasma level with response and survival in patients treated with bevacizumab for recurrent high-grade glioma. *Neuro-Oncol.* **16**, 392–399 (2014).
183. Xue, Q. *et al.* High expression of MMP9 in glioma affects cell proliferation and is associated with patient survival rates. *Oncol. Lett.* **13**, 1325–1330 (2017).
184. Raithatha, S. A. *et al.* Localization of gelatinase-A and gelatinase-B mRNA and protein in humangliomas. *Neuro-Oncol.* **2**, 145–150 (2000).
185. Chou, C. H. *et al.* MMP-9 from sublethally irradiated tumor promotes Lewis lung carcinoma cell invasiveness and pulmonary metastasis. *Oncogene* **31**, 458–468 (2012).
186. Roy, R., Yang, J. & Moses, M. A. Matrix Metalloproteinases As Novel Biomarker s and Potential Therapeutic Targets in Human Cancer. *J. Clin. Oncol.* **27**, 5287–5297 (2009).

187. Benitha, G. *et al.* Evaluation of Serum Levels of Matrix MetalloProteinase-9 (MMP-9) in Oral Squamous Cell Carcinoma and Its Clinicopathological Correlation. *Cureus* (2023) doi:10.7759/cureus.34954.
188. Xu, D. *et al.* Predictive significance of serum MMP-9 in papillary thyroid carcinoma. *Open Life Sci.* **14**, 275–287 (2019).
189. Finn, M. A., Blumenthal, D. T., Salzman, K. L. & Jensen, R. L. Transient postictal MRI changes in patients with brain tumors may mimic disease progression. *Surg. Neurol.* **67**, 246–250 (2007).
190. Ulmer, S. *et al.* Clinical and radiographic features of peritumoral infarction following resection of glioblastoma. *Neurology* **67**, 1668–1670 (2006).
191. Henegar, M. M., Moran, C. J. & Silbergeld, D. L. Early postoperative magnetic resonance imaging following nonneoplastic cortical resection. *J. Neurosurg.* **84**, 174–179 (1996).
192. Kumar, A. J. *et al.* Malignant Gliomas: MR Imaging Spectrum of Radiation Therapy- and Chemotherapy-induced Necrosis of the Brain after Treatment. *Radiology* **217**, 377–384 (2000).
193. Ghodasara, A., Raza, A., Wolfram, J., Salomon, C. & Popat, A. Clinical Translation of Extracellular Vesicles. *Adv. Healthc. Mater.* **12**, e2301010 (2023).
194. Bunda, S. *et al.* Liquid Biomarkers for Improved Diagnosis and Classification of CNS Tumors. *Int. J. Mol. Sci.* **22**, 4548 (2021).
195. Lv, Y. *et al.* Targeting intracellular MMPs efficiently inhibits tumor metastasis and angiogenesis. *Theranostics* **8**, 2830–2845 (2018).
196. Fields, G. B. New strategies for targeting matrix metalloproteinases. *Matrix Biol.* **44–46**, 239–246 (2015).

Supplementary

Table S1 311 membered protein table of DIA mode constructed spectral library
https://docs.google.com/spreadsheets/d/1G8U1Y27iPyY9Z07lqEgLU0mIqsEdmRoh/edit?usp=sharing&ouid=117345183391996855343&rtpof=true&sd=true

Table S2 Sample correlation analysis
https://docs.google.com/spreadsheets/d/1QXmyEB_ZqN0j3n7tGObCRLBRzoqJaVpE/edit?usp=sharing&ouid=117345183391996855343&rtpof=true&sd=true

Table S3 List of the selected proteins

Table S4 Detailed patient characteristics and MMP-9 concentrations measured by ELISA
https://docs.google.com/spreadsheets/d/16JgYOicXftCjnXyDs4-XiPRCnmeJMupS/edit?usp=sharing&ouid=117345183391996855343&rtpof=true&sd=true

Figure S1 Intragroup Coefficients of Variation (CV) distributions

Figure S2 Hierarchical clustering of the sample pools and the intensity of the 311 identified proteins

Figure S3 Matrix metalloproteinase 9 (MMP-9) is the most effective at distinguishing the groups

Figure S4 Comparison of all the preoperative and the postoperative GBM and BM samples in terms of MMP-9 level

Figure S5 Differences among controls and various CNS tumor patients based on MMP-9 level of sEVs originated from preoperative serum samples

Table S2 List of the selected proteins

Whole Serum	UniProt ID	Gene symbol	Protein name	Ratio	Cohen's D	p value
M/CTRL[1]	P09651	HNRNPA1	Heterogeneous nuclear ribonucleoprotein A1	3,3300	4,1813	>0,005
M/CTRL	Q9Y490	TLN1	Talin 1	2,0290	2,1835	>0,005
BM/CTRL	P14780	**MMP9**	Matrix metalloproteinase-9	4,1265	2,0857	>0,005
BM/CTRL	P59665	DEFA1	Neutrophil defensin 1	2,2992	3,8002	>0,005
GBM/CTRL	P04792	**HSPB1**	Heat shock protein beta-1	0,4654	2,4651	>0,005
GBM/CTRL	P01861	IGHG4	Immunoglobulin heavy constant gamma 4	2,3895	2,4491	>0,005
GBM/M	P31944	**CASP14**	Caspase-14	2,2469	3,4752	>0,005
GBM/M[1]	P69891	**HBG1**	Hemoglobin Subunit Gamma 1	4,4472	3,6425	>0,005
GBM/M	P05109	S100A8	Protein S100-A8	2,0844	2,3673	>0,005
GBM/M[1]	P04275	VWF	von Willebrand factor	2,1499	4,2684	>0,005
sEV samples	**UniProt ID**	**Gene symbol**	**Protein name**	**Ratio**	**Cohen's D**	**p value**
M/CTRL	P69891	**HBG1**	Hemoglobin Subunit Gamma 1	0,19	4,54	>0,005
M/CTRL[1]	P02751	FN1	Fibronectin 1	0,46	4,52	>0,005
M/CTRL[1]	P11142	HSPA8	Heat shock 70 kDa protein 8	0,31	2,96	>0,005
M/CTRL	P02776	PF4	Platelet factor 4	0,48	2,58	>0,005
M/CTRL	P15814	IGLL1	Immunoglobulin lambda-like polypeptide 1	2,02	2,29	>0,005
BM/CTRL[1]	P31151	S100A7	S100 calcium-binding protein A7	0,40	6,68	>0,005
BM/CTRL[1]	P14780	**MMP9**	Matrix metalloproteinase-9	5,87	2,98	>0,005
BM/CTRL	P15144	ANPEP	Alanyl Aminopeptidase	2,56	2,53	>0,005
GBM/CTRL	P31944	**CASP14**	Caspase-14	0,30	2,75	>0,005
GBM/CTRL[1]	Q9HCY8	S100A14	S100 Calcium Binding Protein A14	0,42	2,82	>0,005
GBM/CTRL	P22531	SPRR2E	Small Proline Rich Protein 2E	2,74	3,09	>0,005
GBM/M	O75223	GGCT	Gamma-Glutamylcyclotransferase	0,302	3,31	>0,005
GBM/BM	P04792	**HSPB**1	Heat shock protein beta-1	0,355	3,31	>0,005
GBM/BM	Q6UWP8	SBSN	Suprabasin	0,465	2,32	>0,005
BM/M	P02675	FGB	Fibrinogen beta chain	2,947	2,77	>0,005
BM/M	Q13201	MMRN1	Multimerin 1	5,319	2,05	>0,005
BM/M	Q5D862	FLG2	Filaggrin Family Member 2	0,361	2,00	>0,005

[1]These proteins also showed relevant difference in other comparisons,
but only the result of the highest Cohen's d is shown (detailed in Appendix A).

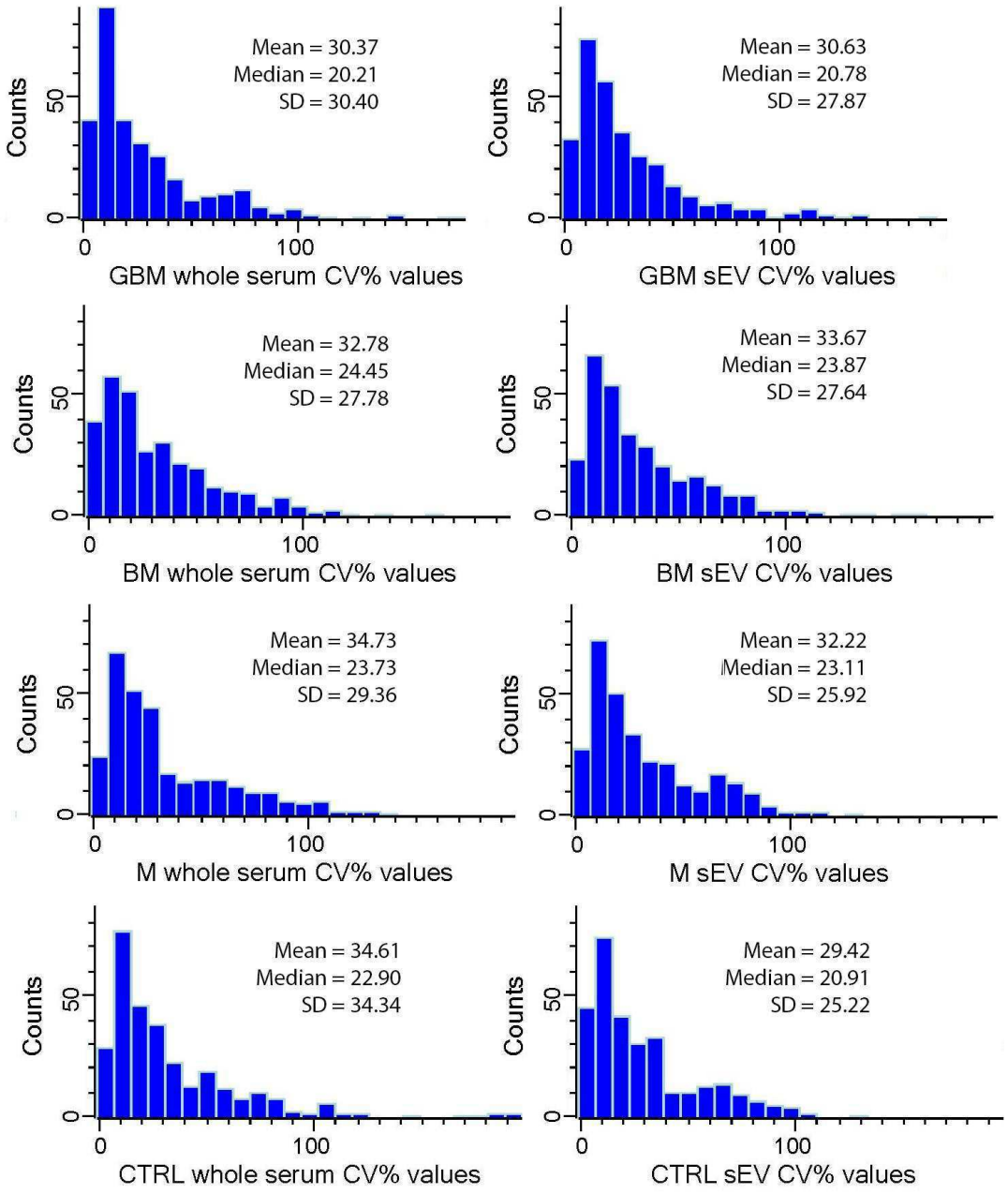

Figure S1. Intragroup Coefficients of variation (CV) distributions

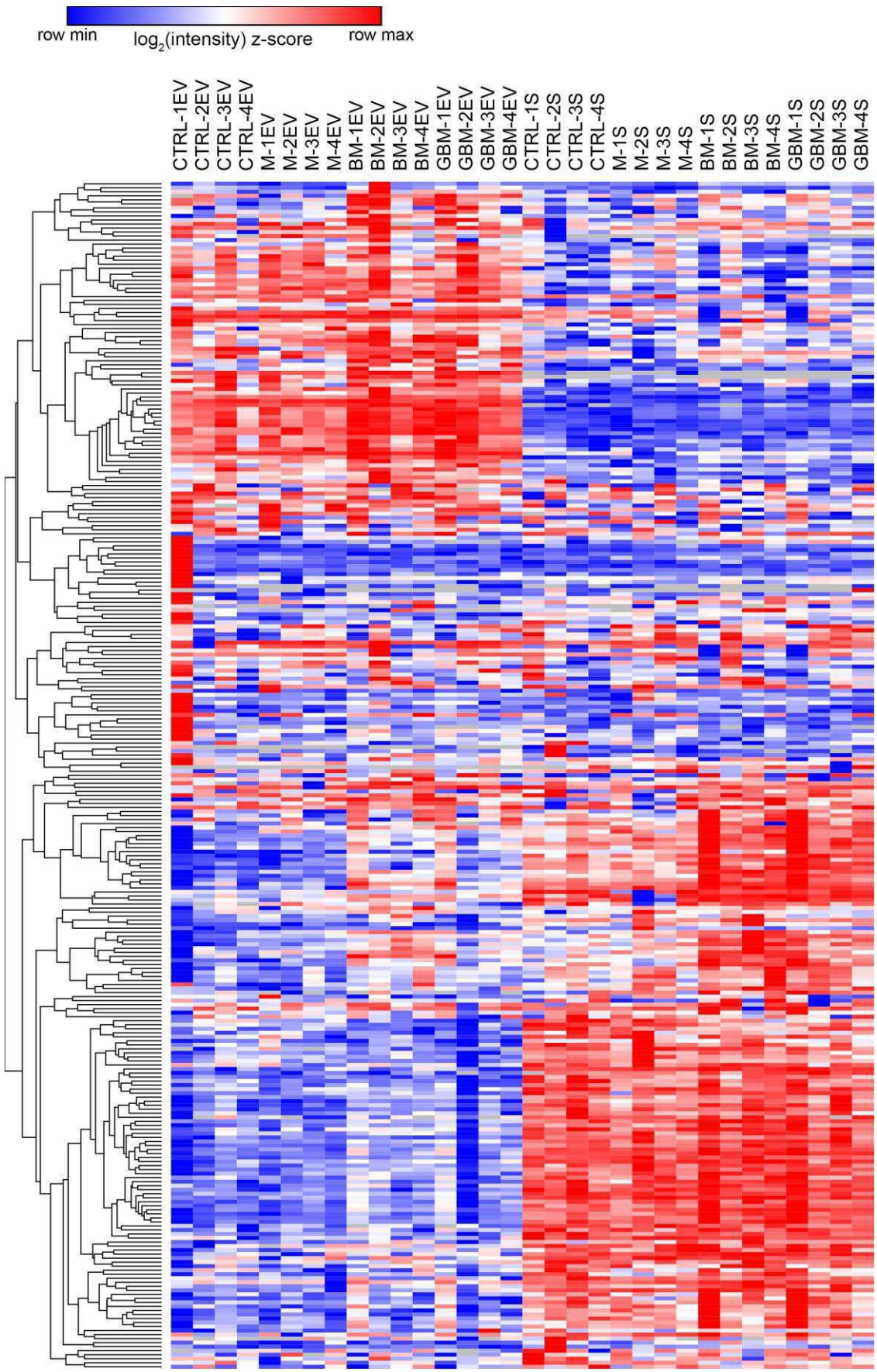

Figure S2. Hierarchical clustering of the sample pools and the intensity of 311 identified proteins

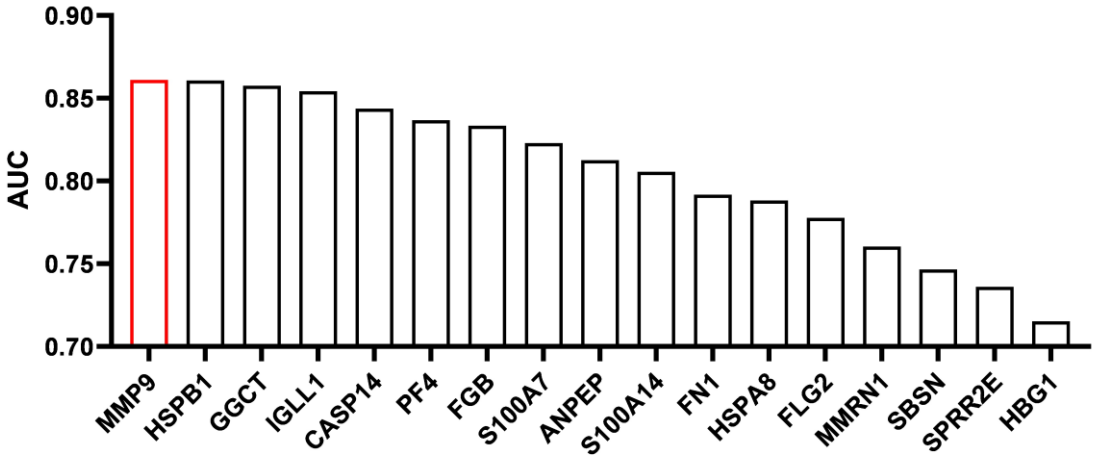

Figure S3 Matrix metalloproteinase 9 (MMP-9) is the most effective at distinguishing the groups among the protein panel of sEVs

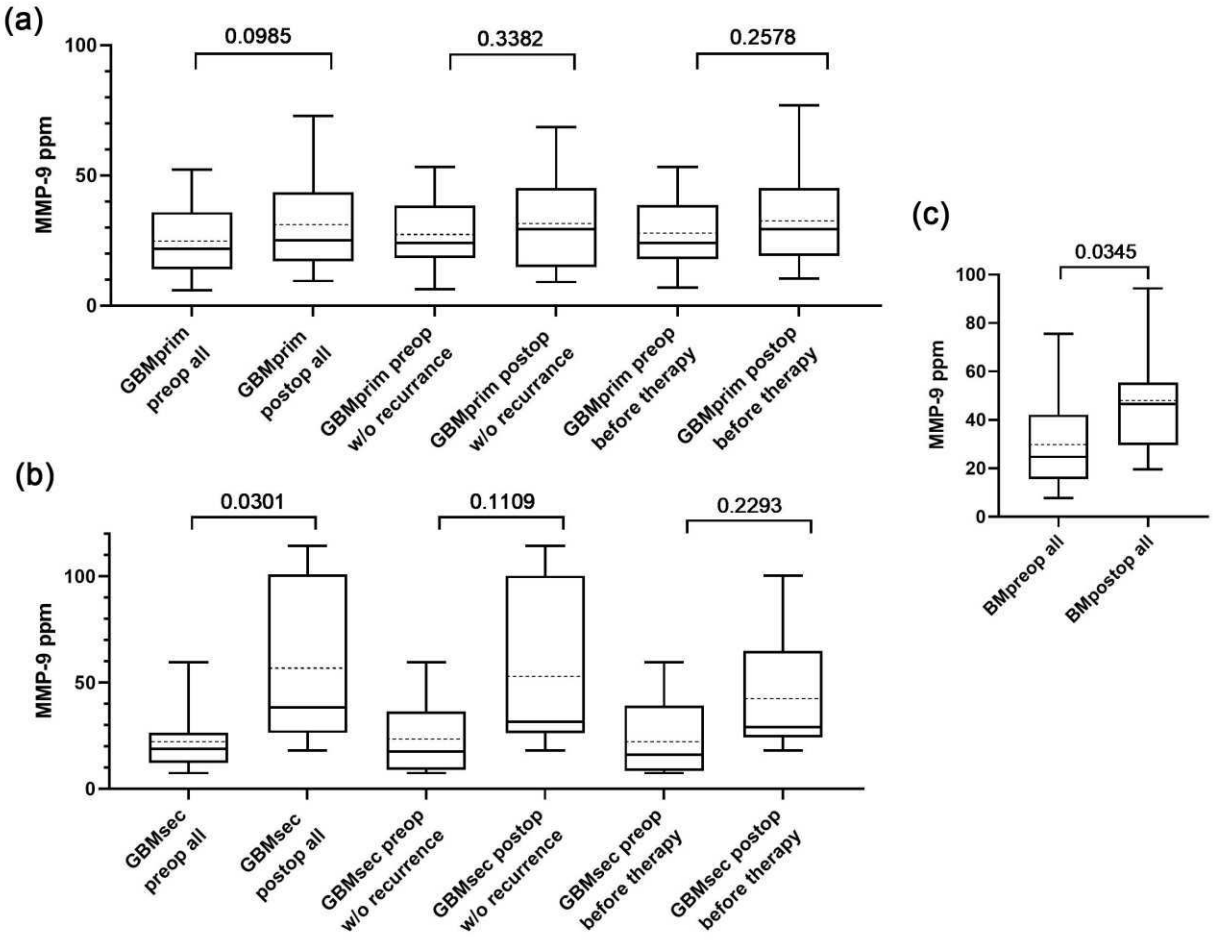

Figure S4. Comparison of all the preoperative and the postoperative GBM and BM samples in terms of MMP-9 level

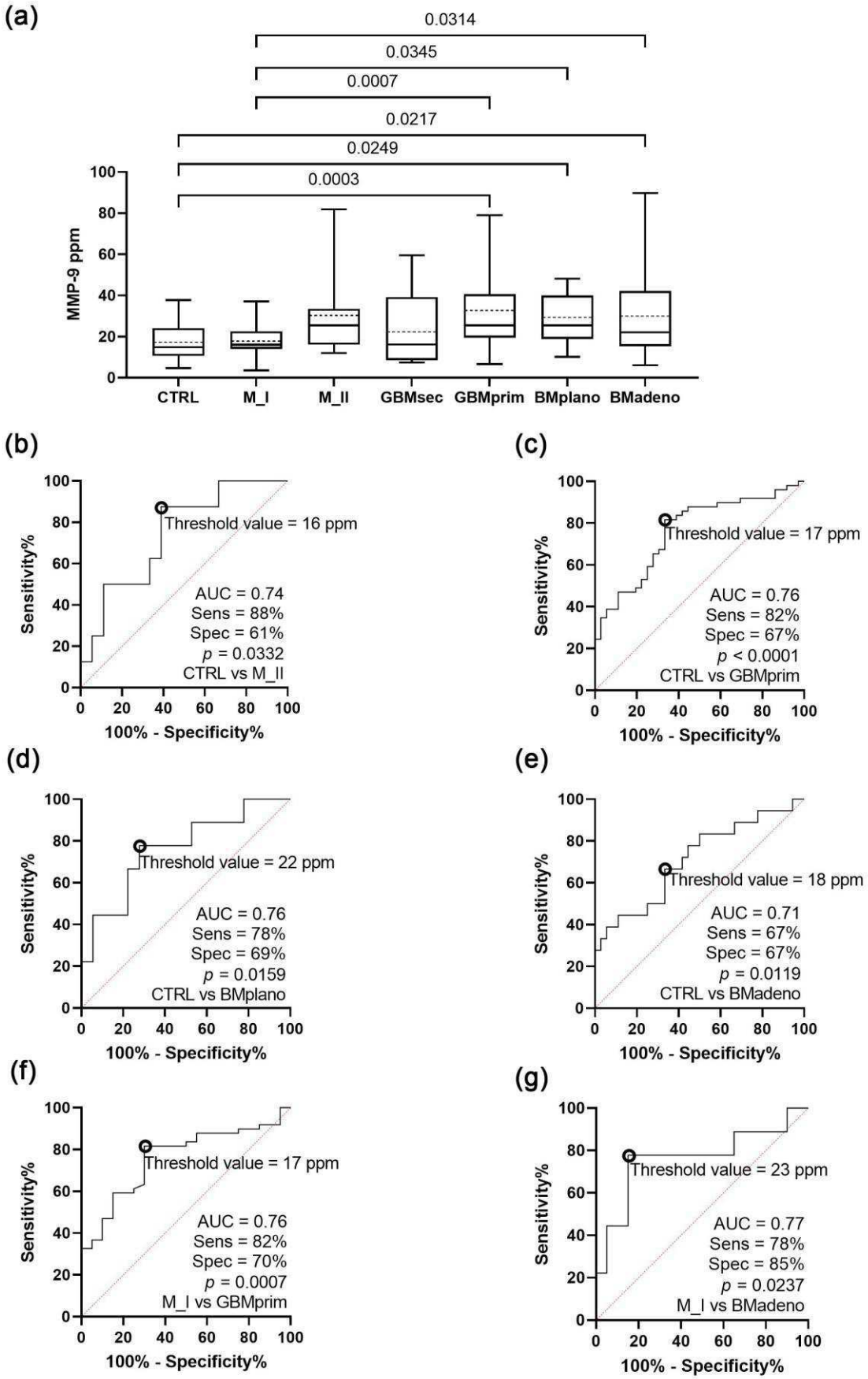

Figure S5. Differences among controls and various CNS tumour patients based on MMP-9 level of sEVs originated from preoperative serum samples

cancers

MDPI

Article

MMP-9 as Prognostic Marker for Brain Tumours: A Comparative Study on Serum-Derived Small Extracellular Vesicles

Gabriella Dobra [1,2,3], Edina Gyukity-Sebestyén [1,3], Mátyás Bukva [1,2,3], Mária Harmati [1,3], Valentina Nagy [1,3], Zoltán Szabó [4], Tibor Pankotai [5,6], Álmos Klekner [7] and Krisztina Buzás [1,3,*]

1 Laboratory of Microscopic Image Analysis and Machine Learning, Institute of Biochemistry, Biological Research Centre, Eötvös Loránd Research Network (ELKH), H-6726 Szeged, Hungary
2 Doctoral School of Interdisciplinary Medicine, Albert Szent-Györgyi Medical School, University of Szeged, H-6720 Szeged, Hungary
3 Department of Immunology, Albert Szent-Györgyi Medical School, Faculty of Science and Informatics, University of Szeged, H-6720 Szeged, Hungary
4 Department of Medical Chemistry, Albert Szent-Györgyi Medical School, University of Szeged, H-6720 Szeged, Hungary
5 Institute of Pathology, Albert Szent-Györgyi Medical School, University of Szeged, H-6720 Szeged, Hungary
6 Genome Integrity and DNA Repair Group, Hungarian Centre of Excellence for Molecular Medicine (HCEMM), University of Szeged, H-6720 Szeged, Hungary
7 Department of Neurosurgery, Faculty of Medicine, University of Debrecen, H-4032 Debrecen, Hungary
* Correspondence: buzas.krisztina@brc.hu; Tel.: +36-62-432-340

Simple Summary: The invasive nature of brain tumours, particularly glioblastoma, severely limits its therapy. Matrix-metalloproteinases (MMPs), enzymes involved in the degradation of the extracellular matrix, are associated with the invasiveness of brain tumours; hence, the determination of MMPs is critical for the monitoring of cancer patients. The aim of our comparative study was to evaluate the possible additional utility of the MMP-9 level of serum-derived small extracellular vesicles (sEVs) for characterising brain tumours. We established a relationship between low MMP-9 content in sEVs and improved survival, and discovered that MMP-9 levels considerably differed between tumour types and stages, showing a positive correlation with aggressiveness. We demonstrated on a large number of samples that the high MMP-9 level of serum-sEVs may serve as a negative prognostic marker for brain tumours.

Abstract: Matrix metalloproteinase-9 (MMP-9) degrades the extracellular matrix, contributes to tumour cell invasion and metastasis, and its elevated level in brain tumour tissues indicates poor prognosis. High-risk tissue biopsy can be replaced by liquid biopsy; however, the blood–brain barrier (BBB) prevents tumour-associated components from entering the peripheral blood, making the development of blood-based biomarkers challenging. Therefore, we examined the MMP-9 content of small extracellular vesicles (sEVs)—which can cross the BBB and are stable in body fluids—to characterise tumours with different invasion capacity. From four patient groups (glioblastoma multiforme, brain metastases of lung cancer, meningioma, and lumbar disc herniation as controls), 222 serum-derived sEV samples were evaluated. After isolating and characterising sEVs, their MMP-9 content was measured by ELISA and assessed statistically (correlation, paired *t*-test, Welch's test, ANOVA, ROC). We found that the MMP-9 content of sEVs is independent of gender and age, but is affected by surgical intervention, treatment, and recurrence. We found a relation between low MMP-9 level in sEVs (<28 ppm) and improved survival (8-month advantage) of glioblastoma patients, and MMP-9 levels showed a positive correlation with aggressiveness. These findings suggest that vesicular MMP-9 level might be a useful prognostic marker for brain tumours.

Keywords: liquid biopsy; small extracellular vesicles; matrix metalloproteinase-9; central nervous system diseases; brain tumour; prognostic marker; survival; glioblastoma

Citation: Dobra, G.; Gyukity-Sebestyén, E.; Bukva, M.; Harmati, M.; Nagy, V.; Szabó, Z.; Pankotai, T.; Klekner, Á.; Buzás, K. MMP-9 as Prognostic Marker for Brain Tumours: A Comparative Study on Serum-Derived Small Extracellular Vesicles. *Cancers* **2023**, *15*, 712. https://doi.org/10.3390/cancers15030712

Academic Editor: Maxim V. Berezovski

Received: 19 December 2022
Revised: 15 January 2023
Accepted: 21 January 2023
Published: 24 January 2023

1. Introduction

In tumour diagnostics, computed tomography (CT) and magnetic resonance imaging (MRI) scans are used to determine disease status, as well as to evaluate the response to treatments [1]; however, these techniques have well-known limitations [2]. MRI, for instance, can only detect tumour masses of sufficient size, and the treatment-related changes may overlap with residual or recurrent tumours [3]. Furthermore, it is also difficult to distinguish between central nervous system (CNS) malignancies such as glioblastoma multiforme and brain metastases [4], and MRI has limited applicability to identify long-term recurrence [5].

Further standard methods for profiling tumours require obtaining tumour samples through invasive surgical procedures. In addition to carrying a high risk of complications, the limitations of such invasive procedures include difficulty in acquiring tumour samples with high heterogeneity or in inaccessible positions and taking multiple biopsies in the occurrence of metastases, as well as monitoring tumour response or relapse. Thus, neuro-oncological research aims to discover novel methods suitable for monitoring CNS tumours in clinical practice [6].

Considering the challenges associated with traditional biopsies, recent oncology research has turned its focus from analysing whole tissues to analysing various biological fluids for tumour-derived components [7–9]; this technique is known as liquid biopsy (LB). LBs have drastically revolutionised the field of clinical oncology, offering ease in tumour sampling, continuous monitoring by repeated sampling, devising personalised therapeutic regimens, and screening for therapeutic resistance [10]. Tumour tissues release proteins, nucleic acids, circulating tumour cells, platelets, and tumour-derived extracellular vesicles into the bloodstream [11]; all these may serve as cancer biomarkers accessible via LB.

Extracellular vesicles (EVs) are small, lipid bilayer-enclosed vesicles released by both normal and neoplastic cells into the extracellular space [12] which enter into the circulation [13–15]. EVs are promising cancer biomarkers accessible through LB because they are cell-secreted, nano-sized, and stable in all body fluids [16,17]. Evs contain a sample of cytosolic milieu of the donor cells, including an abundance of DNA, RNA, proteins, and other analytes [18–21], while externally they also resemble their cell of origin [22]. Mounting evidence indicates that EVs contain a wealth of information that can be used to improve cancer diagnosis and prognostic evaluation [23–25]. The majority of the studies mainly focused on nucleic acids [26], but EV proteins are also receiving more and more attention in cancer diagnostics [27,28].

Finding blood–based biomarkers for CNS tumour monitoring is more challenging, as the blood–brain barrier (BBB) may prevent the release of tumour-related biomarkers into peripheral blood. The available evidence supports that tumour-derived EVs can cross the BBB [29,30]. However, currently no clinically relevant EV biomarkers are accepted for the monitoring of CNS tumours.

In a previous study, we analysed the protein content of whole serum as well as serum-derived small extracellular vesicles (sEVs)—EVs with a diameter of 30–200 nm size [31], theoretically called exosomes—of 96 patients suffering from CNS diseases. Comparative proteomic analysis by liquid chromatography–mass spectrometry (LC-MS) revealed that samples enriched in sEVs can provide an amplified source of relevant information; thus, sEVs may be more suitable than whole sera for separating patients with distinct CNS diseases using a protein panel [32]. Among the proteins of the determined panel, the matrix metalloproteinase-9 (MMP-9) was the most effective candidate in the separation of the patient groups.

Matrix metalloproteinases (MMPs) are zinc-dependent endopeptidases that play an essential role in the physiology of cells by degrading the extracellular matrix (ECM) [33]. It has been found that ECM has an important role also in cancer progression [34]. Some ECM proteins, such as fibronectin, thrombospondin-1, laminin, and osteopontin influence the phenotype of the tumour by affecting cell migration or angiogenesis. Interaction between cancer cells and ECM components is essential for cell transformation as well as

carcinogenesis [35]. In addition to the ECM degradation, MMPs have multiple biological functions in all stages of cancer, from initiation to the development of metastases [36–38]. Although they are associated with cancer cell survival and tumour spread, MMPs are synthetised by cancer cells in a very small amount. By secreting interleukin, interferon, growth factors, and extracellular MMP inductors, cancer cells stimulate surrounding host cells to produce MMPs in a paracrine manner [39]. MMPs secreted by normal cells can be bound to the cancer cell surface and can be utilised by the tumour cells [34].

Matrix metalloproteinase-9 (also known as 92 kDa type IV collagenase or gelatinase B) is one of the most complex forms of MMPs [33]. The role of MMP-9 in tumour tissue invasion and metastasis formation was already described in 1990 [40], and the elevated levels of MMP-9 in human brain tumours was also been reported in the 1990's [41]. Rao et al. also showed that the expression of MMP-9 is significantly upregulated in highly malignant gliomas and correlates with the progression, suggesting a role for MMP-9 in promoting the observed invasiveness [42].

In recent decades, several studies reported the upregulation of MMP-9 in the source of tumour tissue, which provides the opportunity to identify MMP-9 in the serum as well. In the case of some peripheral tumours, elevated MMP-9 levels in plasma were detected and associated with cancer development, invasion, and poorer survival [43]; however, according to other research, MMP-9 in blood samples cannot be considered useful in estimating the invasive capacity of cancer [44]. In the case of brain tumours, specifically for glioblastoma, serum and plasma MMP-9 content analyses yielded conflicting results [45–48].

Based on the findings of our previous study [32], we hypothesised that the contradictions in the literature could be resolved by subjecting the serum-derived sEVs instead of whole serum to the MMP-9 analysis, since EVs are stable in the blood and can cross the BBB, thereby allowing the identification of the tumour-specific distinctive biomolecules using a non-invasive, simple blood test.

For this purpose, in this study, 222 serum samples were collected from four patient groups according to the criteria of the National Ethical Committee, and MMP-9 analysis was performed on serum-derived sEV samples using enzyme-linked immunosorbent assay (ELISA). According to our knowledge, this was the first study that investigated the MMP-9 level of serum sEVs in human brain tumours. The large sample size allowed us to demonstrate the factors influencing the MMP-9 level (age, gender, surgical resection, recurrence, therapy), and was suitable for determining a measurable, significant difference in the sEV MMP-9 level associated with different diseases and patient survival outcomes. Calculating the MMP-9 concentrations of serum-derived sEVs enabled us to establish the cut-off values and the specificity and sensitivity of the analysis required in clinical practice.

2. Materials and Methods

2.1. Patients

Blood samples of 222 patients treated at the Department of Neurosurgery, of the University of Debrecen were analysed. Samples were obtained from patients with glioblastoma multiforme (GBM), meningioma (M), and brain metastasis originating from non-small cell lung cancer (BM). Control samples (CTRL) were collected from patients with lumbar disc herniation without evidence of cancer. In addition to the four main groups, subgroups were also distinguished based on histopathology, sampling time (prior or after to surgery), grading, recurrence, and treatment (Table 1). Detailed patient characteristics can be found in Table S1.

Table 1. Patient cohort and participation in the statistical analyses.

Characteristics	*n* = 222	%
Glioblastoma multiforme (GBM)	**121**	**54%**
secondary glioblastoma (GBMsec)	*18*	*15%*
preoperative samples (GBMsec preop)	9	50%
postoperative samples (GBMsec postop)	9	50%
primary glioblastoma (GBMprim)	*103*	*85%*
preoperative samples (GBMprim preop)	69 (10) [1]	67%
recurrence-related analysis	69	67%
original tumour	54	78%
recurrence	15	22%
therapy involvement analysis	69	67%
patients before therapy	54	78%
patients with therapy	15	22%
survival analysis	27	39%
>65 Years	11	41%
≤65 Years	16	59%
high MMP-9 level (≥28 ppm)	17	63%
low MMP-9 level (<28 ppm)	10	37%
postoperative samples (GBMprim postop)	14 **(10)** [1]	33%
Brain Metastasis (BM)	**37**	**17%**
carcinoma planocellulare (BMplano)	*13*	*35%*
adenocarcinoma (BMadeno)	*24*	*65%*
preoperative samples (BMpreop)	27 (6) [2]	73%
postoperative samples (BMpostop)	10 (6) [2]	27%
Meningioma (M)	**28**	**13%**
meningioma Grade I (M_I)	*20*	*71%*
meningioma Grade II (M_II)	*8*	*29%*
Control (CTRL)	**36**	**16%**
lumbar disc herniation	*36*	*16%*
male	16	44%
female	20	56%

Percentages indicate the participation rates within each statistical analyses; [1] Number of GBM patients involved in paired *t*-test; [2] Number of BM patients involved in paired *t*-test.

Blood samples were collected, processed to serum, and stored by the Neurosurgical Brain Tumour and Tissue Bank of Debrecen according to the criteria of the National Research Ethics Committee. An informed consent form was signed by each patient; the study was conducted in accordance with the Declaration of Helsinki. This study was carried out according to two ethical approvals, namely 51450-2/2015/EKU (0411/15), Medical Research Council, Scientific and Research Ethics Committee, Budapest, 30 October 2015 and 121/2019-SZTE, University of Szeged, Human Investigation Review Board, Albert Szent-Györgyi Clinical Centre, Szeged, 19 July 2019.

2.2. Preparation of Serum Samples

Blood samples were collected into BD Vacutainer SST II Advance Tubes, allowed to clot for at least 1 h at room temperature, and centrifuged for 20 min at 3000× *g*, 10 °C. The serum samples were stored at −80 °C until further processing.

2.3. sEV Isolation and Characterization

sEVs were isolated from the sera via differential centrifugation as described previously [32]. Briefly, after thawing on ice, sera were centrifuged for 30 min at 10,000× *g*, 4 °C, then for 70 min at 110,000 g, 4 °C, using a fixed-angle rotor (T-1270, Thermo Fisher Scientific, Waltham, MA, USA). The pellet was resuspended in particle-free Dulbecco's phosphate-buffered saline (DPBS, Lonza Group Ltd., Basel, Switzerland) and stored at −80 °C until further processing. This sEV isolation protocol served to reach intermediate

recovery and intermediate specificity according to the guideline 'Minimal Information for Studies of Extracellular Vesicles 2018' (MISEV2018) [31].

Following the main suggestions and requirements included in MISEV2018, sEVs were characterised by transmission electron microscopy (TEM), Western blot analysis (WB), and nanoparticle tracking analysis (NTA). The TEM and WB measurements were performed on a representative sample of each main group.

In order to examine sEV morphology, TEM analysis was performed using a Tecnai G2 20 X-Twin type instrument (FEI, Hillsboro, OR, USA), operating at an acceleration voltage of 200 kV. The samples were dropped on a grid (carbon film with 200 mesh copper grids (CF200-Cu, Electron Microscopy Sciences, Hatfield, PA, USA)) and dried without staining or other fixation procedure.

Confirming the presence of sEVs, CD81, CD5L, and calnexin markers were presented by Western blot analyses using NuPAGE reagents and an XCell SureLock Mini-Cell System (Thermo Fisher Scientific, Waltham, MA, USA) according to the manufacturer's protocols. The protein content of sEV samples was determined using a Pierce BCA Protein assay kit (Thermo Fisher Scientific, Waltham, MA, USA) and a benchtop microplate reader (Multiskan RC, Thermo Labsystems, Waltham, MA, USA) according to the manufacturer's instructions. For detection of the sEV markers in the four main groups, rabbit anti-human Alix (1:1000), rabbit anti-human CD5L (1:2000), and rabbit anti-human Calnexin (1:10,000) primary antibodies (all from Sigma-Aldrich, St. Louis, MO, USA), and HRP-conjugated anti-rabbit IgG (1:1000, R&D Systems, Minneapolis, MN, USA) secondary antibody were used. THP-1 cell line (ATCC, Manassas, VA, USA) lysate was used for the positive control for Calnexin.

Determining the nanoparticle size distribution and concentration of the tested samples, sEVs were diluted in particle free DPBS and analysed using a NanoSight NS300 instrument with 532 nm laser (Malvern Panalytical Ltd., Malvern, UK). Six videos of 60 s were recorded for each sample under constant settings (Camera level: 15; Threshold: 4, 25 °C; 60–80 particles/frame).

2.4. MMP-9 Analysis by LC-MS

The LC-MS analysis was performed in a previous study [32] based on the serum sEV samples of 96 from the total of 222 patients. Samples presented the four main groups, namely GBM, BM, M, and CTRL. Each group contained 24 individuals with mixed ages and genders; six-sample-pools were created from the individuals, allowing four parallel samples to be tested per group. Blood samples were collected one day prior to neurosurgical procedure in each tumour case. None of the patients received radio- or chemotherapy before tumour resection.

The detailed methodology of LC-MS measurements was described in the named article [32]. Briefly, for 'in solution' digestion, individual samples containing 20 µg protein were diluted to 26 µL and kept at 60 °C for 30 min to unfold and reduce the proteins, and then kept at RT for 30 min to alkylate the proteins. The samples were digested overnight at 37 °C with trypsin, then stopped by formic acid. The separation of the digested samples was carried out on a nanoAcquity UPLC (Waters, Milford, MA, USA), using Waters ACQUITY UPLC M-Class Peptide C18 column. The LC was coupled to a high-resolution Q Exactive Plus quadrupole-orbitrap hybrid MS (Thermo Scientific, Waltham, MA, USA). The quantitative measurements of digested individual samples were performed in DIA mode, and the analysis was conducted in Encyclopedia 0.81. A comprehensive spectral library of 10,000 human proteins was used for peptide identification.

2.5. MMP-9 Analysis by ELISA

To accurately measure MMP-9 content of sEVs, LEGEND MAX Human MMP-9 ELISA Kit (Biolegend, San Diego, CA, USA) was used according to the manufacturer's protocol. sEV isolates of 222 serum samples were measured individually, and the vesicles were disrupted in a detergent-free manner by five repeated freeze–thaw cycles to expose the

entire protein content. As we examined sEV isolates, potential interferences—observed in clinical immunoassays of sera [49]—are avoided. The assay procedures are briefly summarised below.

A standard curve was applied for each assay, and all samples were run in duplicate on separate plates. In the first step, 50µL assay buffer and 50 uL standard dilutions or 12× diluted samples were added to the appropriate wells, and the plates were sealed and incubated at room temperature for 2 h while shaking at 200 rpm. After the incubation, plates were washed four times with 1× wash buffer. The first step was followed by three more incubation steps, namely 100 µL of human MMP-9 detection antibody solution, 100 µL of Avidin-HRP solution, and 100 µL of substrate solution D were added to each well and incubated at room temperature for 1 h, 30 min, and 15 min, respectively. The plates were washed four times with 1× wash buffer between each incubation procedure. The last step was performed in the dark, and then the reaction was stopped by adding 100 µL of stop solution; the absorbance was immediately read at 450 nm and 570 nm on a benchtop microplate reader (Multiskan RC, Thermo Labsystems, Waltham, MA, USA).

2.6. Statistical Analyses

Before conducting any statistical tests, the MMP-9 level was normalised to the protein content of serum sEVs, meaning that MMP-9 concentration (ng/mL) was divided by protein concentration of the EV-enriched isolates (ng/mL) for every sample. The results of all the analyses are notated in parts-per-million (ppm), describing the individual values of MMP-9 in patients.

Outliers from the analysed groups were always excluded using the ROUT (robust regression followed by outlier identification) method with the Q parameter set to 1%. Then we examined the assumptions of normal distribution utilising the Shapiro–Wilk test and the homogeneity of variances by using the F test (comparing two groups) and the Brown–Forsythe test (comparing more than two groups).

The MMP-9 ppm concentrations of independent groups and matched samples were compared with Welch's test and the paired *t*-test, respectively. One-way ANOVA was used to examine differences between more than two groups.

To determine the relationship between continuous variables, linear regression analyses were conducted. To improve linearity in regression, skewed data were logarithmised.

The diagnostic potential of the MMP-9 ppm was evaluated using receiver operating characteristic (ROC) analyses. Kaplan–Meier analyses with log-rank tests were used to compare the overall survival rates of different groups.

The collected data about the MMP-9 content of sEVs were analysed statistically using GraphPad Prism 8.3.4.

2.7. Data Availability

All datasets generated during the current study are available from the corresponding author upon reasonable request. All relevant data of our experiments had been submitted to the EV-TRACK [50] knowledgebase (EV-TRACK ID: EV230005).

3. Results

3.1. The sEVs' MMP-9 Content Measured by ELISA Is Consistent with the Previous LC-MS Results

Our main goal was to compare the MMP-9 content of serum-derived small extracellular vesicle (sEV) samples from 222 patients with different CNS diseases. The four main investigated groups were glioblastoma (GBM), brain metastasis originated from non-small cell lung cancer (BM), meningioma (M), and lumbar disc hernia patients as controls (CTRL).

In a previous study, following the isolation and characterisation of sEV samples, LC-MS analysis was performed on 96 sEV samples. Each of the four groups (GBM, BM, M, and CTRL) contained 24 individuals, and six sample pools were created from the individuals allowing four parallel samples to be tested per group. As a result of the analysis, a 17 membered protein panel was constructed from the identified proteins which were able to

separate the four groups with 100% efficacy [32]. In this study, we investigated which of the 17 sEV proteins were the most suitable for distinguishing patients, and found MMP-9 to be the most significant (p = 0.0065, multi ROC AUC = 0.86).

Following the candidate selection, in the current study, the MMP-9 content of the 96 sEV samples was measured by ELISA, and the MMP-9 intensities (from LC-MS) were compared with the averaged MMP-9 concentrations (from ELISA) of the six-sample-pools to ascertain that ELISA is also capable of distinguishing the groups. The correlation analysis confirmed that the MMP-9 concentrations measured by ELISA were highly comparable to LC-MS measurements (r = 0.7264; p = 0.0022) (Figure 1).

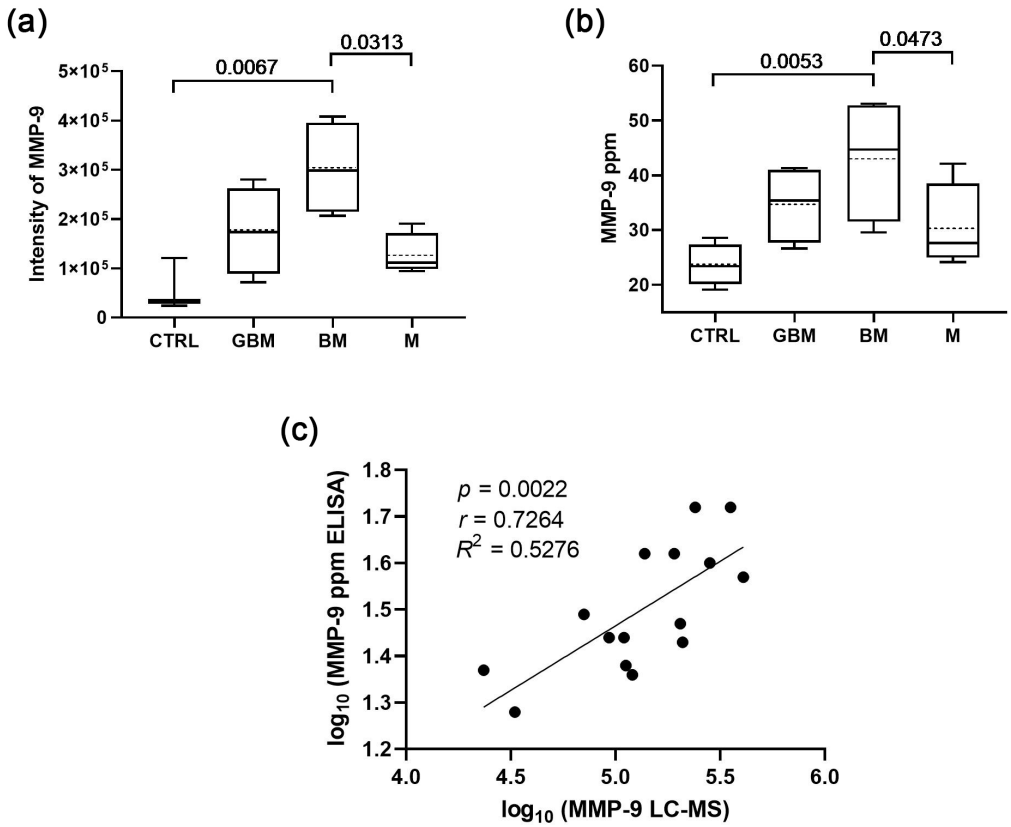

Figure 1. Comparison of the sEV MMP-9 content measured by ELISA with the LC-MS results. (**a**) MMP-9 levels of serum-derived sEVs based on LC-MS data (boxplot shows median with interquartile range, mean with dotted line, error bars range from the 5th–95th percentiles (nCTRL = 3, nGBM = 4, nBM = 4, nM = 4). (**b**) MMP-9 levels of serum-derived sEVs based on ELISA data (nCTRL = 4, nGBM = 4, nBM = 4, nM = 4). Dotted lines indicate mean values. (**c**) Correlation between the MMP-9 levels measured by LC-MS and ELISA.

Therefore, we aimed to perform ELISA measurements on the larger cohort; the MMP-9 concentrations and sEV characteristics can be found in Table S1 and Figure S1, respectively. The large sample size allows us to investigate factors influencing the MMP-9 level, and is suitable for examining whether there is a measurable, significant difference in the sEV MMP-9 level associated with different diseases and patient survival outcome. Measuring the MMP-9 concentrations of serum EVs instead of MMP-9 intensities enables the determination of the cut-off values required in the clinic, as well as the specificity and sensitivity of the test.

3.2. Several Factors Might Influence the MMP-9 Level of the Serum-Derived sEVs

Performing comparative studies between different tumours requires examining what factors (e.g., age, gender, surgical resection, recurrence, and therapy) may influence MMP-9 levels of serum-derived sEVs (Figure 2).

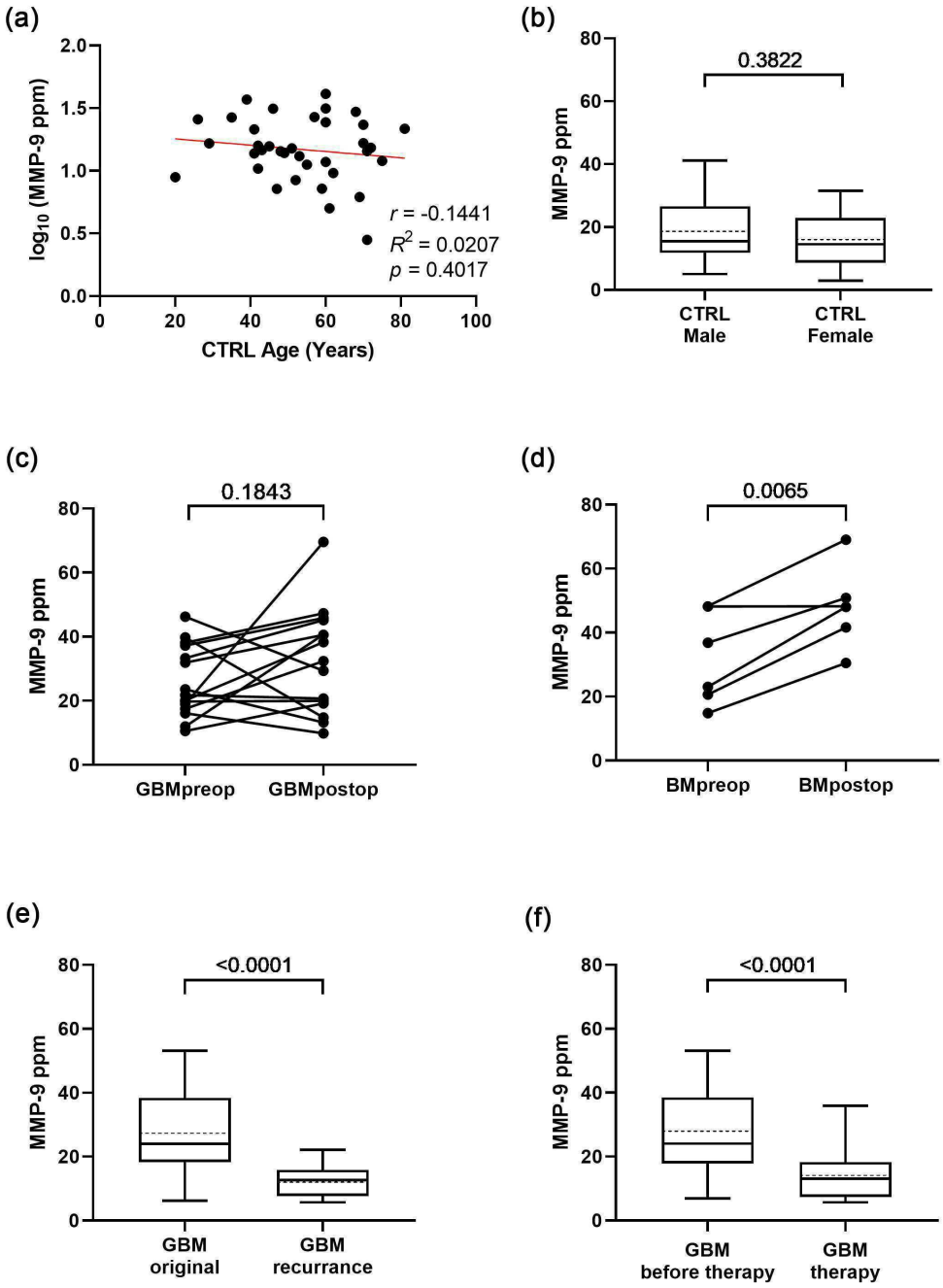

Figure 2. Factors influencing MMP-9 level of serum-derived sEVs. (**a**) Relationship between age and MMP-9 levels in the control group. (nCTRL = 36). (**b**) MMP-9 levels of the two genders in the control group (boxplots show the median with interquartile range, mean with dotted line, error bars range from the 5th–95th percentiles; nCTRL male = 16, nCTRL female = 20). (**c**,**d**) Changes in individual patient's MMP-9 levels before and after surgical resection for the GBM and BM groups, respectively (nGBM preop-postop = 14, nBM preop-postop = 6). (**e**) MMP-9 levels of serum-derived sEVs regarding the original tumour and the recurrence in GBM group before surgical resection (nGBM original = 52, nGBM recurrence = 14). (**f**) MMP-9 levels in GBM group to treatment status (nGBM before therapy = 52, nGBM therapy = 15).

The MMP-9 level was normalised to the total protein content of serum sEVs, meaning that MMP-9 concentration (ng/mL) was divided by protein concentration of the EV-enriched isolates (ng/mL) for every sample. The results of all the analyses are notated in parts-per-million (ppm) describing the individual values of MMP-9 in patients (Table S1).

Age and gender analyses were carried out in the control group, eliminating the possible MMP-9-modifying effect of any tumour disease. Correlation analysis revealed that there is no distinct relationship between age and MMP-9 levels (Figure 2a). The MMP-9 level of serum-derived extracellular vesicles shows no significant difference between male and female patients, as determined by Welch's test (Figure 2b). Based on these findings, further data analyses were conducted regardless of the age or gender of the patients.

Examining the effects of surgical resection on the MMP-9 level of sEVs, paired *t*-tests were completed in the GBM and BM groups (Figure 2c,d, respectively). The MMP-9 levels were similar ($p = 0.1843$, fold change = 15%) before and after the surgical resection in the case of primary GBM patients, while BM samples showed marked increase ($p = 0.0065$, fold change = 209%) after resection.

Further examination on preoperative GBM samples found a distinct difference between the original tumour and the recurrence based on MMP-9 levels of serum sEVs (Figure 2e), and the recurrence showed a lower level of MMP-9 on average ($p < 0.0001$).

Determining the influence of the administered therapy, MMP-9 levels were also compared based on whether or not GBM patients had received treatment at the time of sampling. Our result ($p < 0.0001$) indicates that therapy might decrease the MMP-9 levels of the circulating sEVs (Figure 2f).

In addition to the paired *t*-test shown in Figure 2c,d, unpaired *t*-tests (Welch's tests) were performed on all primary and secondary GBM samples, as well as on all BM samples to determine the effect of surgical resection on a broader cohort (Figure S2). First, all the preoperative and postoperative samples were evaluated; then, subsequent exclusions were made for individuals who had relapsed or received therapy. The unpaired *t*-tests on primary GBM and BM samples (Figure S2a,c) yielded the same results as the paired *t*-tests (Figure 2c,d); however, for the secondary GBM samples, the significant differences were erased when the recurrent or treated samples were excluded from the statistical analysis (Figure S2b).

Based on our findings, we can conclude that in addition to the disease types, surgical resection, recurrence, and therapy might influence the MMP-9 level of the serum-derived sEVs. Due to these findings, all subsequent analyses were conducted exclusively on samples obtained prior to surgical resection and therapy administration.

3.3. MMP-9 Level of Serum sEVs Differs in Various CNS Tumours Showing a Positive Correlation with Tumour Aggressiveness

Further statistical analyses were performed in order to identify if there is a difference between the serum sEV MMP-9 levels of the patient groups (Figure 3).

As a first step, Welch's test was used to compare the control group with all the tumour patients (Figure 3a). Based on ROC analysis, the two groups were significantly distinguishable ($p = 0.0002$) using a cut-off point of 16 MMP-9 ppm with 74% sensitivity, 61% specificity, and an AUC of 0.70 (Figure 3b).

The tumour patients then were divided into M, GBM, and BM, and we found that the differences remained significant between controls and malignant tumours, as well as between the benign and malignant tumours (Figure 3c). Separate comparison resulted in increased specificity, sensitivity values, and AUC scores in the case of control-malignant tumour comparisons at the expense of control-benign comparisons (Figure 3d).

In the last step, the patients were divided into further subgroups based on histopathology. In the subgroup analysis, primary and secondary GBM, patients with grade I and II meningiomas, and brain metastases from patients with adenocarcinoma and carcinoma planocellulare were distinguished. The detailed results are presented in Figure S3. The

comparisons of the patient groups showing significant differences in MMP-9 levels resulted in AUC scores up to 0.77.

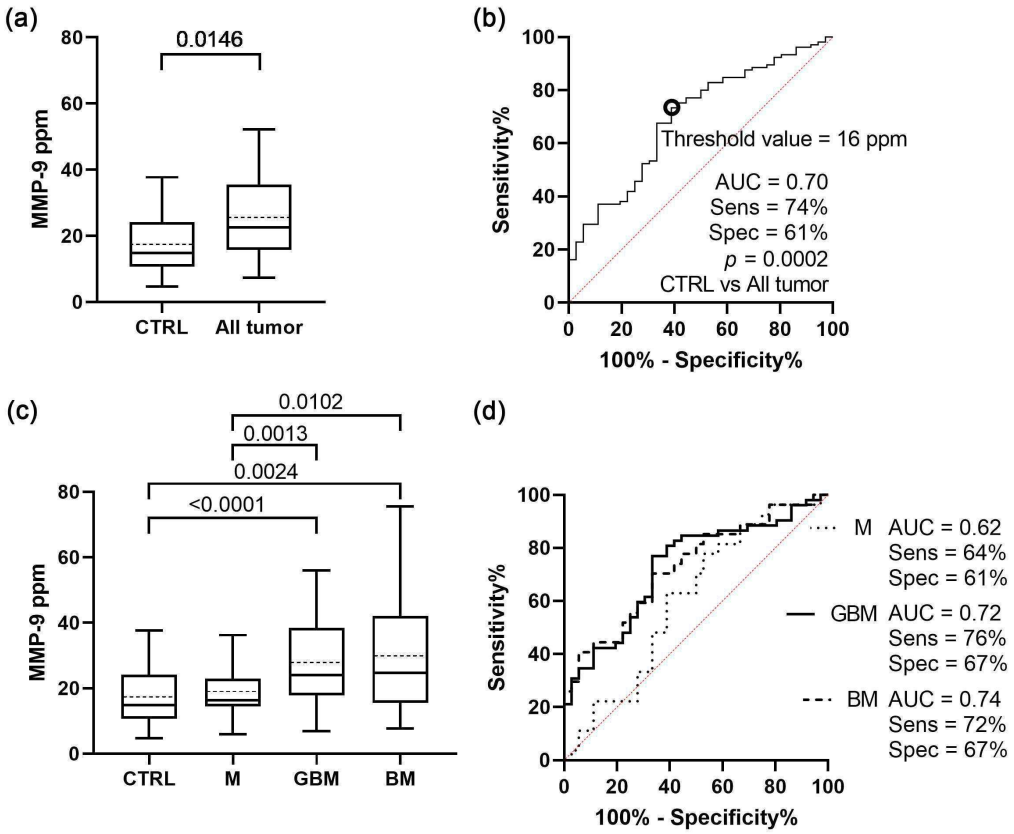

Figure 3. Comparative analyses of MMP-9 level of serum sEVs on the four main groups. (**a**) Graph shows the MMP-9 level of the control group comparing all the tumour patients (median with interquartile range, mean with dotted line, error bars range from the 5th–95th percentiles; nCTRL = 36, nAll tumour = 105). (**b**) ROC curves for exploring the differences between the MMP-9 level of the control group and all the tumour patients (nCTRL = 36, nAll tumour = 109). (**c**) Diagram shows the MMP-9 level of serum sEVs among the four patient groups (nCTRL = 36, nM = 27, nGBM = 52, nBM = 27). (**d**) ROC curves for comparing the three tumour groups to controls (nCTRL = 36, nM = 27, nGBM = 52, nBM = 27).

Our data indicate that patients suffering from malignant, but not benign brain tumours can be distinguished from CTRL patients based on the MMP-9 level of serum sEVs, and that the MMP-9 level of serum sEVs differs between CNS tumour types, showing a positive correlation with tumour aggressiveness.

3.4. The sEVs' MMP-9 Level Might Be a Prognostic Marker for Overall Survival in GBM Patients

After analysing the influencing factors, we aimed to determine whether MMP-9 levels correlate with disease progression/patient survival. To assess the prognostic value of MMP-9 levels in serum sEVs, we analysed the preoperative serum samples from 27 GBM patients. Patients in this study were not administered by any treatment at the time of sampling (Figure 4).

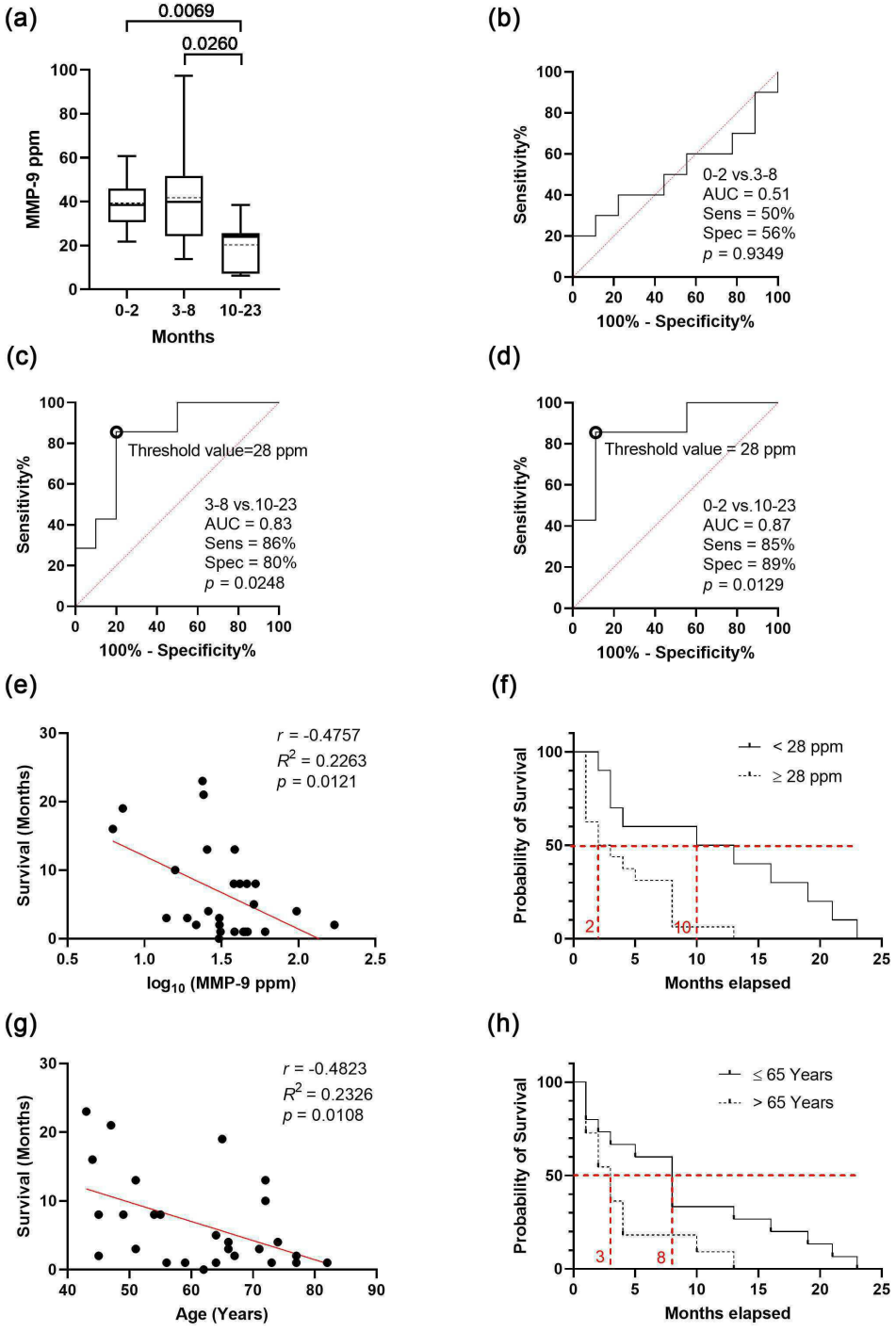

Figure 4. Investigation of survival in GBM patients. (**a**) Differences among the short-, medium- and long-term survival based on MMP-9 level of serum derived sEVs of GBM patients (median with interquartile range, mean with dotted line, error bars range from the 5th–95th percentiles, dotted lines indicate mean values). (**b**–**d**) Receiver operating characteristic (ROC) curves for comparing the short- (0–2 months), medium- (3–8 months) and long-term (10–23 months) survival groups (threshold values of the group-membership score are marked with black circles). (**e**) Correlation between MMP-9 level and survival in the GBM group (nGBM = 27). (**f**) Overall survival according to low and high (n < 28 ppm = 10 and $n \geq$ 28 ppm = 17) MMP-9 level. (**g**) Relationship between age and survival in the GBM group (nGBM = 27); (**h**) Overall survival according to the age ($n \leq$ 65 years = 16 and n > 65 years = 11).

To reveal the prognostic value of sEVs' MMP-9 level on survival, subjects were divided into three groups based on their survival time (short-, medium- and long-term) using 0–2, 3–8, 10–23 months as the cut-offs (Figure 4a). Long-term survival was found to be associated with a significantly lower MMP-9 level compared to the MMP-9 levels of the other two groups (Figure 4b–d). These differences represent a high specificity and sensitivity of 80–89% at a threshold of 28 MMP-9 ppm, and AUC values of 0.83–0.87 in ROC analyses allow efficient distinction of these survival groups.

These results suggest that there should be a correlation between the MMP-9 level of serum sEVs and overall survival (OS), so we performed an analysis where we observed that lower survival time was associated with higher MMP-9 level (Figure 4e). To determine the extent of the influencing effect of MMP-9 levels on survival, patients were separated into two groups, with the previously established threshold of 28 ppm. Based on the Kaplan–Meier chart, patients with low MMP-9 level (<28 ppm) presented with a significant OS benefit (HR 2.401, 95%CI 1.095 to 5.261, $p = 0.0063$), which represents an eight-month increase in the median OS (Figure 4f).

The probability of survival also decreased with age; therefore, we repeated the examination with a cut-off of 65 years. According to the Kaplan–Meier chart, patients under the age of 65 had a five-month increase (HR 2.037, 95%CI 0.8524 to 4.869, $p = 0.0340$) in median survival (Figure 4c). It is crucial to note that age and MMP-9 level are independent (see Figure 2a); we can conclude that the MMP-9 level of serum sEVs may influence survival regardless of age.

To summarise the main findings, analysis of samples taken prior to surgical resection and the administration of therapy revealed a negative correlation between higher MMP-9 levels and the survival, and long-term (10–23 months) survival found to be associated with low MMP-9 level (<28 ppm). Our results support that the high level of MMP-9 in serum-derived sEVs might be a negative prognostic marker of the probability of survival in GBM patients.

4. Discussion

In recent years, oncology research has turned its focus from analysing whole tumour tissues to analysing various biological fluids for tumour-derived components [7,9]. Although several attempts have been made to identify GBM-specific biomarkers in serum [11,51,52], to the best of our knowledge, serum/plasma biomarkers are not routinely used for clinical monitoring of glioblastoma. The lack of reliable non-invasive serum-based biomarkers for GBM can be explained by several reasons, including (1) the extremely high complexity of tumour tissues (hence the name glioblastoma multiforme), (2) the barrier function of BBB that prevents the 'tumour information' from entering the circulation, and (3) the presence of abundant molecules that can 'mask' the potential biomarker candidates.

Using EV samples instead of whole sera, it is possible to amplify the signals released by brain tumours into the circulation [32]. Extracellular vesicles are stable in the blood [12], and can cross the BBB [29,30]; moreover, EVs may contain tumour-related molecules in higher concentrations and are accompanied by less contaminating molecules that may bias the analytical findings. These advantageous properties of EVs increase the possibility of identifying molecules that provide valuable information regarding tumours.

Due to the priority of living-cell secretion, large amounts and stable circulation compared to circulating tumour cells and ctDNA, exosome-based liquid biopsy has been tested in clinical trials and several of them have been approved and reached the market. In 2016, Exosome Diagnostics proposed the first exosome-based liquid biopsy in the world [22], ExoDx™ Lung (ALK), for the isolation and analysis of exosomal RNA from blood samples. In addition, the ExoDx Prostate IntelliScore (EPI) has been certified by FDA [53], and 26% of unnecessary needle biopsies were avoided with an appropriate threshold [54]. High sensitivity was achieved in prospective studies; therefore, they could be used to assist in the early diagnosis of cancer and eliminate unnecessary prostate biopsy [55].

According to Lihares et al., screening for gliomas has no clinical relevance at this time [48]. This is due to the low incidence, absence of sensitive biomarkers in plasma, and the observation that gliomas can develop apparently de novo in a matter of weeks or months. However, a non-invasive biomarker that can be used to estimate tumour state and patient survival would be of great assistance to physicians.

Based on these considerations, we sought to determine whether the MMP-9 (an endopeptidase involved in ECM degradation, thus having a role in tumour invasion) level of serum-derived sEVs can provide information about patient survival. ELISA was used to measure the MMP-9 content of 222 sEV samples isolated from whole serum for this purpose. Serum samples were collected from patients with the most common malignant, benign, and metastatic brain tumours, namely glioblastoma multiforme, meningioma [56], and brain metastasis of non-small cell lung cancer [57], and from control patients with lumbar disc herniation.

Following the measurements, comparative analyses on the MMP-9 level of sEVs were conducted. We determined that surgical resection, recurrence, and therapy can modify the MMP-9 level, but neither age nor gender can. We also detected statistically significant differences in the sEVs' MMP-9 levels associated with various diseases, as well as a correlation between low MMP-9 level and longer survival time, which highlighted the prognostic value of vesicular MMP-9 level. However, functional studies, including MMP-9 activity measurements, would be needed to explore the causal relationship between tumour progression and the MMP-9 level of serum sEVs.

We hypothesise that the higher MMP-9 level of sEVs observed in patients with a poor prognosis is due to the tumour itself. However, there is a debate surrounding the source of the tumour-specific EVs in the blood. Osti et al., as a confirmation of the tumour origin of extracellular vesicles, employed an orthotopic transplantation of tumour-initiating cells (TICs) isolated from human GBM. GBM TICs expressing the exosomal marker CD9 coupled with the GFP protein were produced using lentiviral transduction. Because GBM-derived extracellular vesicles express CD9 on their surface, they were distinguished from natural GFP-negative mouse extracellular vesicles by following the GFP signal. According to their data, nearly half of the extracellular vesicles in the peripheral circulation of transplanted mice were tumour-derived [58]. However, using EV capture and staining techniques that allow differentiation of host cell and GBM-derived EVs, Fraser et al. demonstrated that tumoral EVs often present less than 10% of all EVs with extensive heterogeneity in tumour marker expression in GBM patient plasma [59]. The proportion of tumour-derived sEVs in the blood is a very interesting issue, although its clarification is beyond the scope of our study.

To the best of our knowledge, this study was the first one that analyses the MMP-9 content of serum sEVs; nevertheless, a few serum MMP-9 investigations have been published with contradictory findings. Hormingo et al. found that YKL-40 and MMP-9 could be monitored in patients' serum and help confirm the absence of active disease in GBM [45]. However, after five years, the same group (Iwamoto et al.) conducted a longitudinal prospective study of MMP-9 as a serum marker in gliomas, and the larger cohort could not confirm the previous findings. Serum MMP-9 showed no utility in determining glioma disease status and was not a clinically relevant prognostic marker of survival. There was no statistically significant correlation between serum MMP-9 levels and radiographic disease status. Longitudinal increases in MMP-9 were weakly associated with shorter survival in glioblastoma patients, but they were not independently associated with survival after adjusting for age, extent of resection, and performance status [46]. In contrast, Ricci et al. confirm that MMP-9 levels are significantly higher in high-grade glioma, in low- and high-grade meningioma samples, as well as in metastasis specimens compared to healthy individuals ($p < 0.001$) [47]. This latter research of serum MMP-9 levels is in line with our sEV-based findings.

Several technical issues may have contributed to the poor and contradictory serum/plasma results. It is important to note that the measurement of MMPs in body fluids can be in-

fluenced by the type of fluid and method of collection and storage. EDTA or heparin, for instance, can affect the baseline serum/plasma concentrations of MMP-9 [60]. To solve this issue, for instance, Ricci et al. prepared native serum using plastic tubes without coagulation accelerators, to prevent the release of gelatinases during platelet activation [47]. We used BD Vacutainer SST II Advance Tubes acril gel with only silica particles as clot activators.

Another difficulty is that plasma MMP-9 may be unstable and degrades rapidly even when stored at −80 °C [61,62]. This problem can be alleviated by using sEVs instead of serum, as the high biological stability allows long-term storage of specimens for exosome isolation and detection [63]. Diagnostic analytes, RNA, DNA, or protein cargo in exosomes maintain this informative profile's stability during sample storage, which is essential for the development of biomarkers using retrospective samples [64]. This raises the possibility of monitoring MMP-9 not only at the protein, but also at the mRNA level.

Recently, several research groups have studied vesicular mRNA that can be isolated from body fluids [65–68]. However, the majority of MMP-9 mRNA investigations are conducted on tissue samples [69–71], and there are only a few studies assessing MMP-9 mRNA and MMP-9 protein in serum [72–74]. Although these are not comparative studies of cancer patients, they indicate that increase in MMP-9 is detectable with similar efficiency at both mRNA and protein levels. At the same time, due to the complex regulation of translation and protein degradation, there is no strict correlation between mRNA and protein abundances [75–77]. Thus, we assume that vesicular MMP-9 could be measured at the mRNA level as well, but its prognostic value would need further investigation.

It is also important to note that there is no gold standard method for sEV isolation, which may impede the reproducibility of experimental findings in EV research. The applied technique impacts the isolation efficacy in terms of yield, purity, and EV composition, which may interfere with downstream analyses, including the molecular cargo profiling [78–81]. Another technical issue in EV research is that storage at −80 °C and freeze–thaw cycles may affect stability of EV membranes leading to EV disruption and subsequent fusion phenomena, which may influence the EV characteristics, including biological activity [82–85], but enable the use of repeated freeze-thaw cycles to expose the entire EV cargo prior to downstream analyses (as it was done here and previous studies [86,87], or to load therapeutic cargo into vesicles [88,89]. To enhance the reliability, transparency, and reproducibility of EV studies, the ISEV published the MISEV guidelines, which discuss all technical issues and provide help to set up the experimental protocols best fit to the research question [31,90].

Prior studies have suggested that MMP-9 measurements in serum do not reliably reflect circulating MMP-9 levels and may be artificially high compared to results obtained from plasma samples [43,91–93], but Iwamoto et al. showed that serum and plasma MMP-9 samples were highly correlated in their large sample size, so serum, and thus serum-derived sEV samples, could be used appropriately [46].

In order to find the putative source of the MMP-9 as biomarker, Ricci et al. correlated the expression of serum MMP-9 with the expression of the same protein in the tumour tissue. To address this aim, glioma tissues were subjected to immunohistochemistry with MMP-9 antibody. They discovered that the delocalisation of the MMP-9 signal from glioma cells to endothelial cells of neoplastic blood arteries is directly associated with tumour malignancy. In line with these findings, previous immunohistochemical and in situ hybridization studies demonstrated that, in high-grade glioma, MMP-9 expression is primarily restricted to perivascular regions at the infiltrating borders of the tumour and, in the majority of cases, to endothelial cells, with a close association to tumour malignant behaviour [94,95]. To determine the origin of MMP9 in GBM, Jiguet-Jiglaire et al. analysed its expression by immunohistochemistry. According to their findings, MMP-9 staining was mainly located in the microvascular proliferation, and also in inflammatory cells and circulating intravascular cells. No staining was observed in glioblastoma cells or in the extracellular matrix [39].

The successiveness of a biomarker candidate can be determined by comparing its efficacy to that of existing clinical procedures. We were unable to correlate the sEVs' MMP-9

level of the patients with their MRI status; nevertheless, contradictory findings exist in the literature. Hormigo et al. observed that levels of MMP-9 were higher in the serum samples of patients with high-grade glioma after surgery, while the MMP-9 concentrations were significantly lower in glioblastoma patients with no radiographic evidence of disease in comparison to the subjects with active tumour [45]. In contrast, Iwamoto et al. found that there was no statistically significant correlation between serum MMP-9 levels and radiographic disease status [46]. Moreover, in a very recent study by Jiguet-Jiglaire et al., MMP-9 did not correlate with glioblastoma tumour volume, invasion, or angiogenesis assessed by neuro-imaging [39].

In addition to disease status, other patient characteristics may influence MMP-9 levels in the patient sera. Otero-Estévez et al. found that MMP-9 was significantly correlated with gender and age when examining the serum of colorectal cancer patients [44]. In contrast, in our study on serum-derived sEVs, there was no distinct relationship between age and MMP-9 levels, and there was no significant difference between male and female patients in terms of MMP-9 level (Figure 2). Based on our findings, data analyses on serum-derived sEVs can be conducted regardless of the age or gender of the patients.

The surgical resection also can affect the extracellular vesicle concentration and the MMP-9 content of serum/plasma EVs. Osti et al. measured a significant drop ($p < 0.001$) in plasma extracellular vesicle concentration after surgery [58]. Hormigo et al. observed that levels of MMP-9 were higher in the sera samples of patients with high-grade glioma after surgery, suggesting that increases in the serum level of this protein may be associated with brain inflammation and breakdown of the blood–brain barrier, rather than be a true measure of tumour burden [45]. In our study, the MMP-9 level of serum sEVs were similar before and after the surgical resection in the case of primary GBM patients ($p = 0.1843$; $n = 14$), while BM samples showed marked increase ($p = 0.0116$; fold change = 209%) after resection. This intriguing phenomenon relies on the basis of a few BM samples ($n = 6$), and therefore should be supported by further measurements.

Determining the influence of the administered therapy, MMP-9 levels were also compared based on whether or not GBM patients had received treatment at the time of sampling. Our result ($p < 0.0001$) indicated that therapy might decrease the MMP-9 level of circulating sEVs (Figure 2f). Further examination on preoperative GBM samples found a distinct difference between the original tumour and the recurrence based on the MMP-9 level of serum sEVs (Figure 3e). Although recurrence shows a lower level of MMP-9 on average ($p < 0.0001$), the majority of these GBM patients received treatment, therefore the decrease in MMP-9 cannot be attributed solely to relapse. Tabouret et al. reported that urine protein levels of MMP-2 also decreased and were considered to be related to treatment response, although this was not confirmed in an additional patient cohort [96].

One of the main findings of our study relies on the correlation analysis of samples taken prior to surgical resection and the administration of therapy on MMP-9 level and survival. A negative correlation was revealed between higher MMP-9 levels and the survival, and the long-term (10–23-month) survival was found to be associated with a low MMP-9 level (<28 ppm). Our results support that the high level of MMP-9 in serum-derived sEVs might be a negative prognostic marker of the probability of survival in GBM patients. Osti et al. tested for possible associations between plasma extracellular vesicle concentration and patient outcomes. Patients with GBM were ranked according to their extracellular vesicle content and divided into high-content or low content groups; no significant differences in PFS or OS were found [58]. Jiguet-Jiglaire tested patients with recurrent glioblastoma prior to treatment and found decreased plasma levels of MMP-9 associated with increased OS [39].

By measuring the level of MMP-9, we may determine the efficacy of the treatment. For instance, the majority of patients with GBM will experience relapse despite surgery and standard first-line treatment consisting of radiotherapy with concurrent and adjuvant temozolomide. In certain cases, therapeutic options at the time of recurrence include surgery or reirradiation, whereas in other cases, bevacizumab is the preferred option worldwide. Jiguet-Jiglaire et al. demonstrated that low baseline plasma levels of MMP-9

were associated with a high response rate and a prolonged PFS and OS in patients with recurrent GBM treated with bevacizumab but not cytotoxic chemotherapy. In addition, they observed that MMP-9 plasma levels decreased during treatment with bevacizumab and tended to rise with disease progression. In a retrospective analysis performed in the Avaglio trial (a randomised phase III trial that compared bevacizumab versus placebo in addition to standard of care in newly diagnosed glioblastoma patients), a low plasma level of MMP-9 at baseline consistently predicted PFS and OS gain associated to bevacizumab [39].

Unmet medical need exists for biomarkers able to predict response to antiangiogenic agents. According to the ClinicalTrials.gov database, only a few studies are currently being conducted to determine the predictive value of MMP-9 level on cancer treatment response. One study aims to investigate the predictive impact of circulating MMP-2 and MMP-9 on the progression-free survival of patients with metastatic kidney cancer treated with anti-angiogenic agents (Sunitinib or Pazopanib) in comparison with two untreated cohorts (NCT03185039). Another study evidenced the role for MMP-9 in the primary or acquired resistance to bevacizumab; therefore, in their trial they use monoclonal antibody GS5745 that may overcome resistance to bevacizumab through a specific inhibition of MMP-9. The phase I study is the first step to analyse the tolerance, determine the recommended dose of the combination, and explore the impact of GS5745 on MMP-9 plasma levels and multimodal imaging in patients with recurrent glioblastoma (NCT03631836).

On the other hand, Farina and Mackay draw attention to the Janus-faced nature of MMP-9. This important molecule plays an essential role in tumour biology, from initiation/promotion to angiogenesis, dissemination, immune surveillance, and metastatic growth. However, MMP-9 also possesses antitumour activity and serves essential physiological functions [97]. In order to determine the potential therapeutic efficacy of inhibiting MMP-9 function in cancer therapy, it is necessary to develop specific inhibitors of MMP-9, to inhibit the tumour promoting function of MMP-9 instead of suppressing the anti-tumour effect. Validation of MMP-9's predictive value in a prospective study is a crucial step toward its possible routine therapeutic application. In addition, it may be advantageous to (i) investigate the invasion- and angiogenesis-related molecules co-expressed with MMP-9, or (ii) develop strategies for inhibiting tumour-specific activators of MMP-9 instead of using direct inhibitors.

In summary, we have demonstrated that sEVs' MMP-9 content is suitable for estimating the probability of patient survival and it allows us to obtain information about CNS tumour aggressiveness. This biomarker's benefits include its accessibility (a simple blood test), affordability, fast detectability, ease of implementation, and reproducibility. Collectively, these advantageous characteristics would permit the application of serum sEVs' MMP-9 for non-invasive patient monitoring.

5. Conclusions

Glioblastoma is the most prevalent primary brain tumour in adults, comprising 45.2% of all malignant primary CNS tumours, with a median survival time of 15 months. On average, 5.5% of patients live five years after their diagnosis [98].

The link between the survival of glioblastoma patients and their MMP-9 level of serum-derived sEVs is revealed in our article; hence, the identification of sEVs' MMP-9 is of great importance. Our presented fast-to-perform and non-invasive method can support clinical decision making.

Supplementary Materials: The following supporting information can be downloaded at: https://www.mdpi.com/article/10.3390/cancers15030712/s1, Figure S1: Characterisation of isolated particles; Figure S2: Comparison of all the preoperative and the postoperative GBM and BM samples in terms of MMP-9 level; Figure S3: Differences among controls and various CNS tumour patients based on MMP-9 level of sEVs originated from preoperative serum samples; Table S1: Detailed patient characteristics.

Author Contributions: Conceptualization, G.D. and K.B.; methodology, G.D. and E.G.-S.; validation, M.H.; formal analysis, G.D. and M.B.; investigation, E.G.-S., V.N., M.H., Z.S. and G.D.; resources, Á.K., T.P. and K.B.; writing—original draft preparation, G.D.; writing—review and editing, K.B.; visualisation, G.D. and M.B.; supervision, K.B.; funding acquisition, K.B.; All authors have read and agreed to the published version of the manuscript.

Funding: This study was supported by the following research grants: GINOP-2.2.1-15-2017-00052 (K.B.), TKP-2021-EGA-09 (K.B.), OTKA-K143255 (K.B.), Szent-Györgyi Albert Research Fund provided by University of Szeged (K.B.), "National Brain Research Program NAP 2.0" (Á.K.), ÚNKP-22-5-SZTE-318 (T.P.). The project has received funding from the EU's Horizon 2020 research and innovation program under grant agreement No. 739593. (T.P.), ÚNKP-22-3-New National Excellence Program of the Ministry for Innovation and Technology from the source of the National Research, Development and Innovation Fund (M.B., V.N.) Project no. TKP-2021-EGA-09 has been implemented with the support provided by the Ministry of Culture and Innovation of Hungary from the National Research, Development and Innovation Fund, financed under the TKP2021-EGA funding scheme (K.B.).

Institutional Review Board Statement: The study was conducted in accordance with the Declaration of Helsinki, and ethical approval was obtained from two independent bodies (51450-2/2015/EKU (0411/15), Medical Research Council, Scientific and Research Ethics Committee, Budapest, 30 October 2015, and 121/2019-SZTE, University of Szeged, Human Investigation Review Board, Albert Szent-Györgyi Clinical Centre, Szeged, 19 July 2019).

Informed Consent Statement: Informed consent was obtained from all subjects involved in the study.

Data Availability Statement: All datasets generated during the current study are available from the corresponding author upon reasonable request.

Acknowledgments: The authors thank László Janovák for transmission electron microscopy measurements, Lilla Pintér and Tímea Böröczky for their technical assistance, and Adrienn Jenei and László Szivos for organising serum samples and providing patient data.

Conflicts of Interest: The authors declare no conflict of interest. The funders had no role in the design of the study; in the collection, analyses, or interpretation of data; in the writing of the manuscript, or in the decision to publish the results.

References

1. Macdonald, D.R.; Cascino, T.L.; Schold, S.C.; Cairncross, J.G. Response criteria for phase II studies of supratentorial malignant glioma. *J. Clin. Oncol.* **1990**, *8*, 1277–1280. [CrossRef]
2. Van den Bent, M.J.; Vogelbaum, M.A.; Wen, P.Y.; Macdonald, D.R.; Chang, S.M. End Point Assessment in Gliomas: Novel Treatments Limit Usefulness of Classical Macdonald's Criteria. *J. Clin. Oncol.* **2009**, *27*, 2905–2908. [CrossRef]
3. Pope, W.B.; Brandal, G. Conventional and advanced magnetic resonance imaging in patients with high-grade glioma. *Q. J. Nucl. Med. Mol. Imaging* **2018**, *62*, 239–253. [CrossRef]
4. Neska-Matuszewska, M.; Bladowska, J.; Sąsiadek, M.; Zimny, A. Differentiation of glioblastoma multiforme, metastases and primary central nervous system lymphomas using multiparametric perfusion and diffusion MR imaging of a tumor core and a peritumoral zone—Searching for a practical approach. *PLoS ONE* **2018**, *13*, e0191341. [CrossRef] [PubMed]
5. Garden, G.A.; Campbell, B.M. Glial biomarkers in human central nervous system disease: Glial Biomarkers in Human CNS Disease. *Glia* **2016**, *64*, 1755–1771. [CrossRef]
6. Staedtke, V.; Dzaye, O.D.; Holdhoff, M. Actionable Molecular Biomarkers in Primary Brain Tumors. *Trends Cancer* **2016**, *2*, 338–349. [CrossRef] [PubMed]
7. Cohen, J.D.; Li, L.; Wang, Y.; Thoburn, C.; Afsari, B.; Danilova, L.; Douville, C.; Javed, A.A.; Wong, F.; Mattox, A.; et al. Detection and localization of surgically resectable cancers with a multi-analyte blood test. *Science* **2018**, *359*, 926–930. [CrossRef] [PubMed]
8. Watson, Z.L.; Bitler, B.G. Type I Protein Arginine Methyltransferases Overexpression Promotes Transformation and Potentiates Her2/Neu–Driven Tumorigenesis. *Cancer Res.* **2019**, *79*, 3–4. [CrossRef]
9. Alix-Panabières, C.; Pantel, K. Liquid Biopsy: From Discovery to Clinical Application. *Cancer Discov.* **2021**, *11*, 858–873. [CrossRef]
10. Lone, S.N.; Nisar, S.; Masoodi, T.; Singh, M.; Rizwan, A.; Hashem, S.; El-Rifai, W.; Bedognetti, D.; Batra, S.K.; Haris, M.; et al. Liquid biopsy: A step closer to transform diagnosis, prognosis and future of cancer treatments. *Mol. Cancer* **2022**, *21*, 79. [CrossRef]
11. Best, M.G.; Sol, N.; Zijl, S.; Reijneveld, J.C.; Wesseling, P.; Wurdinger, T. Liquid biopsies in patients with diffuse glioma. *Acta Neuropathol.* **2015**, *129*, 849–865. [CrossRef]
12. Colombo, M.; Raposo, G.; Théry, C. Biogenesis, Secretion, and Intercellular Interactions of Exosomes and Other Extracellular Vesicles. *Annu. Rev. Cell Dev. Biol.* **2014**, *30*, 255–289. [CrossRef] [PubMed]

13. Janowska-Wieczorek, A.; Wysoczynski, M.; Kijowski, J.; Marquez-Curtis, L.; Machalinski, B.; Ratajczak, J.; Ratajczak, M.Z. Microvesicles derived from activated platelets induce metastasis and angiogenesis in lung cancer. *Int. J. Cancer* **2005**, *113*, 752–760. [CrossRef]
14. Théry, C.; Ostrowski, M.; Segura, E. Membrane vesicles as conveyors of immune responses. *Nat. Rev. Immunol.* **2009**, *9*, 581–593. [CrossRef] [PubMed]
15. Ostrowski, M.; Carmo, N.B.; Krumeich, S.; Fanget, I.; Raposo, G.; Savina, A.; Moita, C.F.; Schauer, K.; Hume, A.N.; Freitas, R.P.; et al. Rab27a and Rab27b control different steps of the exosome secretion pathway. *Nat. Cell Biol.* **2010**, *12*, 19–30. [CrossRef] [PubMed]
16. Hu, T.; Wolfram, J.; Srivastava, S. Extracellular Vesicles in Cancer Detection: Hopes and Hypes. *Trends Cancer* **2021**, *7*, 122–133. [CrossRef]
17. Hergenreider, E.; Heydt, S.; Tréguer, K.; Boettger, T.; Horrevoets, A.J.G.; Zeiher, A.M.; Scheffer, M.P.; Frangakis, A.S.; Yin, X.; Mayr, M.; et al. Atheroprotective communication between endothelial cells and smooth muscle cells through miRNAs. *Nat. Cell Biol.* **2012**, *14*, 249–256. [CrossRef] [PubMed]
18. Skog, J.; Würdinger, T.; van Rijn, S.; Meijer, D.H.; Gainche, L.; Curry, W.T.; Carter, B.S.; Krichevsky, A.M.; Breakefield, X.O. Glioblastoma microvesicles transport RNA and proteins that promote tumour growth and provide diagnostic biomarkers. *Nat. Cell Biol.* **2008**, *10*, 1470–1476. [CrossRef]
19. Kahlert, C.; Melo, S.A.; Protopopov, A.; Tang, J.; Seth, S.; Koch, M.; Zhang, J.; Weitz, J.; Chin, L.; Futreal, A.; et al. Identification of Double-stranded Genomic DNA Spanning All Chromosomes with Mutated KRAS and p53 DNA in the Serum Exosomes of Patients with Pancreatic Cancer. *J. Biol. Chem.* **2014**, *289*, 3869–3875. [CrossRef]
20. Al-Nedawi, K.; Meehan, B.; Micallef, J.; Lhotak, V.; May, L.; Guha, A.; Rak, J. Intercellular transfer of the oncogenic receptor EGFRvIII by microvesicles derived from tumour cells. *Nat. Cell Biol.* **2008**, *10*, 619–624. [CrossRef]
21. Demory Beckler, M.; Higginbotham, J.N.; Franklin, J.L.; Ham, A.-J.; Halvey, P.J.; Imasuen, I.E.; Whitwell, C.; Li, M.; Liebler, D.C.; Coffey, R.J. Proteomic Analysis of Exosomes from Mutant KRAS Colon Cancer Cells Identifies Intercellular Transfer of Mutant KRAS. *Mol. Cell. Proteom.* **2013**, *12*, 343–355. [CrossRef]
22. Sheridan, C. Exosome cancer diagnostic reaches market. *Nat. Biotechnol.* **2016**, *34*, 359–360. [CrossRef]
23. Kosaka, N.; Kogure, A.; Yamamoto, T.; Urabe, F.; Usuba, W.; Prieto-Vila, M.; Ochiya, T. Exploiting the message from cancer: The diagnostic value of extracellular vesicles for clinical applications. *Exp. Mol. Med.* **2019**, *51*, 1–9. [CrossRef]
24. Scavo, M.P.; Depalo, N.; Tutino, V.; De Nunzio, V.; Ingrosso, C.; Rizzi, F.; Notarnicola, M.; Curri, M.L.; Giannelli, G. Exosomes for Diagnosis and Therapy in Gastrointestinal Cancers. *Int. J. Mol. Sci.* **2020**, *21*, 367. [CrossRef]
25. Hoshino, A.; Kim, H.S.; Bojmar, L.; Gyan, K.E.; Cioffi, M.; Hernandez, J.; Zambirinis, C.P.; Rodrigues, G.; Molina, H.; Heissel, S.; et al. Extracellular Vesicle and Particle Biomarkers Define Multiple Human Cancers. *Cell* **2020**, *182*, 1044–1061.e18. [CrossRef]
26. Möhrmann, L.; Huang, H.J.; Hong, D.S.; Tsimberidou, A.M.; Fu, S.; Piha-Paul, S.A.; Subbiah, V.; Karp, D.D.; Naing, A.; Krug, A.; et al. Liquid Biopsies Using Plasma Exosomal Nucleic Acids and Plasma Cell-Free DNA Compared with Clinical Outcomes of Patients with Advanced Cancers. *Clin. Cancer Res.* **2018**, *24*, 181–188. [CrossRef]
27. Tao, S.-C.; Guo, S.-C. Role of extracellular vesicles in tumour microenvironment. *Cell Commun. Signal. CCS* **2020**, *18*, 163. [CrossRef]
28. Ruhen, O.; Meehan, K. Tumor-Derived Extracellular Vesicles as a Novel Source of Protein Biomarkers for Cancer Diagnosis and Monitoring. *Proteomics* **2019**, *19*, 1800155. [CrossRef]
29. Choy, C.; Jandial, R. Breast Cancer Exosomes Breach the Blood-Brain Barrier. *Neurosurgery* **2016**, *78*, N10–N11. [CrossRef]
30. García-Romero, N.; Carrión-Navarro, J.; Esteban-Rubio, S.; Lázaro-Ibáñez, E.; Peris-Celda, M.; Alonso, M.M.; Guzmán-De-Villoria, J.; Fernández-Carballal, C.; de Mendivil, A.O.; García-Duque, S.; et al. DNA sequences within glioma-derived extracellular vesicles can cross the intact blood-brain barrier and be detected in peripheral blood of patients. *Oncotarget* **2017**, *8*, 1416–1428. [CrossRef]
31. Théry, C.; Witwer, K.W.; Aikawa, E.; Alcaraz, M.J.; Anderson, J.D.; Andriantsitohaina, R.; Antoniou, A.; Arab, T.; Archer, F.; Atkin-Smith, G.K.; et al. Minimal information for studies of extracellular vesicles 2018 (MISEV2018): A position statement of the International Society for Extracellular Vesicles and update of the MISEV2014 guidelines. *J. Extracell. Vesicles* **2018**, *7*, 1535750. [CrossRef] [PubMed]
32. Dobra, G.; Bukva, M.; Szabo, Z.; Bruszel, B.; Harmati, M.; Gyukity-Sebestyen, E.; Jenei, A.; Szucs, M.; Horvath, P.; Biro, T.; et al. Small Extracellular Vesicles Isolated from Serum May Serve as Signal-Enhancers for the Monitoring of CNS Tumors. *Int. J. Mol. Sci.* **2020**, *21*, 5359. [CrossRef] [PubMed]
33. Mondal, S.; Adhikari, N.; Banerjee, S.; Amin, S.A.; Jha, T. Matrix metalloproteinase-9 (MMP-9) and its inhibitors in cancer: A minireview. *Eur. J. Med. Chem.* **2020**, *194*, 112260. [CrossRef] [PubMed]
34. Noel, A.; Jost, M.; Maquoi, E. Matrix metalloproteinases at cancer tumor–host interface. *Semin. Cell Dev. Biol.* **2008**, *19*, 52–60. [CrossRef]
35. Jabłońska-Trypuć, A.; Matejczyk, M.; Rosochacki, S. Matrix metalloproteinases (MMPs), the main extracellular matrix (ECM) enzymes in collagen degradation, as a target for anticancer drugs. *J. Enzyme Inhib. Med. Chem.* **2016**, *31*, 177–183. [CrossRef]
36. Chambers, A.F.; Matrisian, L.M. Changing views of the role of matrix metalloproteinases in metastasis. *JNCI J. Natl. Cancer Inst.* **1997**, *89*, 1260–1270. [CrossRef]

37. Mannello, F.; Tonti, G.; Papa, S. Matrix Metalloproteinase Inhibitors as Anticancer Therapeutics. *Curr. Cancer Drug Targets* **2005**, *5*, 285–298. [CrossRef]
38. Barillari, G. The Impact of Matrix Metalloproteinase-9 on the Sequential Steps of the Metastatic Process. *Int. J. Mol. Sci.* **2020**, *21*, 4526. [CrossRef]
39. Jiguet-Jiglaire, C.; Boissonneau, S.; Denicolai, E.; Hein, V.; Lasseur, R.; Garcia, J.; Romain, S.; Appay, R.; Graillon, T.; Mason, W.; et al. Plasmatic MMP9 released from tumor-infiltrating neutrophils is predictive for bevacizumab efficacy in glioblastoma patients: An AVAglio ancillary study. *Acta Neuropathol. Commun.* **2022**, *10*, 1. [CrossRef]
40. Stetler-Stevenson, W.G. Type IV collagenases in tumor invasion and metastasis. *Cancer Metastasis Rev.* **1990**, *9*, 289–303. [CrossRef]
41. Rao, J.S.; Steck, P.A.; Mohanam, S.; Stetler-Stevenson, W.G.; Liotta, L.A.; Sawaya, R. Elevated levels of M(r) 92,000 type IV collagenase in human brain tumors. *Cancer Res.* **1993**, *53*, 2208–2211.
42. Rao, J.S.; Yamamoto, M.; Mohaman, S.; Gokaslan, Z.L.; Fuller, G.N.; Stetler-Stevenson, W.G.; Rao, V.H.; Liotta, L.A.; Nicolson, G.L.; Sawaya, R.E. Expression and localization of 92 kDa type IV collagenase/gelatinase B (MMP-9) in human gliomas. *Clin. Exp. Metastasis* **1996**, *14*, 12–18. [CrossRef] [PubMed]
43. Wu, C.-Y.; Wu, M.-S.; Chiang, E.-P.; Chen, Y.-J.; Chen, C.-J.; Chi, N.-H.; Shih, Y.-T.; Chen, G.-H.; Lin, J.-T. Plasma Matrix Metalloproteinase-9 Level Is Better than Serum Matrix Metalloproteinase-9 Level to Predict Gastric Cancer Evolution. *Clin. Cancer Res.* **2007**, *13*, 2054–2060. [CrossRef] [PubMed]
44. Otero-Estévez, O.; Chiara, L.D.; Rodríguez-Girondo, M.; Rodríguez-Berrocal, F.J.; Cubiella, J.; Castro, I.; Hernández, V.; Martínez-Zorzano, V.S. Serum matrix metalloproteinase-9 in colorectal cancer family-risk population screening. *Sci. Rep.* **2015**, *5*, 13030. [CrossRef]
45. Hormigo, A.; Gu, B.; Karimi, S.; Riedel, E.; Panageas, K.S.; Edgar, M.A.; Tanwar, M.K.; Rao, J.S.; Fleisher, M.; DeAngelis, L.M.; et al. YKL-40 and Matrix Metalloproteinase-9 as Potential Serum Biomarkers for Patients with High-Grade Gliomas. *Clin. Cancer Res.* **2006**, *12*, 5698–5704. [CrossRef]
46. Iwamoto, F.M.; Hottinger, A.F.; Karimi, S.; Riedel, E.; Dantis, J.; Jahdi, M.; Panageas, K.S.; Lassman, A.B.; Abrey, L.E.; Fleisher, M.; et al. Longitudinal prospective study of matrix metalloproteinase-9 as a serum marker in gliomas. *J. Neurooncol.* **2011**, *105*, 607–612. [CrossRef]
47. Ricci, S.; Guadagno, E.; Bruzzese, D.; Del Basso De Caro, M.; Peca, C.; Sgulò, F.G.; Maiuri, F.; Di Carlo, A. Evaluation of matrix metalloproteinase type IV-collagenases in serum of patients with tumors of the central nervous system. *J. Neurooncol.* **2017**, *131*, 223–232. [CrossRef] [PubMed]
48. Linhares, P.; Carvalho, B.; Vaz, R.; Costa, B.M. Glioblastoma: Is There Any Blood Biomarker with True Clinical Relevance? *Int. J. Mol. Sci.* **2020**, *21*, 5809. [CrossRef]
49. Luong, J.H.T.; Vashist, S.K. Chemistry of Biotin-Streptavidin and the Growing Concern of an Emerging Biotin Interference in Clinical Immunoassays. *ACS Omega* **2020**, *5*, 10–18. [CrossRef]
50. EV-TRACK Consortium; Van Deun, J.; Mestdagh, P.; Agostinis, P.; Akay, Ö.; Anand, S.; Anckaert, J.; Martinez, Z.A.; Baetens, T.; Beghein, E.; et al. EV-TRACK: Transparent reporting and centralizing knowledge in extracellular vesicle research. *Nat. Methods* **2017**, *14*, 228–232. [CrossRef]
51. Preusser, M. A step towards clinical blood biomarkers of glioblastoma. *Nat. Rev. Neurol.* **2014**, *10*, 681–682. [CrossRef]
52. Kros, J.M.; Mustafa, D.M.; Dekker, L.J.M.; Sillevis Smitt, P.A.E.; Luider, T.M.; Zheng, P.-P. Circulating glioma biomarkers. *Neuro-Oncol.* **2014**, *17*, 343–360. [CrossRef] [PubMed]
53. McKiernan, J.; Donovan, M.J.; O'Neill, V.; Bentink, S.; Noerholm, M.; Belzer, S.; Skog, J.; Kattan, M.W.; Partin, A.; Andriole, G.; et al. A Novel Urine Exosome Gene Expression Assay to Predict High-grade Prostate Cancer at Initial Biopsy. *JAMA Oncol.* **2016**, *2*, 882. [CrossRef] [PubMed]
54. McKiernan, J.; Donovan, M.J.; Margolis, E.; Partin, A.; Carter, B.; Brown, G.; Torkler, P.; Noerholm, M.; Skog, J.; Shore, N.; et al. A Prospective Adaptive Utility Trial to Validate Performance of a Novel Urine Exosome Gene Expression Assay to Predict High-grade Prostate Cancer in Patients with Prostate-specific Antigen 2–10 ng/ml at Initial Biopsy. *Eur. Urol.* **2018**, *74*, 731–738. [CrossRef] [PubMed]
55. Margolis, E.; Brown, G.; Partin, A.; Carter, B.; McKiernan, J.; Tutrone, R.; Torkler, P.; Fischer, C.; Tadigotla, V.; Noerholm, M.; et al. Predicting high-grade prostate cancer at initial biopsy: Clinical performance of the ExoDx (EPI) Prostate Intelliscore test in three independent prospective studies. *Prostate Cancer Prostatic Dis.* **2022**, *25*, 296–301. [CrossRef]
56. Ostrom, Q.T.; Gittleman, H.; Truitt, G.; Boscia, A.; Kruchko, C.; Barnholtz-Sloan, J.S. CBTRUS Statistical Report: Primary Brain and Other Central Nervous System Tumors Diagnosed in the United States in 2011–2015. *Neuro-Oncology* **2018**, *20*, iv1–iv86. [CrossRef]
57. Fox, B.D.; Cheung, V.J.; Patel, A.J.; Suki, D.; Rao, G. Epidemiology of Metastatic Brain Tumors. *Neurosurg. Clin. N. Am.* **2011**, *22*, 1–6. [CrossRef]
58. Osti, D.; Del Bene, M.; Rappa, G.; Santos, M.; Matafora, V.; Richichi, C.; Faletti, S.; Beznoussenko, G.V.; Mironov, A.; Bachi, A.; et al. Clinical Significance of Extracellular Vesicles in Plasma from Glioblastoma Patients. *Clin. Cancer Res.* **2019**, *25*, 266–276. [CrossRef]
59. Fraser, K.; Jo, A.; Giedt, J.; Vinegoni, C.; Yang, K.S.; Peruzzi, P.; Chiocca, E.A.; Breakefield, X.O.; Lee, H.; Weissleder, R. Characterization of single microvesicles in plasma from glioblastoma patients. *Neuro-Oncology* **2019**, *21*, 606–615. [CrossRef]

60. Jung, K.; Laube, C.; Lein, M.; Lichtinghagen, R.; Tschesche, H.; Schnorr, D.; Loening, S.A. Kind of sample as preanalytical determinant of matrix metalloproteinase 2 and 9 and tissue inhibitor of metalloproteinase 2 in blood. *Clin. Chem.* **1998**, *44*, 1060–1062. [CrossRef]
61. Rouy, D.; Ernens, I.; Jeanty, C.; Wagner, D.R. Plasma storage at −80°C does not protect matrix metalloproteinase-9 from degradation. *Anal. Biochem.* **2005**, *338*, 294–298. [CrossRef] [PubMed]
62. Zucker, S.; Cao, J. Measurement of Matrix Metalloproteinases in Serum of Patients with Melanoma: Snarled in Technical Pitfalls. *Clin. Cancer Res.* **2005**, *11*, 5069–5070. [CrossRef]
63. Yu, D.; Li, Y.; Wang, M.; Gu, J.; Xu, W.; Cai, H.; Fang, X.; Zhang, X. Exosomes as a new frontier of cancer liquid biopsy. *Mol. Cancer* **2022**, *21*, 56. [CrossRef] [PubMed]
64. Yu, W.; Hurley, J.; Roberts, D.; Chakrabortty, S.K.; Enderle, D.; Noerholm, M.; Breakefield, X.O.; Skog, J.K. Exosome-based liquid biopsies in cancer: Opportunities and challenges. *Ann. Oncol.* **2021**, *32*, 466–477. [CrossRef] [PubMed]
65. Lai, H.; Li, Y.; Zhang, H.; Hu, J.; Liao, J.; Su, Y.; Li, Q.; Chen, B.; Li, C.; Wang, Z.; et al. exoRBase 2.0: An atlas of mRNA, lncRNA and circRNA in extracellular vesicles from human biofluids. *Nucleic Acids Res.* **2022**, *50*, D118–D128. [CrossRef]
66. Li, Y.; Zhao, J.; Yu, S.; Wang, Z.; He, X.; Su, Y.; Guo, T.; Sheng, H.; Chen, J.; Zheng, Q.; et al. Extracellular Vesicles Long RNA Sequencing Reveals Abundant mRNA, circRNA, and lncRNA in Human Blood as Potential Biomarkers for Cancer Diagnosis. *Clin. Chem.* **2019**, *65*, 798–808. [CrossRef]
67. Bracht, J.W.P.; Gimenez-Capitan, A.; Huang, C.-Y.; Potie, N.; Pedraz-Valdunciel, C.; Warren, S.; Rosell, R.; Molina-Vila, M.A. Analysis of extracellular vesicle mRNA derived from plasma using the nCounter platform. *Sci. Rep.* **2021**, *11*, 3712. [CrossRef]
68. Kumar, S.R.; Kimchi, E.T.; Manjunath, Y.; Gajagowni, S.; Stuckel, A.J.; Kaifi, J.T. RNA cargos in extracellular vesicles derived from blood serum in pancreas associated conditions. *Sci. Rep.* **2020**, *10*, 2800. [CrossRef]
69. Taran, K.; Wnęk, A.; Kobos, J.; Andrzejewska, E.; Przewratil, P. Tissue and serum mRNA profile of MMPs-2/9 as a potential novel biomarker for the most individual approach in infantile hemangiomas and cancer disease. *Immunobiology* **2017**, *222*, 1035–1042. [CrossRef]
70. Wu, Z.-S.; Wu, Q.; Yang, J.-H.; Wang, H.-Q.; Ding, X.-D.; Yang, F.; Xu, X.-C. Prognostic significance of MMP-9 and TIMP-1 serum and tissue expression in breast cancer. *Int. J. Cancer* **2008**, *122*, 2050–2056. [CrossRef]
71. Guo, C.-B.; Wang, S.; Deng, C.; Zhang, D.-L.; Wang, F.-L.; Jin, X.-Q. Relationship between matrix metalloproteinase 2 and lung cancer progression. *Mol. Diagn. Ther.* **2007**, *11*, 183–192. [CrossRef] [PubMed]
72. Zhou, L.; Kou, D.-Q. Correlation between acute myocardial infarction complicated with cerebral infarction and expression levels of MMP-2 and MMP-9. *Eur. Rev. Med. Pharmacol. Sci.* **2019**, *23*, 297–302. [CrossRef] [PubMed]
73. Vira, H.J.; Pradhan, V.D.; Umare, V.D.; Chaudhary, A.K.; Rajadhyksha, A.G.; Nadkar, M.Y.; Ghosh, K.; Nadkarni, A.H. Expression of the matrix metalloproteinases MMP-2 and MMP-9 and their inhibitors TIMP-1 and TIMP-2 in systemic lupus erythematosus patients. *Neth. J. Med.* **2020**, *78*, 261–268. [PubMed]
74. Prasetyo, E.; Asadul Islam, A.; Hatta, M.; Widodo, D.; Pattelongi, I. The Profile of MMP-9, MMP-9 mRNA Expression, -1562 C/T Polymorphism and Outcome in High-risk Traumatic Brain Injury: The Effect of Therapeutic Mild Hypothermia. *Neurol. Med. Chir.* **2017**, *57*, 612–619. [CrossRef]
75. Liu, Y.; Beyer, A.; Aebersold, R. On the Dependency of Cellular Protein Levels on mRNA Abundance. *Cell* **2016**, *165*, 535–550. [CrossRef]
76. Mund, A.; Brunner, A.-D.; Mann, M. Unbiased spatial proteomics with single-cell resolution in tissues. *Mol. Cell* **2022**, *82*, 2335–2349. [CrossRef]
77. Buccitelli, C.; Selbach, M. mRNAs, proteins and the emerging principles of gene expression control. *Nat. Rev. Genet.* **2020**, *21*, 630–644. [CrossRef]
78. Jia, Y.; Yu, L.; Ma, T.; Xu, W.; Qian, H.; Sun, Y.; Shi, H. Small extracellular vesicles isolation and separation: Current techniques, pending questions and clinical applications. *Theranostics* **2022**, *12*, 6548–6575. [CrossRef]
79. Freitas, D.; Balmaña, M.; Poças, J.; Campos, D.; Osório, H.; Konstantinidi, A.; Vakhrushev, S.Y.; Magalhães, A.; Reis, C.A. Different isolation approaches lead to diverse glycosylated extracellular vesicle populations. *J. Extracell. Vesicles* **2019**, *8*, 1621131. [CrossRef]
80. Clos-Sansalvador, M.; Monguió-Tortajada, M.; Roura, S.; Franquesa, M.; Borràs, F.E. Commonly used methods for extracellular vesicles' enrichment: Implications in downstream analyses and use. *Eur. J. Cell Biol.* **2022**, *101*, 151227. [CrossRef]
81. Veerman, R.E.; Teeuwen, L.; Czarnewski, P.; Güclüler Akpinar, G.; Sandberg, A.; Cao, X.; Pernemalm, M.; Orre, L.M.; Gabrielsson, S.; Eldh, M. Molecular evaluation of five different isolation methods for extracellular vesicles reveals different clinical applicability and subcellular origin. *J. Extracell. Vesicles* **2021**, *10*, e12128. [CrossRef] [PubMed]
82. Gelibter, S.; Marostica, G.; Mandelli, A.; Siciliani, S.; Podini, P.; Finardi, A.; Furlan, R. The impact of storage on extracellular vesicles: A systematic study. *J. Extracell. Vesicles* **2022**, *11*, e12162. [CrossRef] [PubMed]
83. Wu, Y.; Deng, W.; Klinke II, D.J. Exosomes: Improved methods to characterize their morphology, RNA content, and surface protein biomarkers. *Analyst* **2015**, *140*, 6631–6642. [CrossRef] [PubMed]
84. Bosch, S.; de Beaurepaire, L.; Allard, M.; Mosser, M.; Heichette, C.; Chrétien, D.; Jegou, D.; Bach, J.-M. Trehalose prevents aggregation of exosomes and cryodamage. *Sci. Rep.* **2016**, *6*, 36162. [CrossRef] [PubMed]
85. Cheng, Y.; Zeng, Q.; Han, Q.; Xia, W. Effect of pH, temperature and freezing-thawing on quantity changes and cellular uptake of exosomes. *Protein Cell* **2019**, *10*, 295–299. [CrossRef]

86. Sallai, I.; Marton, N.; Szatmári, A.; Kittel, Á.; Nagy, G.; Buzás, E.I.; Khamari, D.; Komlósi, Z.; Kristóf, K.; Drahos, L.; et al. Activated polymorphonuclear derived extracellular vesicles are potential biomarkers of periprosthetic joint infection. *PLoS ONE* **2022**, *17*, e0268076. [CrossRef]
87. Yang, J.E.; Rossignol, E.D.; Chang, D.; Zaia, J.; Forrester, I.; Raja, K.; Winbigler, H.; Nicastro, D.; Jackson, W.T.; Bullitt, E. Complexity and ultrastructure of infectious extracellular vesicles from cells infected by non-enveloped virus. *Sci. Rep.* **2020**, *10*, 7939. [CrossRef]
88. Zhang, Y.-F.; Shi, J.-B.; Li, C. Small extracellular vesicle loading systems in cancer therapy: Current status and the way forward. *Cytotherapy* **2019**, *21*, 1122–1136. [CrossRef]
89. Antimisiaris, S.; Mourtas, S.; Marazioti, A. Exosomes and Exosome-Inspired Vesicles for Targeted Drug Delivery. *Pharmaceutics* **2018**, *10*, 218. [CrossRef]
90. Lötvall, J.; Hill, A.F.; Hochberg, F.; Buzás, E.I.; Di Vizio, D.; Gardiner, C.; Gho, Y.S.; Kurochkin, I.V.; Mathivanan, S.; Quesenberry, P.; et al. Minimal experimental requirements for definition of extracellular vesicles and their functions: A position statement from the International Society for Extracellular Vesicles. *J. Extracell. Vesicles* **2014**, *3*, 26913. [CrossRef]
91. Jung, K.; Lein, M.; Laube, C.; Lichtinghagen, R. Blood specimen collection methods influence the concentration and the diagnostic validity of matrix metalloproteinase 9 in blood. *Clin. Chim. Acta* **2001**, *314*, 241–244. [CrossRef] [PubMed]
92. Gerlach, R.F.; Uzuelli, J.A.; Souza-Tarla, C.D.; Tanus-Santos, J.E. Effect of anticoagulants on the determination of plasma matrix metalloproteinase (MMP)-2 and MMP-9 activities. *Anal. Biochem.* **2005**, *344*, 147–149. [CrossRef] [PubMed]
93. Souza-Tarla, C.D.; Uzuelli, J.A.; Machado, A.A.; Gerlach, R.F.; Tanus-Santos, J.E. Methodological issues affecting the determination of plasma matrix metalloproteinase (MMP)-2 and MMP-9 activities. *Clin. Biochem.* **2005**, *38*, 410–414. [CrossRef] [PubMed]
94. Forsyth, P.A.; Wong, H.; Laing, T.D.; Rewcastle, N.B.; Morris, D.G.; Muzik, H.; Leco, K.J.; Johnston, R.N.; Brasher, P.M.A.; Sutherland, G.; et al. Gelatinase-A (MMP-2), gelatinase-B (MMP-9) and membrane type matrix metalloproteinase-1 (MT1-MMP) are involved in different aspects of the pathophysiology of malignant gliomas. *Br. J. Cancer* **1999**, *79*, 1828–1835. [CrossRef]
95. Vince, G.H.; Wagner, S.; Pietsch, T.; Klein, R.; Goldbrunner, R.H.; Roosen, K.; Tonn, J.C. Heterogeneous regional expression patterns of matrix metalloproteinases in human malignant gliomas. *Int. J. Dev. Neurosci.* **1999**, *17*, 437–445. [CrossRef] [PubMed]
96. Tabouret, E.; Boudouresque, F.; Barrie, M.; Matta, M.; Boucard, C.; Loundou, A.; Carpentier, A.; Sanson, M.; Metellus, P.; Figarella-Branger, D.; et al. Association of matrix metalloproteinase 2 plasma level with response and survival in patients treated with bevacizumab for recurrent high-grade glioma. *Neuro-Oncol.* **2014**, *16*, 392–399. [CrossRef] [PubMed]
97. Farina, A.; Mackay, A. Gelatinase B/MMP-9 in Tumour Pathogenesis and Progression. *Cancers* **2014**, *6*, 240–296. [CrossRef] [PubMed]
98. Kanderi, T.; Gupta, V. Glioblastoma Multiforme. In *StatPearls*; StatPearls Publishing: Treasure Island, FL, USA, 2022.

International Journal of
Molecular Sciences

MDPI

Article

Small Extracellular Vesicles Isolated from Serum May Serve as Signal-Enhancers for the Monitoring of CNS Tumors

Gabriella Dobra [1,2], Matyas Bukva [1,2], Zoltan Szabo [3], Bella Bruszel [3], Maria Harmati [1], Edina Gyukity-Sebestyen [1], Adrienn Jenei [4], Monika Szucs [5,6], Peter Horvath [1], Tamas Biro [7], Almos Klekner [4] and Krisztina Buzas [1,8,9,*]

1 Laboratory of Microscopic Image Analysis and Machine Learning, Institute of Biochemistry, Biological Research Centre, H-6726 Szeged, Hungary; dobragab@yahoo.co.uk (G.D.); bukvamatyas@gmail.com (M.B.); harmatimarcsi@gmail.com (M.H.); e.gyukity.sebestyen@gmail.com (E.G.-S.); horvath.peter@brc.hu (P.H.)
2 Department of Medical Genetics, Doctoral School of Interdisciplinary Medicine, University of Szeged, H-6720 Szeged, Hungary
3 Department of Medical Chemistry, Faculty of Medicine, University of Szeged, H-6720 Szeged, Hungary; szabo.zoltan@med.u-szeged.hu (Z.S.); bruszel.bella@med.u-szeged.hu (B.B.)
4 Department of Neurosurgery, Clinical Centre, University of Debrecen, H-4032 Debrecen, Hungary; jenei.adrienn@med.unideb.hu (A.J.); aklekner@yahoo.com (A.K.)
5 Department of Medical Physics and Informatics, Faculty of Medicine, University of Szeged, H-6720 Szeged, Hungary; szucs.monika@med.u-szeged.hu
6 Department of Medical Physics and Informatics, Faculty of Science and Informatics, University of Szeged, H-6720 Szeged, Hungary
7 Department of Immunology, Faculty of Medicine, University of Debrecen, H-4032 Debrecen, Hungary; biro.lcmp@gmail.com
8 Department of Immunology, Faculty of Medicine, University of Szeged, H-6720 Szeged, Hungary
9 Department of Immunology, Faculty of Science and Informatics, University of Szeged, H-6720 Szeged, Hungary
* Correspondence: kr.buzas@gmail.com; Tel.: +36-62-432-340

Received: 26 June 2020; Accepted: 24 July 2020; Published: 28 July 2020

Abstract: Liquid biopsy-based methods to test biomarkers (e.g., serum proteins and extracellular vesicles) may help to monitor brain tumors. In this proteomics-based study, we aimed to identify a characteristic protein fingerprint associated with central nervous system (CNS) tumors. Overall, 96 human serum samples were obtained from four patient groups, namely glioblastoma multiforme (GBM), non-small-cell lung cancer brain metastasis (BM), meningioma (M) and lumbar disc hernia patients (CTRL). After the isolation and characterization of small extracellular vesicles (sEVs) by nanoparticle tracking analysis (NTA) and atomic force microscopy (AFM), liquid chromatography -mass spectrometry (LC-MS) was performed on two different sample types (whole serum and serum sEVs). Statistical analyses (ratio, Cohen's d, receiver operating characteristic; ROC) were carried out to compare patient groups. To recognize differences between the two sample types, pairwise comparisons (Welch's test) and ingenuity pathway analysis (IPA) were performed. According to our knowledge, this is the first study that compares the proteome of whole serum and serum-derived sEVs. From the 311 proteins identified, 10 whole serum proteins and 17 sEV proteins showed the highest intergroup differences. Sixty-five proteins were significantly enriched in sEV samples, while 129 proteins were significantly depleted compared to whole serum. Based on principal component analysis (PCA) analyses, sEVs are more suitable to discriminate between the patient groups. Our results support that sEVs have greater potential to monitor CNS tumors, than whole serum.

Keywords: extracellular vesicles; cancer biomarker; proteomics

1. Introduction

According to the World Health Organization (WHO), cancer is the second leading cause of death, accounting for an estimated 9.6 million cases in 2018. Globally, 1 in 6 deaths is due to cancer [1]. The cancer burden continues to grow worldwide, exerting tremendous physical, emotional and financial strain on individuals, families, communities and on health systems [2].

The diagnosis of central nervous system (CNS) tumors is based on CT and MRI scans, as well as on the histopathological analysis of samples obtained by biopsy or via surgical resection. However, these procedures are highly invasive, uncomfortable for the patient, bear a considerable risk of complications and provide limited information on tumor status. Therefore, biomarkers appropriate for monitoring disease progression and response to treatment are eagerly required. While repeated MRI scans serve as the standard method to follow patients, it has little prognostic value for long-term recurrence [3]. Thus, neuro-oncological research aims to identify novel biomarkers suitable for monitoring CNS tumors in clinical practice [4].

Liquid biopsy is in the spotlight of biomarker-focused research, as body fluids are easily accessible sources of biomarkers and are available with minimally invasive and low cost sampling procedures. Also, multiple sampling allows the monitoring of disease progression and therapeutic response [5]. Every cell, including neoplastic cells, release molecular markers into the circulation. Tumor-derived biomarkers include proteins, nucleic acids, circulating tumor cells, platelets and tumor-derived extracellular vesicles that accumulate in urine, cerebrospinal fluid, saliva and blood [6].

Blood is the most easily accessible source for biomarkers, thus it is frequently used to assess disease status in malignancies such as prostate, liver and ovarian cancers based on the serum concentrations of PSA, AFP and CA125, respectively. In neuro-oncology, blood-based biomarkers are mainly used to evaluate toxicity and safety of treatments to guide patient management. For example, myelosuppression is a common risk associated with temozolomide treatment and radiotherapy, thus standard practice dictates weekly tests of complete blood count, including whole blood cell differential and platelet counts during definitive chemoradiotherapy [7]. Finding biomarkers for blood-based CNS tumor monitoring is more challenging, as the blood-brain barrier (BBB) prevents the release of tumor-related biomarkers into peripheral blood. However, it would have outstanding benefits in clinical patient management, thus efforts to identify blood based biomarkers, including proteins, nucleic acids, circulating tumor cells and extracellular vesicles are currently in the forefront of neuro-oncological research [8].

Extracellular vesicles (EVs) are promising cancer biomarkers accessible via liquid biopsy, because they are cell-secreted, nano-sized and stably exist in all types of body fluids. EVs contain a sample of the cytosolic milieu, including an abundance of DNA, RNA, proteins and other analytes, while externally they also resemble their cell of origin [9]. EVs are small, lipid bilayer-enclosed vesicles released by both cancer and non-cancerous cells into the extracellular space [10].

EVs secreted by cancer cells communicate with neighboring stromal cells or even with cells at distant sites, inducing an alteration of the cell program [11,12]. Pre-metastatic niche formation has been shown in several tumors, for example, in pancreatic, lung, colorectal and ovarian cancers [13–16]. Also, EVs may be taken up by immune cells, leading to immunosuppression [17]. More recently, EVs have even gained a role in cancer diagnosis and therapy [18–20] as biomarker molecules that may be identified in different primary tumors with high sensitivity and specificity [21]. Regarding pancreatic cancer, Kalluri and colleagues found that glypican-1 (GPC1), a cell surface proteoglycan, is specifically enriched in circulating exosomes (30–200 nm endosome-derived EVs). GPC1 is suitable to differentiate early- and late-stage pancreatic cancer from benign diseases of the pancreas, with an accuracy of 100% [22]. The available evidence also supports that tumor-derived EVs can cross the BBB [23,24], however, currently no clinically relevant EV biomarkers are accepted for the monitoring of CNS tumors.

Several studies report on gene or protein expression analyses of CNS tumor tissue (specifically, glioblastoma), allowing to identify biomarkers that could be secreted into the blood and thus could be detected from serum samples. Recent studies have aimed to identify one and two specific biomarkers

for the reliable evaluation of actual tumor status [25–27] but none of these proteins alone was found to be sufficiently specific and sensitive to serve as a monitoring marker.

Regarding that previous attempts to find surrogate serum markers for brain tumors have failed when based on a single or only few candidate factors, we made an attempt to identify a characteristic protein fingerprint of 10–20 candidate markers associated with CNS tumors.

For this purpose, 96 serum samples were collected from four patient groups according to the criteria of the National Ethical Committee and proteomics analysis was performed using liquid chromatography and mass spectrometry (LC-MS). The serum samples were obtained from patients diagnosed with the two most common types of brain tumors [28], namely malignant glioblastoma multiforme (GBM) and benign meningioma (M), as well as from patients with a prevalent brain metastasis [29] originating from non-small-cell lung cancer (BM). Patients with lumbar disc herniation served as controls (CTRL). Following a statistical selection, these four patient groups were compared with respect to the identified proteins. In parallel, small extracellular vesicles (sEVs) were isolated from the serum samples by differential centrifugation and proteomics and statistical analyses were also performed on these sEV samples, allowing to compare the suitability of these two different sample types. According to the best of our knowledge, this is the first study that compares the proteome of whole serum and serum-derived sEV samples. Results from the proteomics analysis indicate that using a protein fingerprint of serum-derived sEVs instead of analyzing whole serum increases the accuracy of distinguishing between the clinical samples, that is, between the patient groups. Our results support that sEVs have a greater potential for the proteomics-based monitoring of CNS tumors compared to whole serum analysis.

2. Results

2.1. EV Samples Show sEV Properties with Similar Concentration and Size Distribution in the Different Patient Groups

To verify the value of circulating extracellular vesicles as potential biomarkers for CNS tumors, EVs were isolated from the serum of patients with glioblastoma multiforme (GBM), single brain metastasis originating from non-small-cell lung cancer (BM) and meningioma (M), as well as from control patients with lumbar disc herniation (CTRL). Each group included 24 individuals of both genders with various ages. Extracellular vesicles were isolated from the sera by differential centrifugation and were characterized by atomic force microscopy (AFM) and nanoparticle tracking analysis (NTA). Pools of 6 samples were formed in all groups, allowing four parallel samples to be tested per group (see in Section 4.1). Western blot analyses were also performed to demonstrate the EV nature (Figure S1).

EVs were divided into subtypes based on their size range, separating small EVs (sEVs) and medium/large EVs (m/lEVs) [30]. AFM analysis revealed that the small EV subtype includes various structures. Mean and mode diameters of the particles, represented by an average of the 16 sample pools, were measured as 112 nm and 86 nm by NTA, respectively (Figure 1A).

The quantitative characterization of serum sEVs by NTA (Figure 1B) revealed no significant differences between the four patient groups regarding the size and concentration of circulating sEVs. However, within the groups high individual differences were observed in the measured parameters of the sEVs.

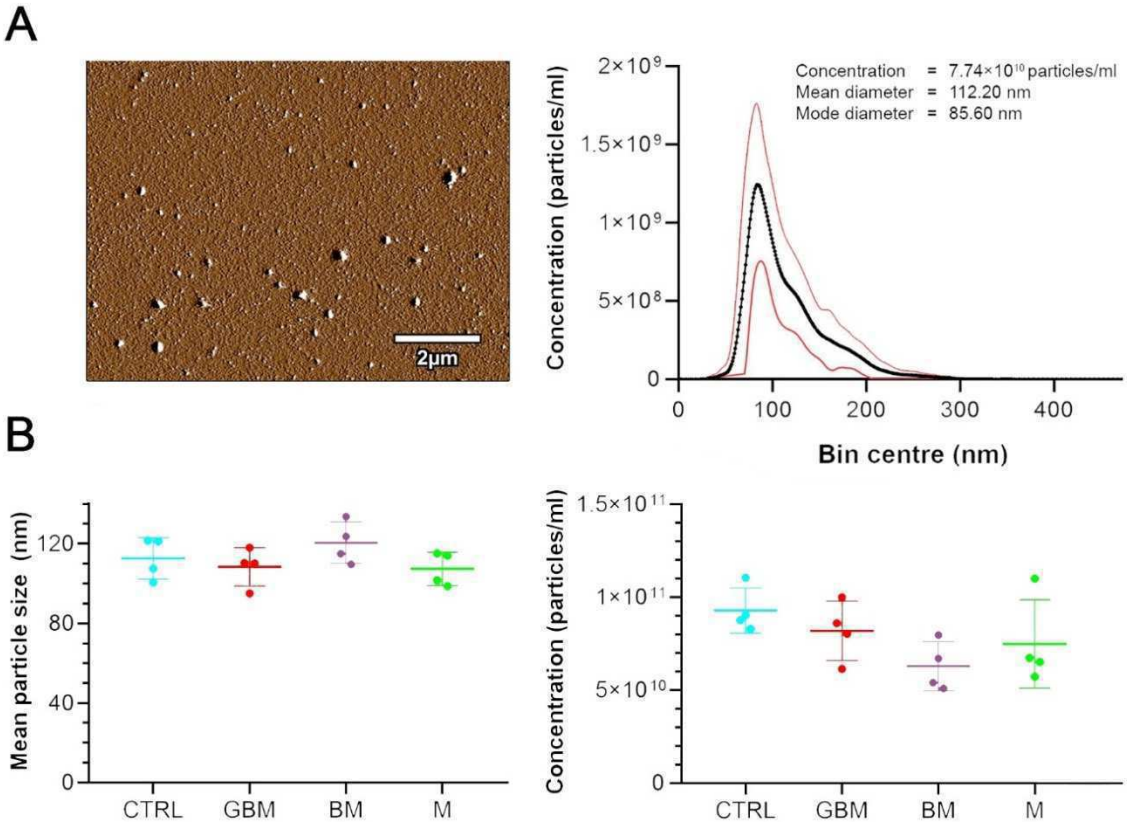

Figure 1. Characterization and quantitative properties of the small extracellular vesicle (sEV) samples. (**A**) Atomic force microscopy (AFM) image of sEV isolates displays vesicles with diameters within the range of 50–140 nm. The diagram shows the size distribution of the 96 sEV samples isolated from the serum, presenting the mean +/−95% CI values measured by nanoparticle tracking analysis (NTA). (**B**) Dot plots show the number and size distribution of small extracellular vesicles (sEVs) displayed in mean size (left) and concentration (right) values for each sample pools (4 samples/group).

2.2. Statistical Analysis of LC-MS Data Reveals Characteristic Proteomic Fingerprints for Each Patient Group and Informs on the Suitability of the Two Different Sample Types in Distinguishing CNS Tumors

We aimed to identify the differences between the four patient groups to reveal the characteristic protein profiles associated with the CNS tumors in point. Using an intensity ratio of >2 or <0.5 with Cohen's d effect size of 2 as a cut-off, we investigated which proteins show reliable intensity difference and which proteins can separate at least one group from the others based on a receiver operating characteristic (ROC) analysis. Moreover, utilizing principal component analysis (PCA) with k-means clustering, we were able to compare the suitability of the two different sample types to distinguish between the CNS tumors in point. Figure 2 shows the flowchart of LC-MS data processing and the results of the statistical analyses.

Proteomics analyses by LC-MS (Step 1) were performed on whole serum and sEV samples obtained from patients with GBM, BM, M and CTRL. Individual samples (n = 24) in each group were arranged into 4 pools (see in Section 4.1) to eliminate individual variances, reduce sample number, shorten the time of LC-MS measurements and reduce the need for materials. The Data independent acquisition (DIA) mode constructed spectral library revealed 311 proteins (see Table S1). Based on Pearson's correlation analyses (Step 2), one of the sEV control samples had to be excluded from further statistical analyses (Table S2). After excluding unreliable proteins, as well as proteins with missing values (Step 3), a total of 262 proteins remained for the final analysis.

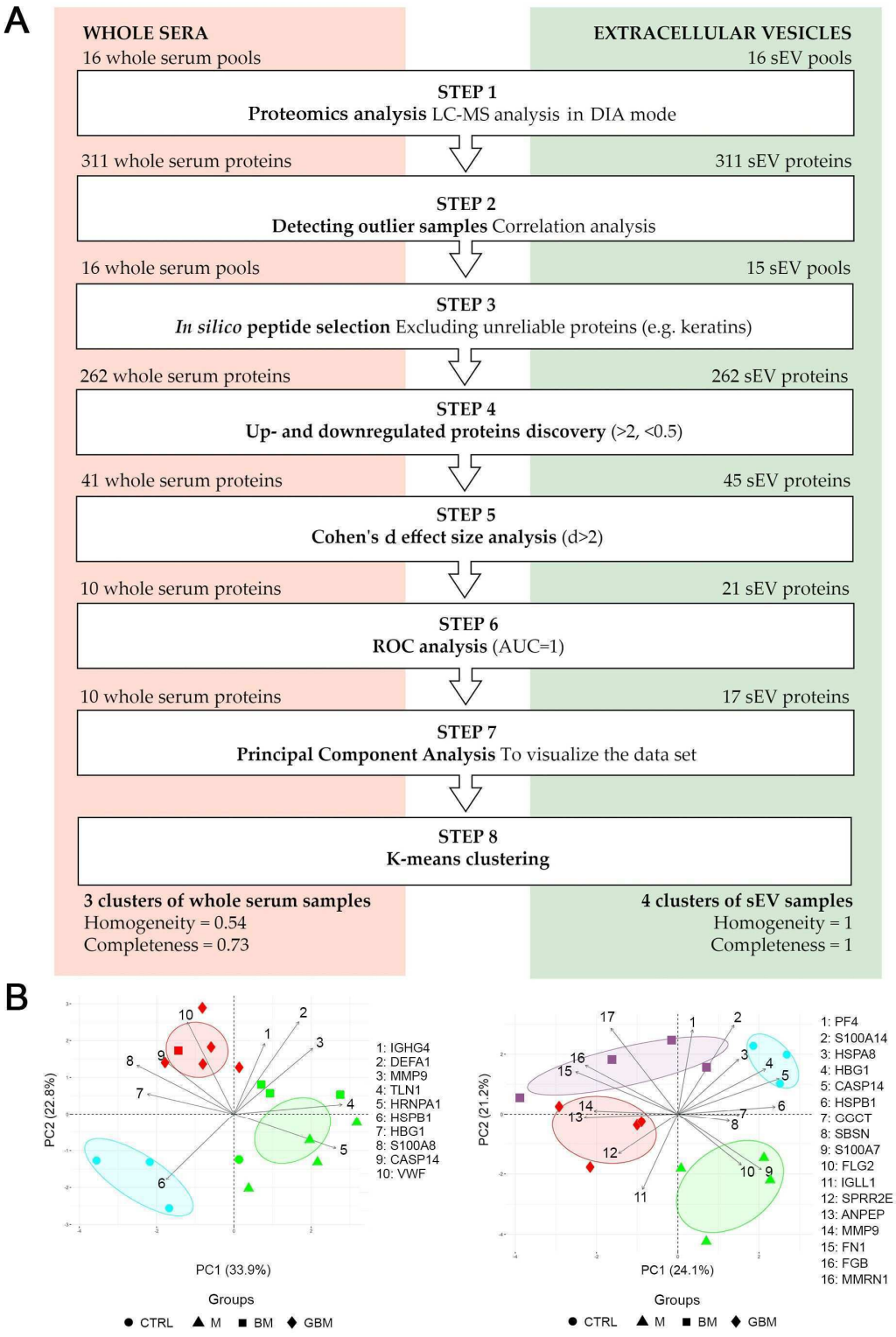

Figure 2. Statistical analysis of the proteome of whole serum (left) and sEV samples (right). (**A**) The flowchart shows the steps of selecting the proteins revealed by liquid chromatography and mass spectrometry (LC-MS) (**B**) The diagrams visualize the results of the principal component analysis (PCA) and k-means clustering. X and Y axes of PCA biplots show principal component 1 (PC1) and principal component 2 (PC2) with explained variances. Arrows represent the coefficients of each protein for PC1 versus the coefficients for PC2, showing the significance of each protein in influencing PCs. Different dots represent the 4 patient groups. Colors indicate the clusters formed by k-means clustering; ellipses indicating the 95% confidence interval were constructed around the barycenters of the clusters.

Following basic processing, up- and down-regulated protein discovery (Step 4) resulted in 41 whole serum proteins and 45 sEV proteins. In addition to comparing each CNS tumor group to CTRL, between-group differences among the CNS tumor groups were also assessed in the protein selection process. As clinically relevant incidence is an important consideration for selecting the proteins identified, Cohen's d effect size was adopted as an indicator of between-groups difference. The Cohen's d effect size analysis (Step 5) with a threshold of d > 2 yielded 10 and 21 proteins in the whole serum and sEV samples, respectively. In the ROC analyses (Step 6) 10 whole serum proteins (MMP9, HSPB1, CASP14, HBG1, IGHG4, DEFA1, VWF, HNRNPA1, S100A8, TLN1) and 17 sEV proteins (MMP9, HSPB1, CASP14, HBG1, FGB, GGCT, PF4, S100A7, FN1, ANPEP, FLG2, HSPA8, IGLL1, MMRN1, S100A14, SBSN, SPRR2E) were found to meet the AUC = 1 selection criteria. Table S3 includes the UniProt ID, Gene symbol, ratio of intensity means > 2 or < 0.5 and Cohen's d effect size > 2 parameters for the selected proteins. The two sample groups shared four significantly altered proteins (highlighted in Table S3), namely MMP9, CASP14, HBG1 and HSPB1.

Following protein selection, PCA (Step 7) was performed to visualize the dataset, where several potentially correlated proteins were projected into a smaller number of variables. K-means clustering (Step 8) on the whole serum PCA biplot resulted in 3 inhomogeneous or incomplete clusters. Calculated cluster homogeneity and completeness scores are 0.56 and 0.73, respectively. In contrast to whole serum samples, the clustering of sEV samples formed homogeneous and complete clusters, with homogeneity and completeness scores of 1. The results of the PCA analyses and k-means clustering indicate considerable differences between the whole serum and sEV samples (Figure 2B). We found that the accuracy of distinguishing between various CNS tumors can be increased using a protein panel from serum-derived sEVs, compared to analyzing whole serum samples.

2.3. Statistical Evaluation and IPA of LC-MS Data Revealed the Background of Suitability Differences between Whole Serum and sEV Samples

2.3.1. Quantitative Changes of the Proteome May Affect the Suitability of sEV Samples to Provide Biomarkers for CNS Tumor Status Monitoring

Statistical comparison of the proteome of sEV and whole serum samples was performed to reveal quantitative differences affecting the suitability of different sample types to provide biomarkers for CNS tumor status monitoring. Pairwise statistical comparison (Welch's test) was used to identify proteins significantly enriched or depleted in sEV samples compared to whole serum samples (Figure 3). Sixty-five proteins were found to be significantly enriched in sEV samples, while 129 proteins were significantly depleted ($p < 0.05$). Using our sEV purification protocol detailed in the Section 4, we obtained a uniform particle size range of sEVs but the magnitude of quantitative changes in the sEV versus whole serum proteome suggested the possible presence of lipoprotein and serum protein contaminations. The level of apolipoproteins was decreased in sEV enriched samples (sEV/serum mean ratio is 0.66), however this fraction could not be completely eliminated. Besides, well known high abundance serum proteins (e.g., ALB) dominated the protein content of sEV enriched samples too. However, the enrichment of non-tissue specific (ITGA2B, ITGB3, LGALS3BP), epithelial cell (CD5L) and platelet related (STOM, TSPAN9) EV marker proteins [31] confirms sEV enrichment (sEV/serum mean ratio is 26.58), while it also demonstrates the presence of sEVs produced during clotting.

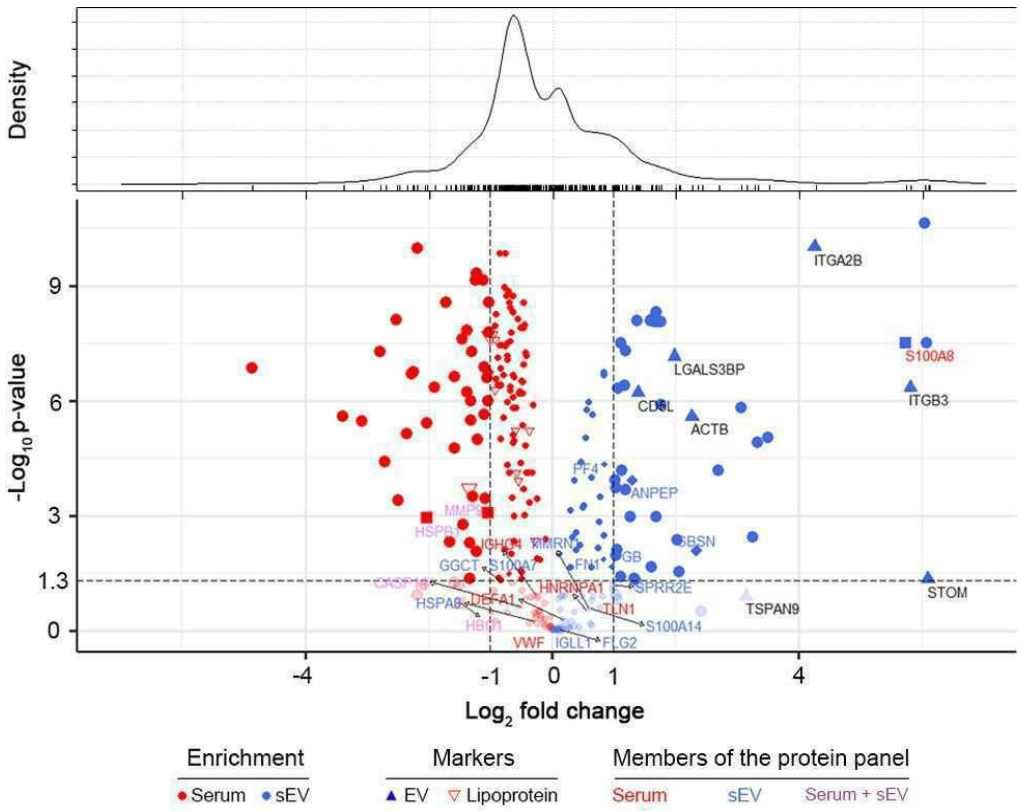

Figure 3. Quantitative comparison of the proteome of sEV and whole serum samples. Volcano plot represents the observed changes in average MS intensities in paired sEV vs. serum comparisons. Protein enrichment is marked with red and blue colored symbols in whole serum and sEVs, respectively. Lipoproteins (empty red upside-down triangles), elements of our whole serum protein panel (red letters, square symbols), sEV protein panel (blue letters, diamond symbols) and common members of the two protein panels (purple letters) are highlighted. Values of –log (p) were obtained from paired Welch's test in sEV/serum comparisons. Density estimation of log2 (fold change) values is shown on top.

Among the 17 proteins of the sEV marker panel described in Section 2.2 only 6 were significantly enriched in the sEV samples and 5 of the 10 proteins comprising the specific serum panel had higher abundance in whole serum (Figure 3). These findings suggest that the better suitability of sEV enriched samples to serve a biomarker source is not explained by a total increase in the abundance of specific proteins. (Detailed proteomics findings, protein annotation and sEV enrichment data are available in Table S1).

Additional sample processing (sEV isolation) may introduce higher technical variance in case of sEV samples, thus it may reduce the analytical suitability of this sample type. Our analysis revealed a similar level of variance for proteins quantified in each sample type (excluding contaminants)—median coefficients of variation within each patient group were in the ranges of 20.78–23.87% for sEV and 20.21–24.45% for serum samples (see Figure S2 for CV distributions).

2.3.2. Biological Background Might Be Responsible for the Increased Suitability of sEV Samples to Provide Biomarkers for CNS Tumor Status Monitoring

To gain insight into the biological background of the obtained proteomics data, IPAwas applied. We performed 'Core Analyses' for whole serum and sEV data separately, yielding a list of significantly influenced 'Diseases and Functions' in each patient group ($p < 0.05$). Using 'Comparison Analysis,' we were able to develop heatmaps covering the relevant systemic and tumor-related functions, as well as the activated or inhibited immune functions (Figure 4A). Regarding whole serum samples, many of the significantly influenced functions identified are related to CNS involvement and active immune

regulatory processes but the patient groups are not clearly distinguished on the heatmaps (Figure 4A, left panels). In contrast, on two of the three sEV proteome-based heatmaps M was evidently separated from the malignant tumor groups (Figure 4A, right panels), where tumor progression-related functions (e.g., angiogenesis, proliferation and migration of tumor cells) were detected to be highly activated and the activated immune functions (e.g., cell movement or activation of myeloid cells) predominate over inhibited immune functions (e.g., phagocytosis).

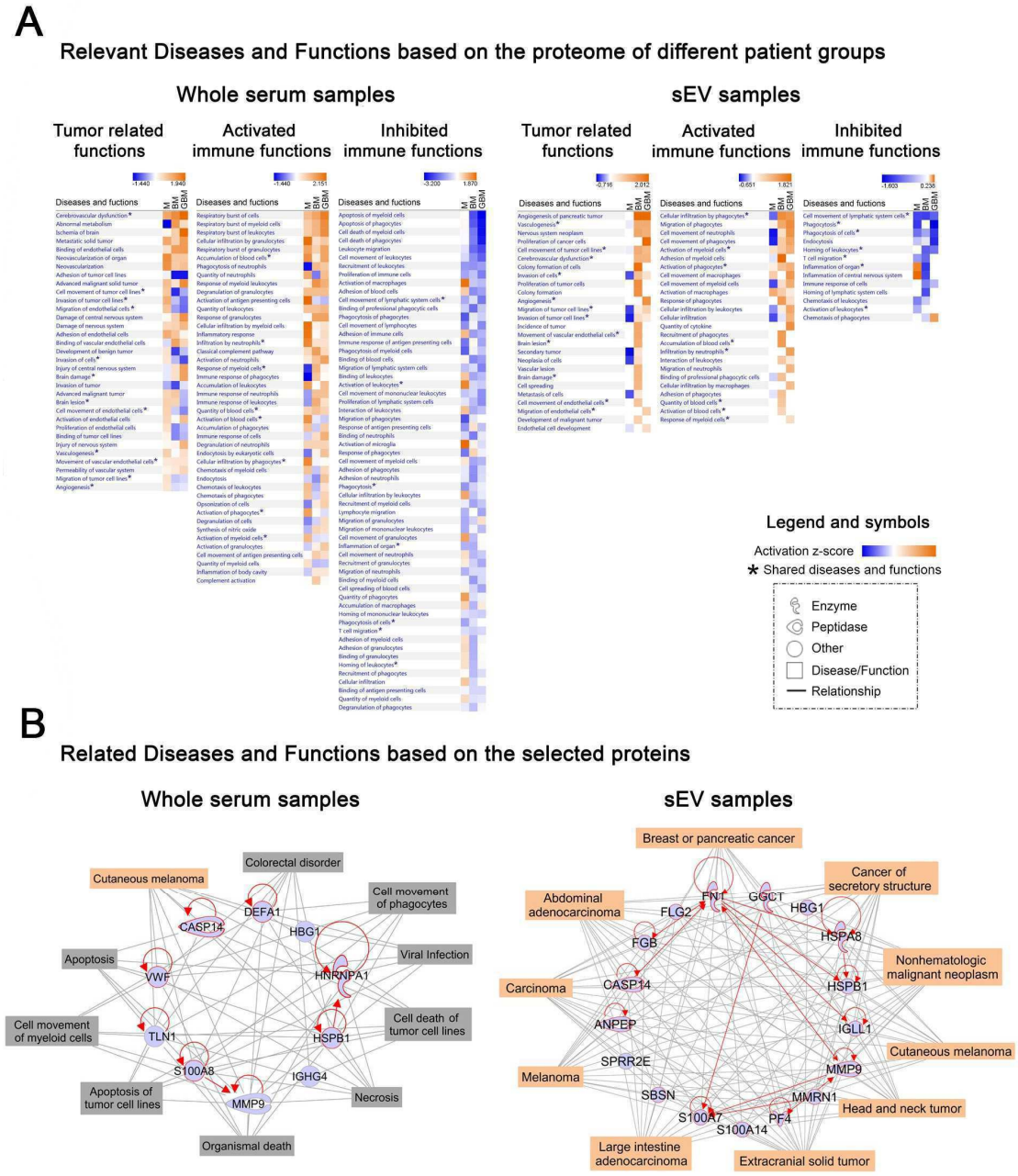

Figure 4. Ingenuity Pathway Analysis (IPA) analyses of whole serum (left) and sEV (right) data derived from the LC-MS analysis. (**A**) Heatmaps show relevant 'Diseases and Functions' in three separated panels related to systemic and tumor-related functions, as well as activated and inhibited immune functions. Z-score indicates activation or inhibition rates of the relevant 'Diseases and Functions' in the three tumorous patient groups compared to the control group. * symbol indicates the shared diseases and functions in whole serum and sEVs. (**B**) Networks display the selected 10 whole serum or 17 sEV proteins (blue symbols) and their relationships (red lines). Top ten related 'Diseases (highlighted in orange symbols) and Functions (highlighted in grey)' are connected by grey lines.

Next, we attempted to specify the common biological role of the characteristic protein profiles identified. Therefore, we elaborated two networks containing the selected 10 and 17 proteins identified based on whole serum and the sEV data, respectively (Figure 4B). Using the 'Grow tool,' the top ten influenced 'Diseases and Functions' were integrated into the networks. In case of the whole serum network (Figure 4B, left panel), nine different related 'Diseases and Functions' were identified, including viral infection, apoptosis, necrosis or cell movement of phagocytes and myeloid cells and only one was cancer-related. In contrast, the top ten influenced diseases identified on the sEV network based on the identified 17 proteins (Figure 4B, right panel) were all tumor-associated, suggesting their potential involvement in the pathophysiology of cancers.

3. Discussion

Non-invasive diagnostic tests are of outstanding clinical importance because of their minimal burden and risk to the patient, their repeatability, low cost, high information content and easy accessibility. In CNS tumors, a minimally invasive technique for describing the actual tumor status should be particularly important. Conventional MRI tests commonly used for the monitoring of CNS tumors are not absolutely appropriate for discriminating between various tumor types (e.g., cannot differentiate between glioblastomas and solitary metastases, CNS lymphomas or other glioma grades [32]) and cannot distinguish recurrence from pseudoprogression. Brain biopsies, as another option, are highly challenging and risky, especially when multiple sampling is required for long-term follow-up [33]. For several cancer types, blood-based tumor markers, such as PSA, AFP and CA125 have been introduced into clinical practice and research for the identification of further noninvasive biomarkers applicable for monitoring a wider scale of malignant diseases is ongoing [34]. However, regarding CNS tumors these studies have generally failed, presumably explained by several reasons, including (1) the barrier function of BBB (releasing less tumor 'information' into the systemic circulation), (2) the presence of molecules released into the blood from other sources and (3) possibly because of the complexity of tumor tissues (such as glioblastoma multiforme). These issues hamper attempts to use a single or only a few biomarkers to diagnose and monitor CNS tumors.

Based on these considerations, we aimed to detect the characteristic protein fingerprint of some common CNS tumors, trying to amplify the signal/information that brain tumors release into the circulation. For this purpose, the protein content of 96 clinical serum samples and related sEV samples isolated from the whole serum was measured by LC-MS. Serum samples were collected from three brain tumor groups considered as the most common malignant, benign and metastatic brain tumors (glioblastoma multiforme, meningioma [28] and brain metastasis of non-small-cell lung cancer [29]) and a control group (lumbar disc herniation).

To examine whether the proteomes of serum and sEV samples are suitable for differentiating between the CNS tumors in point, that is, whether they are applicable to diagnose and monitor the disease, the proteomes of these four patient groups were compared. The effectiveness of tumor type distinction may be increased if the analysis is restricted to proteins which exhibit significant between-group differences. Protein selection was carried out as described in literature [35] (using ratio of intensity means; Cohen's d effect size; ROC) but much stricter thresholds were applied (>2, <0.5; d > 2; AUC = 1, respectively). Statistical selection yielded a collection of proteins whose intensity showed significant between-group differences and thus these proteins could be reckoned as the most suitable molecules for distinguishing between the tumor types examined. Specifically, protein selection yielded a 10- and 17-membered protein panel for whole serum and sEV samples, respectively. While none of these proteins appeared to be able to distinguish between the patient groups individually, their combination was found to reliably discriminate between the different patient groups suggesting that instead of a few candidates, a specific protein panel is required for a perfect differentiation between various tumor types.

To evaluate group distinction efficiency, PCA with k-means clustering was carried out according to literature [36]. Homogeneity and completeness scores of the clusters were calculated to measure the

performance of k-means clustering. Cluster homogeneity and completeness mean that each cluster contains only samples from the same group and all samples of a given group are assigned to the same cluster. Both scores are bounded below by 0 and above by 1. A score of 1 indicates perfect homogeneity or completeness. PCA revealed that sEV samples were more suitable for group distinction. Despite carefully selected and perfectly identical statistical analyses for the two sample types, the homogeneity and completeness scores for the whole serum analysis were 0.56 and 0.73, respectively, compared to scores 1 and 1 for the analysis of sEV samples. The explanation for these findings is illustrated on a PCA biplot (Figure 2). Regarding serum samples, the proteins that can separate two given groups by the appropriate ratio and effect size may have similar intensities in other groups as well. For example, DEFA1 is important in distinguishing the CTRL group from the BM and GBM groups, however, it shows similar intensities in the GBM and BM groups, hampering the separation of these groups (see DEFA1 arrow pointing between the BM and GBM groups in the whole serum PCA plot). Still, DEFA1 cannot be removed, because it plays a key role in separating the CTRL group from malignant tumors. In contrast, the majority of the proteins identified in the sEV samples were able to separate any given group from all the others.

To check whether the poorer performance of whole serum proteins in distinguishing between the patient groups is attributed to the number of the proteins considered, we performed another PCA analysis including only up- and down-regulated proteins selected from the whole identified panel (see Figure 2, Step 4), yielding a similar number of proteins for the two sample types. The PCA analysis of these 41 whole serum and 45 sEV proteins yielded similar results as the previous analysis of carefully selected proteins only and the sEV sample type proved to perform better again. Although the sEV sample was far from being perfect in this case (4 groups were recognized with a homogeneity score of 0.66 and a completeness score of 0.66), the results for the whole serum analysis indicated that not even the sample groups can be recognized based on these proteins only 2 groups were recognized, homogeneity—0.07, completeness: 0.40) (Figure S3). These findings support that sEVs have a better efficiency in distinguishing between various patient groups, irrespective of the order of magnitude of proteins analyzed for the comparison of sEV and whole serum samples.

To investigate the background of our observations, we performed a quantitative proteomics comparison of the two sample types. A quantitative evaluation of sEV purification protocols was suggested based on quantitative LC-MS based proteomics approach, using enrichment analysis of carefully selected sEV markers along with medium specific contamination marker proteins (e.g., lipoproteins and serum). To the best of our knowledge, we are the first group to quantitatively compare the proteome of serum derived small extracellular vesicles with that of the original whole serum samples. sEV enrichment may increase the relative abundance of proteins present in higher concentration within sEVs and the increased signal-to-noise ratio may be beneficial for the quantitative LC-MS analysis of such proteins. On the other hand, proteins in serum are originating from different sources of the human body. Any fractionation (e.g., enrichment of a specific sEV population) may decrease the suppressing effect of the uninformative protein fraction released from sources not specific for the target disease. No association was revealed between being a sEV marker and sEV enrichment, suggesting that it not the overall enrichment process that should be responsible for the increased suitability of sEV samples to provide biomarkers for CNS tumor monitoring. Instead, the removal of an uninformative protein fraction, providing a more specific sample, may explain why the sEV sample is more applicable for distinguishing between various CNS cancer patient groups. Compared to whole serum samples, EVs may be more suitable for investigating tumor related molecular patterns, as the characteristic fingerprint molecules are present in higher concentrations in sEV samples and are accompanied by less contaminating molecules that may bias the analytical findings.

To understand the biological background for our proteomics-based data, IPA was used for the separate analyses of whole serum and sEV data. 'Core Analyses' were performed, yielding a list of significantly influenced 'Diseases and Functions' comprising tumor-related functions as well as activated or inhibited immune functions in each patient group ($p < 0.05$). 'Comparison Analysis' was

carried out to compare the affected 'Diseases and Functions' in the different patient groups. Regarding whole serum samples, many of the significantly influenced functions identified were associated with CNS involvement and active immune regulatory processes but the patient groups were not clearly distinguished on the heatmaps. In contrast, on the sEV proteome-based heatmaps the benign M was clearly separated from the malignant tumors, for which numerous tumor progression-related functions (e.g., angiogenesis, proliferation and migration of tumor cells) were found to be highly activated. The generated IPA heatmaps also revealed that the proteome of sEV samples may provide more specific information on the immune reactions characteristic to the patient groups. We assume that activated immune functions (e.g., cellular infiltration and migration of phagocytes) may play a crucial role in the development of an immune-suppressive microenvironment, while antitumoral immune responses (e.g., phagocytosis, inflammation) might be inhibited.

Serum is a dual source of biomolecular information on cancer, as it contains the molecules released by cancer cells, as well as those released during the immune system's tumor-specific responses [37]. Therefore, the differences observed in the serum vesicles isolated from different patient groups may not only mirror tumor-specific processes but also those related to the associated immune responses [38,39]. Samples enriched in sEVs can offer an amplified source of relevant information, representing not only the specific tumor tissue but also the associated immune responses. Thus, an appropriate protein panel, covering both sources, may have improved efficiency for CNS tumor classification and monitoring.

In addition, the networks developed based on the IPA 'Grow tool' demonstrated that the biological background of the sEV-based characteristic protein profile is more specifically associated with the tumor types compared with the whole serum based protein profile. The role of some of the proteins included in the sEV-based characteristic protein profile has already been described, for example in GBM biology, making these proteins promising targets for extracellular vesicle-based biomarker development [25].

In addition to the proteomics-based comparison of EV samples, we also examined the EV concentration of individual serum samples. Interestingly, no significant differences were detected between the four patient groups regarding the concentration of serum sEVs, with a mean size of 112.2 nm. Osti et al. observed higher EV plasma levels in GBM patients, brain metastases and extra-axial brain tumors compared to healthy controls. Other researchers also demonstrated higher EV concentration in tumorous patients, when unfractionated EV isolates [40] or a wider spectra of EVs were analyzed [41,42]. However, other non-neoplastic diseases of the central nervous system may also increase the number of small-sized circulating EVs, as it was demonstrated in acute ischemic stroke [43] or multiple sclerosis patients [44]. Our vesicle number measurement results, as well as the findings detailed above suggest that the elevated sEV concentration cannot be clearly attributed to the presence of the tumor as immune responses or other systemic responses also contribute to the circulating EV population. Our proteomics-based findings, coupled with the available literature data, suggest that circulating small-sized EVs show important qualitative but not quantitative differences between benign or malignant brain tumors and spinal disc herniation.

Liu and colleagues highlighted that serum is not the perfect choice for a representative sampling of circulating EVs [45], as a high fraction of EVs may be lost during coagulation and also blood components (e.g., platelets) may release microvesicles (MV) during clotting, altering the original MV content of blood samples. However, serum is still the preferred sample form for blood-based clinical diagnoses and it is a practical choice for future clinical developments. It should be noted that co-purification of proteins [46] and lipoprotein particles [47] in EV isolation methods is a common and well known challenge [31]. The presence of protein aggregates [48] and lipoproteins in sEV isolates may provide additional explanation for the lack of increase in the concentration of enriched sEV particles in cancer patients' serum, contrary to literature data on plasma [49] or serum samples [40]. Efforts to eliminate lipoproteins are described in numerous papers reporting on attempts to introduce more sophisticated methods (e.g., combination of ultracentrifugation and size-exclusion chromatography) [50]. In fact, these laborious and instrumentation demanding methods are of high importance in scientific research of the molecular contents of EVs but they may not be applicable in routine clinical practice. Our sEV

isolation protocol has several advantages, as it does not require expensive equipment or highly trained professionals and the entire procedure (along with characterization) is performed within 4 h, therefore, this technique could be easily incorporated into clinical practice.

Our quantitative proteomics results demonstrate that even a simple sEV enrichment protocol can increase the diagnostic potential of serum samples for the identification and classification of patients with different CNS cancers. This finding also supports that even a low-efficacy sEV enrichment/purification method may be appropriate to enhance the analytical applicability of serum samples for CNS cancer monitoring, however, in such cases a quantitative description of enrichment efficiency is definitely required for the right interpretation of the analytical results [51].

In conclusion, our findings support that extracellular vesicles have a greater potential for the monitoring of CNS tumors compared to whole serum samples. Using EV samples is a possible way to amplify the signals released by brain tumors into the circulation. Given the easy-to-implement isolation and enrichment protocol established in this study, the introduction of EV analysis would be beneficial in clinical practice.

4. Materials and Methods

4.1. Patients

Blood samples of 96 patients treated between March 2015 and January 2018 in the Department of Neurosurgery, University of Debrecen were analyzed. Samples were obtained from patients with primary glioblastoma multiforme (GBM), meningioma (M) and single brain metastasis originating from non-small-cell lung cancer (BM). Control samples (CTRL) were collected from patients with spinal disc herniation without evidence of cancer. This non-tumor patient group served as control group in comparison to the patients having different intracranial tumor to distinguish the effects of tumorous processes from the CNS involvement on circulating sEVs. Each group contained 24 individuals with mixed ages and genders. As shown in the Table 1, six-sample-pools were created from the individuals, allowing four parallel samples to be tested per group. Blood samples were collected one day prior to neurosurgical procedure in each tumor case. None of the patients received radio- or chemotherapy before tumor resection. Blood samples were stored by the Neurosurgical Brain Tumor and Tissue Bank of Debrecen according to the criteria of the National Research Ethics Committee. An informed consent form was signed by each patient; the study was conducted in accordance with the Declaration of Helsinki. This study was carried out according to two ethical approvals, namely 51450-2/2015/EKU (0411/15), Medical Research Council, Scientific and Research Ethics Committee, Budapest, October 30, 2015 and 121/2019-SZTE, University of Szeged, Human Investigation Review Board, Albert Szent-Györgyi Clinical Centre, Szeged, 19 July 2019.

Table 1. Patient cohort [1].

♦ Glioblastoma Multiforme	GBM	GBM1	GBM2	GBM3	GBM4
Total No. of patients	***n* = 24**	*n* = 6	*n* = 6	*n* = 6	*n* = 6
Age, Median (range)	**67 (33–82)**	64.5 (38–82)	69.5 (33–76)	67.5 (49–74)	66.5 (63–77)
Mean	**64.9**	62.7	63.8	64.7	68.5
Sex (%), Male	**13 (54.2)**	3 (50)	3 (50)	5 (83.3)	2 (33.3)
Female	**11 (45.8)**	3 (50)	3 (50)	1 (16.7)	4 (66.7)
■ Brain Metastasis	**BM**	**BM1**	**BM2**	**BM3**	**BM4**
Total No. of patients	***n* = 24**	*n* = 6	*n* = 6	*n* = 6	*n* = 6
Age, Median (range)	**64 (42–82)**	66.5 (51–82)	68 (62–71)	63.5 (42–81)	59.5 (53–64)
Mean	**64**	67.7	67.5	59.7	59.5
Sex (%), Male	**13 (54.2)**	2 (33.3)	3 (50)	4 (66.7)	4 (66.7)
Female	**11 (45.8)**	4 (66.7)	3 (50)	2 (33.3)	2 (33.3)
▲ Meningioma	**M**	**M1**	**M2**	**M3**	**M4**

Table 1. *Cont.*

♦ Glioblastoma Multiforme	GBM	GBM1	GBM2	GBM3	GBM4
Total No. of patients	***n* = 24**	*n* = 6	*n* = 6	*n* = 6	*n* = 6
Age, Median (range)	**60 (30–79)**	54.5 (39–69)	62 (30–66)	61.5 (44–75)	66.5 (52–79)
Mean	**58.0**	53.5	53	59.3	66
Sex (%), Male	**4 (16.7)**	0 (0)	0 (0)	1 (16.7)	3 (50)
Female	**20 (83.3)**	6 (100)	6 (100)	5 (83.3)	3 (50)
• Control	**CTRL**	**CTRL1**	**CTRL2**	**CTRL3**	**CTRL4**
Total No. of patients	***n* = 24**	*n* = 6	*n* = 6	*n* = 6	*n* = 6
Age, Median (range)	**50.5 (20–81)**	46.5 (26–71)	47 (20–62)	70.5 (49–81)	52.5 (41–69)
Mean	**52.9**	46.5	45	67.2	53
Sex (%), Male	**9 (37.5)**	2 (33.3)	4 (66.7)	4 (66.7)	4 (66.7)
Female	**15 (62.5)**	4 (66.7)	2 (33.3)	2 (33.3)	2 (33.3)

[1] The table summarizes the main characteristics of the patient groups examined. Each group (average values highlighted in bald) included 24 individuals, converted into six-sample-pools to yield four samples per group for further analysis.

4.2. Preparation of Serum Samples, sEV Isolation and Characterization

Blood samples were collected into BD Vacutainer SST II Advance Tubes (Becton, Dickinson and Company, Franklin Lakes, NJ, USA), allowed to clot for at least 1 h at room temperature and centrifuged for 20 min at 3000× *g*, 10 °C to remove cells. Following the 3000× *g* centrifugation, the supernatant serum was transferred to new Eppendorf tubes and centrifuged for 30 min at 10,000× *g*, 4 °C to remove debris and large vesicles. One milliliter serum aliquot was diluted with DPBS (Ca^{2+}-free, Mg^{2+}-free, Lonza Group Ltd., Basel, Switzerland) to 8 mL and ultracentrifuged for 70 min, at 100,000× *g*, 4 °C (polycarbonate tubes, fixed angle T-1270 rotor, Thermo Fisher Scientific, Waltham, MA, USA). The pellet was resuspended in 100 uL DPBS and stored at −80 °C until further processing. This sEV isolation protocol served to reach intermediate recovery and intermediate specificity according to MISEV2018 [31].

SEVs were characterized by AFM (Oxford Instruments Asylum Research, Abingdon, UK), as described previously [52] and NTA using a NanoSight NS300 instrument (Malvern Panalytical Ltd., Malvern, UK) as it described below. Classical EV markers were presented by Western blot analyses using NuPAGE reagents and an XCell SureLock Mini-Cell System (Thermo Fisher Scientific, Waltham, MA, USA) according to manufacturer's protocols. For detection of the CD81 and Alix markers, we used rabbit anti-human CD81 (1:1000, Sigma-Aldrich, St. Louis, MO, USA) and rabbit anti-human Alix (1:1000, Sigma-Aldrich, St. Louis, MO, USA) primary antibody and HRP-conjugated anti-rabbit IgG (1:1000, R&D Systems, Minneapolis, MN, USA) secondary antibody.4.3. Quantitative analysis of sEVs by NTA.

As suggested by a recent study [53], sEVs were diluted in particle free DPBS and analyzed using a NanoSight NS300 instrument with 532 nm laser (Malvern Panalytical Ltd., Malvern, UK). The measurements were performed on the 16 sEV sample pools (described in 4.1). Six videos of 60 s were recorded for each sample under constant settings (Camera level: 15; Treshold: 4, 25 °C; 60–80 particles/frame) and analyzed to obtain data on size distribution and particle concentration.

4.3. Proteomic Analysis by LC-MS

4.3.1. 'In Solution' Digestion

Individual samples containing 20 µg protein were diluted to 10 µL with 0.1 M NH_4HCO_3 (pH = 8.0) buffer; 12 µL 0.1% RapiGest SF (Waters, Milford, MA, USA) and 2 µL 55 mM dithioeritritol solution was added and kept at 60 °C for 30 min to unfold and reduce proteins. A volume of 2 µL 200 mM iodo acetamide solution was added to alkylate the proteins which were kept for an additional 30 min in the dark at room temperature. The samples were digested overnight at 37 °C with trypsin (Thermo

Scientific, Waltham, MA, USA, enzyme/protein ratio: 0.4 to 1). The digestion was stopped by addition of 1 µL of concentrated formic acid.

4.3.2. LC-MS

The separation of the digested samples was carried out on a nanoAcquity UPLC, (Waters, Milford, MA, USA) using Waters ACQUITY UPLC M-Class Peptide C18 (130 Å, 1.78 µm, 75 µm × 250 mm) column with a nonlinear 90 min gradient. Eluents were water (A) and acetonitrile (B) containing 0.1 *V*/*V*% formic acid and the separation of the peptide mixture was performed at 45 °C with 0.35 µL/min flow rate using an optimized nonlinear LC gradient (3–40% B). The LC was coupled to a high-resolution Q Exactive Plus quadrupole-orbitrap hybrid mass spectrometer (Thermo Scientific, Waltham, MA, USA). The quantitative measurements of digested individual samples were performed in DIA mode. The survey scan for DIA method operated with 35,000 resolution. The full scan was performed between 380 to 1020 *m*/*z*. The AGC target was set to 5 × 106 or 120 ms maximum injection time. In the 400–1000 *m*/*z* region 22 *m*/*z* wide overlapping windows were acquired at 17,500 resolution (AGC target: 3 × 106 or 100 ms injection time, normalized collision energy: 27 for charge 2). The quantitative analysis was performed in Encyclopedia 0.81 [54] using default settings after deconvolution, peak picking and conversion of raw MS files to mzML format in Proteowizard [55]. A comprehensive spectral library [56] of 10,000 human proteins was used for peptide identification. Protein quantities calculated by the Encyclopedia software based on summed intensities of the automatically filtered peptides were used in further statistical evaluations.

4.4. Statistical Analysis

The collected data about the whole serum and extracellular vesicles were reduced and analyzed using statistical methods. Pearson's correlation analysis was used to investigate the outlier samples [57], contaminating proteins (cytokeratins) and proteins with missing values were excluded from the proteomic data [58]. Data were log-transformed to reduce skewness and increase linearity [59]. Cohen's d effect size was calculated to measure the difference between the protein intensity means, outcomes in two different groups [60,61]. Pairwise ROC analysis allowed us to find those proteins which can separate at least one group to the others [62]. The calculated ROC AUC (area under the ROC curve) values are accepted if it equals to 1. In order to transform several (potentially) correlated proteins into a (smaller) number of uncorrelated variables and visualize the dataset, PCA with k-means clustering was performed [63–66]. Homogeneity and completeness scores of the clusters were calculated to measure the performance of k-means clustering [67]. Two-tailed Welch's *t*-test was performed to identify the significantly enriched or depleted proteins in sEV samples. The statistical analyses were performed using R statistical program (version 3.6.3 with pROC, FactoMineR, factoextra and ggplot2 packages; Vienna, Austria), Python programming language (version 3.8, Scotts Valley, CA, USA) and Perseus (MaxQuant, Munich, Germany). Values of $p < 0.05$ were considered significant (see in Appendix A more detailed). GraphPad Prism 8 (San Diego, CA, USA) was used for further data visualization.

4.5. In Silico Analysis of LC-MS Data

Protein data derived from the LC-MS were analyzed by the IPA (Qiagen Bioinformatics, Hilden, Germany). Using fold change values, 'Core Analysis' were performed for whole serum and sEV data separately to identify 'Diseases and Functions,' which can be significantly influenced by the described proteomes ($p < 0.05$). After 'Comparison Analysis,' we created heatmaps of the relevant 'Diseases and Functions,' that is, tumor-related and immunological functions showing regulatory differences between the three CNS tumor groups. Activation z-score calculated by IPA indicates the extent and direction of the effect that given proteins have on function/disease.

The selected 10 whole serum proteins and 17 sEV proteins were introduced to custom pathways as well. Then, 'Connect tool' of IPA was used to reveal the relationships between these molecules and

'Grow tool' was applied to search the top ten 'Diseases and Functions' assigned to the 10 whole serum proteins or 17 sEV proteins. Results are displayed in two networks created by the IPA Path Designer.

Confidence level was set to 'Experimentally observed' for all IPA procedures, which enables literature data-based analysis but excludes unproven predictions.

4.6. Data Availability

All datasets generated during the current study are available from the corresponding author upon reasonable request.

We have submitted all relevant data of our experiments to the EV-TRACK [68] knowledgebase EV-TRACK ID: EV200080.

5. Conclusions

Our study aimed to detect the characteristic protein fingerprint of the most common CNS tumors. Intending to amplify the signal that brain tumors release into the circulation, in addition to the whole serum's, the protein content of the small extracellular vesicles isolated from the serum was also examined.

Comparative proteomic analysis suggests that sEVs may be more suitable for investigating tumor related molecular patterns, because these molecules are present in higher concentrations in sEV samples compared to whole serum samples and have less 'noise' that may bias the analytical findings. In silico analyses revealed that the biological background of the sEV-based characteristic protein profile of the samples is more specifically associated with the tumor types compared with the whole serum based protein profile. Samples enriched in sEVs can offer an amplified source of relevant information, representing not only the specific tumor tissue but also the associated immune responses.

These findings revealed that circulating small-sized extracellular vesicles were more suitable for separating different patient groups. The number of proteins applied for monitoring cannot be reduced to a few individual molecules, instead, a specific protein panel is required for perfect differentiation. To the best of our knowledge, we are the first group to quantitatively compare the proteome of serum derived small extracellular vesicles with that of the original whole serum samples.

In conclusion, our findings support that extracellular vesicles have a greater potential for monitoring CNS tumors, compared to whole serum samples. Considering that analyzing sEVs can be performed easily, incorporating our method into clinical practice would be of great benefit.

Supplementary Materials: Supplementary materials can be found at http://www.mdpi.com/1422-0067/21/15/5359/s1. Figure S1: Western blot analyses of classical EV markers, Figure S2: Intragroup Coefficients of variation (CV) distributions, Figure S3: PCA dotplot constructed after statistical selection based on the means of intensity ratio; Table S1: 311 membered protein table of DIA mode constructed spectral library; Table S2: Sample correlation matrix; Table S3: List of the selected proteins.

Author Contributions: Conceptualization, K.B.; methodology, G.D. and K.B.; validation, G.D., B.B. and A.J.; formal analysis G.D., M.B., Z.S., M.H., M.S.; investigation, G.D., M.B. and E.G.-S.; resources, A.K., P.H., T.B. and K.B.; writing—original draft preparation, G.D., M.B., Z.S. and M.H.; writing—review and editing, G.D. and K.B.; visualization, G.D, M.B., Z.S. and M.H.; supervision, A.K. and K.B.; project administration, G.D. and K.B.; funding acquisition, K.B. All authors have read and agreed to publish the final version of the manuscript.

Funding: This study was founded by the following research grants: GINOP-2.3.2-15-2016-00015 (K.B.); GINOP-2.2.1-15-2017-00052 (K.B.), 2017-1.2.1-NKP-2017-00002 "National Brain Research Program NAP 2.0" (A.K.), UNKP-19-4-SZTE-63 (K.B.), Janos Bolyai Research Scholarship of the Hungarian Academic of Sciences (K.B.).

Acknowledgments: The authors thank Lilla Pinter for her technical assistance and Zsolt Szegletes for taking the AFM images. The authors thank Dora Bokor, PharmD, for proofreading the manuscript.

Conflicts of Interest: The authors declare no conflict of interest. The funders had no role in the design of the study; in the collection, analyses, or interpretation of data; in the writing of the manuscript, or in the decision to publish the results.

Abbreviations

AFM	Atomic force microscopy
BBB	Blood brain barrier
BM	Brain metastasis originating from non-small-cell lung cancer
CNS	Central nervous system
CTRL	Controls – lumbar disc hernia patients
DIA	Data independent acquisition
EVs	Extracellular Vesicles
GBM	Primary glioblastoma multiforme
IPA	Ingenuity Pathway Analysis
LC-MS	Liquid chromatography - mass spectrometry
M	Meningioma
NTA	Nanoparticle tracking analysis
PCA	Principal component analysis
ROC	Receiver operating characteristic
sEVs	small extracellular vesicles

Appendix A. Detailed Description of the Statistical Analyses.

The collected data about the whole serum and extracellular vesicles were reduced and analyzed using statistical methods. Pearson's correlation analysis was used to investigate the outlier samples [57]. Contaminating proteins (cytokeratins) and proteins with missing values were excluded from the proteomic data [58]. Data were log-transformed to reduce skewness and increase linearity [59].

Cohen's d effect size was calculated to measure the difference between the protein intensity mean, outcomes in two different groups. The formula of the Cohen's d effect size

$$d = \frac{\left|\overline{X}_1 - \overline{X}_2\right|}{\sqrt{\frac{(n_1-1)SD_1^2+(n_2-1)SD_2^2}{n_1+n_2-2}}}$$

where X is the mean protein intensity in a given group, SD is standard deviation and n is sample size [60]. In this study we say at least 2 effect size is necessary. It indicates that the mean of group 1 is at the 97.7 percentile of group 2, and the nonoverlapping area of the two distributions at least is 81.1% [61].

Pairwise ROC analysis allowed us to find those proteins which can separate at least one group to the others [62]. The ROC analysis use the true positive rate (sensitivity) and the true negative rate (specificity) at various threshold settings. Plotting the sensitivity against the 1-specificity we get the ROC curve, under the area under this curve measure the separability of the given variable (protein). AUC = 0.5 represents an unsuitable variable to the separate two groups. If AUC = 1, the separation using the actual variable is error-free. In our study the calculated AUC (area under the curve) values are accepted if it equals to 1.

In order to transform several (potentially) correlated proteins into a (smaller) number of uncorrelated variables, and visualize the dataset, principal component analysis (PCA) with k-means clustering was performed. The goal of PCA is to reduce a large number of correlated variables with a set of uncorrelated principal components. These components can be thought of as linear combinations of the original variables that are optimally weighted and derived from the correlation matrix of the data [63].

K-means clustering was performed on the obtained PCA score plots by Hartigan-Wong algorithm [64,65]. Optimal numbers of clusters were determined with Silhouette method and these recommended values were used for clustering [66].

Homogeneity and completeness scores of the clusters were calculated to measure the performance of k-means clustering Cluster homogeneity and completeness mean that each cluster contains only

samples from the same group, and all samples of a given group are assigned to the same cluster. Both scores are bounded below by 0 and above by 1. A score of 1 indicates the perfect homogeneity or completeness. [67].

Two-tailed Welch's t-test was performed to identify significantly enriched or depleted proteins in sEV samples.

The statistical analyses were performed using R statistical program (version 3.6.3 with pROC, FactoMineR, factoextra and ggplot2 packages), Python programming language (version 3.8) and Perseus (MaxQuant). Values of $p < 0.05$ were considered significant. GraphPad Prism 8 was used for further data visualization.

References

1. World Health Organization. *WHO Guidelines for the Pharmacological and Radiotherapeutic Management of Cancer Pain in Adults and Adolescents*; World Health Organization, 2018; License: CC BY-NC-SA 3.0 IGO. Available online: https://apps.who.int/iris/handle/10665/279700 (accessed on 1 June 2020).
2. World Health Organization. *Guide to Cancer Early Diagnosis*; World Health Organization, 2017; License: CC BY-NC-SA 3.0 IGO. Available online: https://apps.who.int/iris/handle/10665/254500 (accessed on 1 June 2020).
3. Garden, G.A.; Campbell, B.M. Glial biomarkers in human central nervous system disease. *Glia* **2016**, *64*, 1755–1771. [CrossRef] [PubMed]
4. Staedtke, V.; Dzaye, O.; Holdhoff, M. Actionable molecular biomarkers in primary brain tumors. *Trends Cancer* **2016**, *2*, 338–349. [CrossRef] [PubMed]
5. Good, D.M.; Thongboonkerd, V.; Novak, J.; Bascands, J.L.; Schanstra, J.P.; Coon, J.J.; Dominiczak, A.; Mischak, H. Body fluid proteomics for biomarker discovery: Lessons from the past hold the key to success in the future. *J. Proteome Res.* **2007**, *6*, 4549–4555. [CrossRef] [PubMed]
6. Best, M.G.; Sol, N.; Zijl, S.; Reijneveld, J.C.; Wesseling, P.; Wurdinger, T. Liquid biopsies in patients with diffuse glioma. *Acta Neuropathol.* **2015**, *129*, 849–865. [CrossRef] [PubMed]
7. Gerber, D.E.; Grossman, S.A.; Zeltzman, M.; Parisi, M.A.; Kleinberg, L. The impact of thrombocytopenia from temozolomide and radiation in newly diagnosed adults with high-grade gliomas. *Neuro Oncol.* **2007**, *9*, 47–52. [CrossRef]
8. Cagney, D.N.; Sul, J.; Huang, R.Y.; Ligon, K.L.; Wen, P.Y.; Alexander, B.M. The FDA NIH Biomarkers, EndpointS and other Tools (BEST) resource in neuro-oncology. *Neuro Oncol.* **2018**, *20*, 1162–1172. [CrossRef]
9. Sheridan, C. Exosome cancer diagnostic reaches market. *Nat. Biotechnol.* **2016**, *34*, 359–360. [CrossRef]
10. Colombo, M.; Raposo, G.; Théry, C. Biogenesis, secretion and intercellular interactions of exosomes and other extracellular vesicles. *Annu. Rev. Cell Dev. Biol* **2014**, *30*, 255–289. [CrossRef] [PubMed]
11. Nogués, L.; Benito-Martin, A.; Hergueta-Redondo, M.; Peinado, H. The influence of tumour-derived extracellular vesicles on local and distal metastatic dissemination. *Mol. Asp. Med.* **2018**, *60*, 15–26. [CrossRef]
12. Hoshino, A.; Costa-Silva, B.; Shen, T.L.; Rodrigues, G.; Hashimoto, A.; Tesic Mark, M.; Molina, H.; Kohsaka, S.; Di Giannatale, A.; Ceder, S.; et al. Tumour exosome integrins determine organotropic metastasis. *Nature* **2015**, *527*, 329–335. [CrossRef] [PubMed]
13. Costa-Silva, B.; Aiello, N.M.; Ocean, A.J.; Singh, S.; Zhang, H.; Thakur, B.K.; Becker, A.; Hoshino, A.; Mark, M.T.; Molina, H.; et al. Pancreatic cancer exosomes initiate pre-metastatic niche formation in the liver. *Nat. Cell Biol.* **2015**, *17*, 816–826. [CrossRef] [PubMed]
14. Liu, Y.; Gu, Y.; Han, Y.; Zhang, Q.; Jiang, Z.; Zhang, X.; Huang, B.; Xu, X.; Zheng, J.; Cao, X. Tumor Exosomal RNAs Promote Lung Pre-metastatic Niche Formation by Activating Alveolar Epithelial TLR3 to Recruit Neutrophils. *Cancer Cell* **2016**, *30*, 243–256. [CrossRef] [PubMed]
15. Zeng, Z.; Li, Y.; Pan, Y.; Lan, X.; Song, F.; Sun, J.; Zhou, K.; Liu, X.; Ren, X.; Wang, F.; et al. Cancer-derived exosomal miR-25-3p promotes pre-metastatic niche formation by inducing vascular permeability and angiogenesis. *Nat. Commun.* **2018**, *9*, 5395. [CrossRef] [PubMed]
16. Feng, W.; Dean, D.C.; Hornicek, F.J.; Shi, H.; Duan, Z. Exosomes promote pre-metastatic niche formation in ovarian cancer. *Mol. Cancer* **2019**, *18*, 124. [CrossRef] [PubMed]
17. Chen, G.; Huang, A.C.; Zhang, W.; Zhang, G.; Wu, M.; Xu, W.; Yu, Z.; Yang, J.; Wang, B.; Sun, H.; et al. Exosomal PD-L1 contributes to immunosuppression and is associated with anti-PD-1 response. *Nature* **2018**, *560*, 382–386. [CrossRef] [PubMed]

18. Scavo, M.P.; Depalo, N.; Tutino, V.; De Nunzio, V.; Ingrosso, C.; Rizzi, F.; Notarnicola, M.; Curri, M.L.; Giannelli, G. Exosomes for Diagnosis and Therapy in Gastrointestinal Cancers. *Int. J. Mol. Sci.* **2020**, *21*, 367. [CrossRef] [PubMed]
19. Basu, B.; Ghosh, M.K. Extracellular Vesicles in Glioma: From Diagnosis to Therapy. *Bioessays* **2019**, *41*, e1800245. [CrossRef]
20. Kosaka, N.; Kogure, A.; Yamamoto, T.; Urabe, F.; Usuba, W.; Prieto-Vila, M.; Ochiya, T. Exploiting the message from cancer: The diagnostic value of extracellular vesicles for clinical applications. *Exp. Mol. Med.* **2019**, *51*, 31. [CrossRef]
21. Möhrmann, L.; Huang, H.J.; Hong, D.S.; Tsimberidou, A.M.; Fu, S.; Piha-Paul, S.A.; Subbiah, V.; Karp, D.D.; Naing, A.; Krug, A. Liquid biopsies using plasma exosomal nucleic acids and plasma cell-free DNA compared with clinical outcomes of patients with advanced cancers. *Clin. Cancer Res.* **2018**, *24*, 181–188. [CrossRef]
22. Melo, S.A.; Luecke, L.B.; Kahlert, C.; Fernandez, A.F.; Gammon, S.T.; Kaye, J.; LeBleu, V.S.; Mittendorf, E.A.; Weitz, J.; Rahbari, N.; et al. Glypican-1 identifies cancer exosomes and detects early pancreatic cancer. *Nature* **2015**, *523*, 177–182. [CrossRef]
23. Choy, C.; Jandial, R. Breast Cancer Exosomes Breach the Blood-Brain Barrier. *Neurosurgery* **2016**, *78*, N10-1. [CrossRef] [PubMed]
24. García-Romero, N.; Carrión-Navarro, J.; Esteban-Rubio, S.; Lázaro-Ibáñez, E.; Peris-Celda, M.; Alonso, M.M.; Guzmán-De-Villoria, J.; Fernández-Carballal, C.; de Mendivil, A.O.; García-Duque, S.; et al. DNA sequences within glioma-derived extracellular vesicles can cross the intact blood-brain barrier and be detected in peripheral blood of patients. *Oncotarget* **2017**, *8*, 1416–1428. [CrossRef] [PubMed]
25. Gollapalli, K.; Ray, S.; Srivastava, R.; Renu, D.; Singh, P.; Dhali, S.; Bajpai Dikshit, J.; Srikanth, R.; Moiyadi, A.; Srivastava, S. Investigation of serum proteome alterations in human glioblastoma multiforme. *Proteomics* **2012**, *12*, 2378–2390. [CrossRef] [PubMed]
26. Gállego Pérez-Larraya, J.; Paris, S.; Idbaih, A.; Dehais, C.; Laigle-Donadey, F.; Navarro, S.; Capelle, L.; Mokhtari, K.; Marie, Y.; Sanson, M.; et al. Diagnostic and prognostic value of preoperative combined GFAP, IGFBP-2 and YKL-40 plasma levels in patients with glioblastoma. *Cancer* **2014**, *120*, 3972–3980. [CrossRef] [PubMed]
27. Figueroa, J.M.; Carter, B.S. Detection of glioblastoma in biofluids. *J. Neurosurg.* **2018**, *129*, 334–340. [CrossRef] [PubMed]
28. Ostrom, Q.T.; Gittleman, H.; Truitt, G.; Boscia, A.; Kruchko, C.; Barnholtz-Sloan, J.S. CBTRUS Statistical Report: Primary Brain and Other Central Nervous System Tumors Diagnosed in the United States in 2011-2015. *Neuro Oncol.* **2018**, *20*, iv1–iv86. [CrossRef]
29. Fox, B.D.; Cheung, V.J.; Patel, A.J.; Suki, D.; Rao, G. Epidemiology of Metastatic Brain Tumors. *Neurosurg. Clin. N. Am.* **2011**, *22*, 1–6. [CrossRef]
30. Théry, C.; Witwer, K.W.; Aikawa, E.; Alcaraz, M.J.; Anderson, J.D.; Andriantsitohaina, R.; Antoniou, A.; Arab, T.; Archer, F.; Atkin-Smith, G.K.; et al. Minimal information for studies of extracellular vesicles 2018 (MISEV2018): A position statement of the International Society for Extracellular Vesicles and update of the MISEV2014 guidelines. *J. Extracell. Vesicles* **2018**, *7*, 1535750. [CrossRef]
31. de Menezes-Neto, A.; Sáez, M.J.; Lozano-Ramos, I.; Segui-Barber, J.; Martin-Jaular, L.; Ullate, J.M.; Fernandez-Becerra, C.; Borrás, F.E.; Del Portillo, H.A. Size-exclusion chromatography as a stand-alone methodology identifies novel markers in mass spectrometry analyses of plasma-derived vesicles from healthy individuals. *J. Extracell. Vesicles* **2015**, *4*, 27378. [CrossRef]
32. Weber, M.A.; Zoubaa, S.; Schlieter, M.; Jüttler, E.; Huttner, H.B.; Geletneky, K.; Ittrich, C.; Lichy, M.P.; Kroll, A.; Debus, J.; et al. Essig Diagnostic performance of spectroscopic and perfusion MRI for distinction of brain tumors. *Neurology* **2006**, *66*, 1899–1906. [CrossRef]
33. Shankar, G.M.; Balaj, L.; Stott, S.L.; Nahed, B.; Carter, B.S. Liquid biopsy for brain tumors. *Expert Rev. Mol. Diagn.* **2017**, *17*, 943–947. [CrossRef] [PubMed]
34. Marrugo-Ramírez, J.; Mir, M.; Samitier, J. Blood-Based Cancer Biomarkers in Liquid Biopsy: A Promising Non-Invasive Alternative to Tissue Biopsy. *Int. J. Mol. Sci.* **2018**, *21*, 2877. [CrossRef] [PubMed]
35. Miyauchi, E.; Furuta, T.; Ohtsuki, S.; Tachikawa, M.; Uchida, Y.; Sabit, H.; Obuchi, W.; Baba, T.; Watanabe, M.; Terasaki, T.; et al. Identification of blood biomarkers in glioblastoma by SWATH mass spectrometry and quantitative targeted absolute proteomics. *PLoS ONE* **2018**, *13*, e0193799. [CrossRef] [PubMed]

36. Rhie, S.K.; Perez, A.A.; Lay, F.D.; Schreiner, S.; Shi, J.; Polin, J.; Farnham, P.J. A high-resolution 3D epigenomic map reveals insights into the creation of the prostate cancer transcriptome. *Nat. Commun.* **2019**, *10*, 4154. [CrossRef] [PubMed]
37. Anderson, K.S.; LaBaer, J. The sentinel within: Exploiting the immune system for cancer biomarkers. *J. Proteome Res.* **2005**, *4*, 1123–1133. [CrossRef] [PubMed]
38. Wen, C.; Seeger, R.C.; Fabbri, M.; Wang, L.; Wayne, A.S.; Jong, A.Y. Biological roles and potential applications of immune cell-derived extracellular vesicles. *J. Extracell. Vesicles* **2017**, *6*, 1400370. [CrossRef] [PubMed]
39. Veerman, R.E.; Güçlüler Akpinar, G.; Eldh, M.; Gabrielsson, S. Immune Cell-Derived Extracellular Vesicles –Functions and Therapeutic Applications. *Trends Mol. Med.* **2019**, *25*, 382–394. [CrossRef]
40. Gercel-Taylor, C.; Atay, S.; Tullis, R.H.; Kesimer, M.; Taylor, D.D. Nanoparticle analysis of circulating cell-derived vesicles in ovarian cancer patients. *Anal. Biochem.* **2012**, *428*, 44–53. [CrossRef]
41. Lázaro-Ibáñez, E.; Sanz-Garcia, A.; Visakorpi, T.; Escobedo-Lucea, C.; Siljander, P.; Ayuso-Sacido, A.; Yliperttula, M. Different gDNA content in the subpopulations of prostate cancer extracellular vesicles: Apoptotic bodies, microvesicles and exosomes. *Prostate* **2014**, *74*, 1379–1390. [CrossRef]
42. König, L.; Kasimir-Bauer, S.; Bittner, A.K.; Hoffmann, O.; Wagner, B.; Santos Manvailer, L.F.; Kimmig, R.; Horn, P.A.; Rebmann, V. Elevated levels of extracellular vesicles are associated with therapy failure and disease progression in breast cancer patients undergoing neoadjuvant chemotherapy. *Oncoimmunology* **2017**, *27*, e1376153. [CrossRef]
43. Ji, Q.; Ji, Y.; Peng, J.; Zhou, X.; Chen, X.; Zhao, H.; Xu, T.; Chen, L.; Xu, Y. Increased Brain-Specific MiR-9 and MiR-124 in the Serum Exosomes of Acute Ischemic Stroke Patients. *PLoS ONE* **2016**, *11*, e0163645. [CrossRef] [PubMed]
44. Galazka, G.; Mycko, M.P.; Selmaj, I.; Raine, C.S.; Selmaj, K.W. Multiple sclerosis: Serum-derived exosomes express myelin proteins. *Mult. Scler.* **2018**, *24*, 449–458. [CrossRef] [PubMed]
45. Liu, M.-L.; Werth, V.P.; Williams, K.J. Blood plasma versus serum: Which is right for sampling circulating membrane microvesicles in human subjects? *Ann. Rheum. Dis.* **2020**, *79*, e73. [CrossRef] [PubMed]
46. Smolarz, M.; Pietrowska, M.; Matysiak, N.; Mielańczyk, Ł.; Widłak, P. Proteome Profiling of Exosomes Purified from a Small Amount of Human Serum: The Problem of Co-Purified Serum Components. *Proteomes* **2019**, *7*, 18. [CrossRef]
47. Sódar, B.W.; Kittel, Á.; Pálóczi, K.; Vukman, K.V.; Osteikoetxea, X.; Szabó-Taylor, K.; Németh, A.; Sperlágh, B.; Baranyai, T.; Giricz, Z.; et al. Low-density lipoprotein mimics blood plasma-derived exosomes and microvesicles during isolation and detection. *Sci. Rep.* **2016**, *6*, 24316. [CrossRef] [PubMed]
48. Filipe, V.; Hawe, A.; Jiskoot, W. Critical evaluation of Nanoparticle Tracking Analysis (NTA) by NanoSight for the measurement of nanoparticles and protein aggregates. *Pharm. Res.* **2010**, *27*, 796–810. [CrossRef] [PubMed]
49. Osti, D.; Del Bene, M.; Rappa, G.; Santos, M.; Matafora, V.; Richichi, C.; Faletti, S.; Beznoussenko, G.V.; Mironov, A.; Bachi, A.; et al. Clinical Significance of Extracellular Vesicles in Plasma from Glioblastoma Patients. *Clin. Cancer Res.* **2019**, *25*, 266–276. [CrossRef]
50. Karimi, N.; Cvjetkovic, A.; Jang, S.C.; Crescitelli, R.; Hosseinpour Feizi, M.A.; Nieuwland, R.; Lötvall, J.; Lässer, C. Detailed analysis of the plasma extracellular vesicle proteome after separation from lipoproteins. *Cell Mol. Life Sci.* **2018**, *75*, 2873–2886. [CrossRef]
51. Xu, R.; Greening, D.W.; Zhu, H.J.; Takahashi, N.; Simpson, R.J. Extracellular vesicle isolation and characterization: Toward clinical application. *J. Clin. Investig.* **2016**, *126*, 1152–1162. [CrossRef]
52. Harmati, M.; Tarnai, Z.; Decsi, G.; Kormondi, S.; Szegletes, Z.; Janovak, L.; Dekany, I.; Saydam, O.; Gyukity-Sebestyen, E.; Dobra, G.; et al. Stressors alter intercellular communication and exosome profile of nasopharyngeal carcinoma cells. *J. Oral Pathol. Med.* **2017**, *46*, 259–266. [CrossRef]
53. Parsons, M.E.M.; McParland, D.; Szklanna, P.B.; Guang, M.H.Z.; O'Connell, K.; O'Connor, H.D.; McGuigan, C.; Ní Áinle, F.; McCann, A.; Maguire, P.B. A Protocol for Improved Precision and Increased Confidence in Nanoparticle Tracking Analysis Concentration Measurements between 50 and 120 nm in Biological Fluids. *Front. Cardiovasc. Med.* **2017**, *4*, 68. [CrossRef] [PubMed]
54. Searle, B.C.; Pino, L.K.; Egertson, J.D.; Ting, Y.S.; Lawrence, R.T.; MacLean, B.X.; Villén, J.; MacCoss, M.J. Chromatogram libraries improve peptide detection and quantification by data independent acquisition mass spectrometry. *Nat. Commun.* **2018**, *9*, 5128. [CrossRef] [PubMed]

55. Chambers, M.; Maclean, B.; Burke, R.; Amodei, D.; Ruderman, D.L.; Neumann, S.; Gatto, L.; Fischer, B.; Pratt, B.; Egertson, J.; et al. A cross-platform toolkit for mass spectrometry and proteomics. *Nat. Biotechnol.* **2012**, *30*, 918–920. [CrossRef] [PubMed]
56. Rosenberger, G.; Koh, C.C.; Guo, T.; Röst, H.L.; Kouvonen, P.; Collins, B.C.; Heusel, M.; Liu, Y.; Caron, E.; Vichalkovski, A.; et al. A repository of assays to quantify 10,000 human proteins by SWATH-MS. *Sci. Data* **2014**, *1*, 140031. [CrossRef] [PubMed]
57. Metz, T.O.; Qian, W.J.; Jacobs, J.M.; Gritsenko, M.A.; Moore, R.J.; Polpitiya, A.D.; Monroe, M.E.; Camp, D.G., 2nd; Mueller, P.W.; Smith, R.D. Application of proteomics in the discovery of candidate protein biomarkers in a diabetes autoantibody standardization program sample subset. *J. Proteome Res.* **2008**, *7*, 698–707. [CrossRef] [PubMed]
58. Hodge, K.; Have, S.T.; Hutton, L.; Lamond, A.I. Cleaning up the masses: Exclusion lists to reduce contamination with HPLC-MS/MS. *J. Proteom.* **2013**, *88*, 92–103. [CrossRef] [PubMed]
59. Curran-Everett, D. Explorations in statistics: The log transformation. *Adv. Physiol. Educ.* **2018**, *42*, 343–347. [CrossRef]
60. Lakens, D. Calculating and reporting effect sizes to facilitate cumulative science: A practical primer for t-tests and ANOVAs. *Front. Psychol.* **2013**, *4*, 863. [CrossRef]
61. Cohen, J. *Statistical Power Analysis for the Behavioral Sciences*, 2nd ed.; Routledge: New York, NY, USA, 1988. [CrossRef]
62. Fawcett, T. An introduction to ROC analysis. *Pattern Recognit. Lett.* **2006**, *27*, 861–874. [CrossRef]
63. Husson, F.; Le, S.; Pagès, J. *Exploratory Multivariate Analysis by Example Using R*, 2nd ed.; Chapman and Hall/CRC: New York, NY, USA, 2017. [CrossRef]
64. Hartigan, J.A.; Wong, M.A. Algorithm AS 136: A K-Means Clustering Algorithm. *J. Appl. Stat.* **1979**, *28*, 100. [CrossRef]
65. Ding, C.; He, X. K-means clustering via principal component analysis. In Proceedings of the Twenty-First International Conference on Machine Learning, Banff, AB, Canada, 4–8 July 2004; Association for Computing Machinery: New York, NY, USA, 2004. [CrossRef]
66. Rousseeuw, P.J. Silhouettes: A graphical aid to the interpretation and validation of cluster analysis. *J. Comput. Appl. Math.* **1987**, *20*, 53–65. [CrossRef]
67. Pedregosa, F.; Varoquaux, G.; Gramfort, A.; Michel, V.; Thirion, B.; Grisel, O.; Blondel, M.; Prettenhofer, P.; Weiss, R.; Dubourg, V.; et al. Scikit-learn: Machine Learning in Python. *J. Mach. Learn. Res.* **2012**, *12*, 2825–2830.
68. Van Deun, J.; Mestdagh, P.; Agostinis, P.; Akay, Ö.; Anand, S.; Anckaert, J.; Martinez, Z.A.; Baetens, T.; Beghein, E.; Bertier, L.; et al. EV-TRACK: Transparent reporting and centralizing knowledge in extracellular vesicle research. *Nat. Methods* **2017**, *14*, 228–232. [CrossRef] [PubMed]